STABILITY AND FOLDING OF THE H2A/H2B DIMER: EFFECT OF N-TERMINAL TAIL REMOVAL AND INCORPORATION OF THE HISTONE VARIANT H2A.Z

By

BRANDON JEREMY PLACEK

A dissertation/thesis submitted in partial fulfillment of
the requirements for the degree of

DOCTOR OF PHILOSOPHY

WASHINGTON STATE UNIVERSITY
School of Molecular Biosciences

December 2004

To the Faculty of Washington State University:

The members of the Committee appointed to examine the dissertation/thesis of BRANDON JEREMY PLACEK find it satisfactory and recommend that it be accepted.

_____

Chair

_____

_____

ACKNOWLEDGMENT

I would like to acknowledge to my mentor Lisa Gloss, without whom none of this work would have been possible. She has taught me how to think critically, take criticism and to be a good scientist. I would also like to thank all of my current and past committee members, Michael Smerdon, Bill Davis, Rodney Croteau and Jeremy N. S. Evans. Even if I did not like it at the time, my committee meetings were an invaluable part of my education as a graduate student. Finally, I would like to thank all of my family and friends who have put up with me during this entire process. Don't fret it is finally about over.

STABILITY AND FOLDING OF THE H2A/H2B DIMER: EFFECT OF N-TERMINAL TAIL REMOVAL AND INCORPORATION OF THE HISTONE VARIANT H2A.Z

Abstract

by Brandon Jeremy Placek, Ph. D.
Washington State University
December 2004

Chair: Lisa M. Gloss

The stabilities of the histone oligomers H2A/H2B and H2A.Z/H2B were characterized to further the understanding of the stability and dynamics of the nucleosome core particle. The equilibrium stabilities of the oligomers were determined by urea-induced denaturation, using circular dichroism and intrinsic tyrosine fluorescence. Each of the histone proteins contains a highly basic, unstructured N-terminal tail region, the major sites of post-translational modifications. Truncations of these regions in H2A and H2B were created and the equilibrium stabilities of these were determined and compared to the wild-type. The free energy of unfolding for the wild-type H2A/H2B dimer was 11.8 kcal mol^{-1}, for the three truncated dimers, □N_H2A/H2B, H2A/□N_H2B, and □N_H2A/□N_H2B, the free energy of unfolding were 11.1 kcal mol^{-1}, 12.2 kcal mol^{-1}, and 11.8 kcal mol^{-1} respectively. The stability of the H2A.Z/H2B dimer was determined in the presence of 1 M TMAO; the stability of H2A/H2B was also determined in 1 M TMAO for comparison. The stability of H2A.Z/H2B is 7.3 kcal mol^{-1} and H2A/H2B is 15.5 kcal mol^{-1} in 1 M Trimethylamine-N-oxide.

Stopped-flow fluorescence and circular dichroism techniques were utilized to elucidate the folding mechanism of the H2A/H2B dimer. The folding mechanism was determined to involve two sequential steps: 1) During the dead-time of the instrument (~5 ms), the two monomers come together to form a dimeric intermediate. This intermediate contains greater than 50% of the stability and helical structure. Double-jump experiments confirmed that the

dimeric intermediate is obligatory and on-pathway. 2) In step two, this dimeric intermediate is converted via a first order process to the native dimer. A kinetic folding pathway requiring a dimeric intermediate is seen in other intertwined, helical dimers, including FIS and H3/H4.

TABLE OF CONTENTS

Page

LIST OF TABLES

LIST OF FIGURES

CHAPTER ONE
INTRODUCTION

The work described in this dissertation determines the equilibrium stability and kinetic folding mechanism of the H2A/H2B histone dimer, and compares these results with those obtained following removal of the N-terminal tail domains of these proteins. This work has added to the knowledge of how these highly basic N-terminal tail domains influence the stability and folding of the H2A/H2B heterodimer and therefore of the entire nucleosome core particle. This work also contributes to the general understanding of oligomeric protein folding and provides insights into the redundancies within the protein folding code by comparing these results to those determined from proteins of similar structure. Finally, this work also examines the effect on the stability of the oligomeric histone proteins by the incorporation of a particular histone variant, H2A.Z.

Protein function and structure

Proteins are ubiquitous in nature and play a vital role in life (1). Nearly all biological processes involve the function of one or more proteins. Proteins are linear, unbranched polymers of amino acids, which are linked together by peptide bonds between adjacent amino acids. As a class of biomolecules, proteins have a variety of cellular functions, including but not limited to, catalysis, structure, receptors, regulators, motion and storage. Proteins can function as enzymes catalyzing the vital chemical reactions of life. They may also function as regulators of enzyme activity, interacting directly with an enzyme and altering the enzyme activity. Proteins function as receptors, transducing extracellular signals to their intracellular targets. Mechanical motions of a cell whether it is contractile motion such as in muscle cells or flagellar movement in microorganisms is brought about by the action of proteins. Finally, proteins are involved in the transport and storage of all biomolecules. This brief list indicates the central importance of proteins to the maintenance of all life.

The hierarchy of protein structure can be divided in to four distinct levels: The primary structure (1°) is the linear sequence of amino acids that define a given protein. This order of amino acids is determined by the DNA sequence of the gene encoding a particular protein. The

next level of protein structure is secondary structure (2°). This is the arrangement of the peptide backbone without regard to side chain conformation. The most common types of secondary structure are the α-helix and the β-sheet. Both of these structures are stabilized by a network of hydrogen bonds between the carbonyl group (-C=O) of one residue and the amide group (-N-H) of another (Figure 1). A protein's tertiary structure (3°) is the three dimensional structure of a single polypeptide chain. This involves not only interactions between backbone atoms but also interactions between the side chain atoms. Finally, many proteins are part of complexes involving two or more polypeptide chains. Quaternary structure (4°) is the spatial arrangement of these multiple polypeptide subunits. While the primary structure of a protein is held together by covalent bonds between each amino acid, higher order protein structures are held together by many weak, noncovalent interactions, except in the case of disulfide bonds. Forces that stabilize these structures are electrostatic interactions, hydrogen bonds, van der Waals contacts, and hydrophobic interactions.

Protein stability

Understanding protein structure begins with the observation that the information required to achieve a protein's three dimensional structure is encoded in its primary sequence of amino acids (1, 2). Evidence for this came from the observation that denaturant unfolded ribonuclease A could spontaneously refold to its native state upon removal of denaturant (3). This was the first direct evidence that the primary sequence encodes a protein's three dimensional structure. Since this observation was made in the 1960's, many proteins, ranging from small, monomeric proteins to large, oligomeric complexes have been shown to refold spontaneously (4, 5).

The goal of studying protein folding is to understand how a linear sequence of amino acids is converted from a random coil form to its folded functional form. These studies can be divided into two types, equilibrium experiments to determine a protein's stability, and kinetic experiments which examine the pathway or mechanism by which a protein achieves its folded

state. When studying protein stability, the goal is to determine the difference in Gibb's free energy between the native (N) and unfolded (U) states of a given protein (Figure 2).

$$\Delta G = G_N - G_U \qquad (1)$$

To achieve this goal, the concentration of the unfolded state, relative to the concentration of the native state, must be determined. For a protein of marginal stability (ΔG = 5 kcal/mol), the ratio of U to N is approximately 1 in 20,000, and as the stability increases this ratio is shifted even further toward the native. Currently, there is no practical method for measuring this small number of unfolded molecules in a sea of folded proteins. To determine protein stability, it is necessary to shift this equilibrium such that the concentrations of both the native and unfold species are measurable. The most common denaturation methods are temperature, pH and chemical denaturants (such as urea and guanidinium hydrochloride). Spectroscopic techniques such as circular dichroism and intrinsic tyrosine fluorescence may be used to monitor protein structure (these techniques are discussed later in this thesis). In the case of a dimeric protein, the relative amounts of N and U as a function of denaturant are related to the stability by the following set of equations:

$$K_{eq} = \frac{[U]^2}{[N]} \qquad (2)$$

$$\Delta G^\circ = -RT \ln K_{eq} \qquad (3)$$

This ΔG° is the difference in free energy between the N and U states at a given denaturant concentration. To determine the stability in the absence of denaturant the following equation is used:

$$\Delta G^\circ = \Delta G^\circ_{(H_2O)} - m[Denaturant] \qquad (4)$$

where $\Delta G°(H_2O)$ is the stability in the absence of denaturant and *m* is the sensitivity of the transition to denaturant. This *m* value has previously been demonstrated to be proportional to the change in solvent-accessible surface area (ΔASA) as the protein unfolds (6).

Protein folding

The primary structure of a protein not only encodes its stability, but also the mechanism for its folding from the unfolded state. Conceptually, the simplest model to describe how a protein is converted from the unfolded to the folded form is a random search through all possible conformations until the most stable fold is found. However, Cyrus Levinthal performed a simple calculation that showed if a protein of 100 amino acids in length randomly searched through all possible conformations, it would take longer then the lifetime of the universe for this process to be completed (7). Yet, it is known that most proteins fold on a time scale in the range of milliseconds to minutes. Therefore, a protein must fold by a pathway, not by a random search, and this pathway must be dictated by the amino acid sequence.

One goal of studying a protein's folding pathway is to identify and characterize any obligatory intermediates that occur during this process. It should be noted that these intermediates are not well defined structures, but instead are ensembles of species with closely related structures and thermodynamic properties. The *in vitro* study of protein folding begins with the protein under conditions favoring the unfolded state. Like equilibrium studies, these conditions can include low pH, high temperature or high pressure, as well as the use of chaotropic chemicals, such as urea or guanidium hydrochloride. Initiation of the folding pathway begins with rapidly converting the conditions favoring the unfolded state to conditions favoring the folded form. When the conditions favor the folded form, the protein will begin to fold and the formation of structure can be monitored as a function of time.

The work described in this thesis utilized the techniques of stopped-flow circular dichroism (SF-CD) and stopped-flow fluorescence (SF-FL) to monitor the formation of protein structure. A stopped flow apparatus consists of mechanically driven syringes (Figure 3) that

push solution into a mixer where the liquid is rapidly and efficiently mixed. The protein solution then enters a cuvette where the CD and FL signal change is monitored. For example, urea unfolded protein is placed in one syringe while buffer without urea is placed in a second syringe. The syringe drive motors push the two solutions into the mixer in a predetermined ratio that significantly reduces the concentration of urea to a low enough level such that the folded state is now favored. The primary reason for using a stopped-flow is to significantly reduce the time required for mixing. It is possible to manually mix the unfolded protein with refolding buffer; however, the time required for manual mixing is significantly longer then stopped-flow. The time required for manual mixing is on the time scale of seconds (5-10 seconds), stopped flow allows mixing times as fast as 5 milliseconds. Since many proteins fold in a matter of seconds, it is vital that a rapid mixing technique be used.

Circular dichroism is a technique that monitors the conformation of the peptide backbone and therefore provides a sensitive measure of a protein's secondary structure. Monitoring the change in intrinsic tyrosine fluorescence allows the formation of its tertiary and quaternary structure to be quantified. This technique takes advantage of the fact that in the unfolded state, tyrosines are exposed to solvent and their fluorescence is quenched. In general, tyrosines are buried within the hydrophobic core of the native protein. As folding occurs, the tyrosine residues are removed from solvent, quenching is decreased and the fluorescence signal increases. By monitoring this change in fluorescence, the formation of tertiary and quaternary structure can be quantified in a time dependent manner. All of the kinetic data presented here were able to adequately modeled by the following equation:

$$Y(t) = Y \quad + Y_i \exp(\square t / \square_i) \tag{5}$$

where Y(t) is the spectroscopic signal measured at any time t, Y is the signal at t = , Y_i is the amplitude of the signal change and is the relaxation time in seconds (= 1/k, where k is the rate constant of the reaction). To determine the kinetic parameters in the absence of denaturant, the

relaxation times as a function of final denaturant concentration were fitted to the following equation:

$$\frac{1}{\tau_i} = k_{(H_2O)} \exp\left[\frac{m^{\ddagger}[Urea]}{RT}\right] \qquad (6)$$

where $k_{(H2O)}$ is the rate constant in the absence of denaturant and $m^{\ddagger}$ reflects the sensitivity of the rate to denaturant and is proportional to the ΔASA between the ground state and the transition state.

Chromatin structure and function

Within the nucleus of all eukaryotic cells, the DNA is packaged in a nucleoprotein complex called chromatin. In the case of humans, this complex allows the cell to efficiently package and organize 6 x 10^9 base pairs of DNA, greater than 2 meters in length, into nuclei which are only ~ 6 μm in diameter (8). Initially, it was thought the only role of chromatin was static packaging of DNA in the nucleus. Currently, it is known that the molecular machinery controlling replication, transcription, repair and recombination all utilize DNA when it is packaged into chromatin. There are two general forms of chromatin, the transcriptionally inactive, highly compacted heterochromatin and the transcriptionally active, open form called euchromatin. In order for replication, repair or transcription to occur on DNA, which is packaged in chromatin, the chromatin must first be rearranged to allow access to the DNA. This understanding indicates that chromatin must be a dynamic structure continually being altered. A brief discussion of how this is achieved is presented in a later section of this introduction. Therefore, an understanding of the structural and functional properties of the nucleosome is essential for the complete understanding of the biology of the cell.

Nucleosome core particle structure

The basic repeating unit of chromatin is the Nucleosome Core Particle (NCP). These NCP's occur every 200 ± 40 bp throughout eukaryotic genomes (9). Adjacent NCPs are connected by linker DNA which is no less than 20 bp in length. This linker DNA is bound by another histone protein, H1, which facilitates the further compaction of the DNA. Two copies of each of the four histone proteins H2A, H2B, H3 and H4 form the core of the NCP which is wrapped by ~ 150 bp of DNA in 1.65 superhelical turns.

Each of the histone proteins has a highly conserved structure that can be divided into two domains (10), the N-terminal tail domain and the C-terminal globular domain. The N-terminal tail domain is unstructured, highly basic and the major site of post-translational modifications. The C-terminal domain forms the core of the protein and is the dimerization domain. Despite low sequence identity between the histones (~ 4%) (11), all histones fold to a similar structure called the histone fold. The histone fold is made up of a long central α-helix flanked on each end by a loop and a shorter α-helix. The histone fold is highly conserved and found in a number of DNA binding proteins (11, 12). H2A forms a heterodimer with H2B in a head-to-tail manner called the 'handshake' motif. H3 and H4 form a similar heterodimer, two of these H3/H4 dimers come together to form the H3/H4 heterotetramer via a four-helix bundle between the C-terminal helices of the H3 and H3' proteins (Figure 4).

Two major steps are involved in NCP formation *in vitro* (13, 14). In the first step, the H3/H4 tetramer is deposited onto the DNA near the replication fork. This tetramer/DNA complex is stable, isolatable, and this interaction provides some protection of the DNA from nuclease digestion. In the second step, addition of two H2A/H2B dimers converts this intermediate to the fully assembled NCP.

Altering Chromatin Structure

The packaging of DNA into chromatin potentially blocks the access of the cellular machinery to the DNA. Incorporation of DNA into nucleosomal arrays represses both

transcription initiation and elongation by RNA polymerase III (15). Similarly, nucleosomes could also inhibit replication and repair. It is clear that cells must be able to alter the structure of chromatin to allow access to the DNA. To accomplish this, cells have developed several mechanisms for altering chromatin structure: 1) Post-translational modification of the histone proteins; 2) Chromatin remodeling complexes; and 3) Altering the biochemical makeup of the histone octamer by incorporation of histone variants.

Post-translational modification of the histone proteins

The histone proteins are subject to a complex and dynamic set of covalent modifications, which influence all of the pathways involving DNA, such as, replication, transcription, repair and recombination. The modifications that have been identified to date are acetylation, phosphorylation, methylation, ADP ribosylation, and ubiquitination (for review, (16)). These modifications occur primarily on side chains located in the N-terminal tail domain; many residues on each histone are subject to modification. Acetylation of lysine residues located in the N-terminal tails is the best characterized modification of the histone proteins (17). Acetylation of the histone proteins is carried out by enzymes called histone acetyltransferases (HATs). These enzymes transfer the acetyl group from acetyl-CoA to the amino group in lysine side chains. Acetylation has been implicated in a variety of cellular pathways, including gene activation, histone deposition and DNA replication (18). Another well studied modification is methylation of both lysine and arginine residues. This modification is carried out by histone methyltransferases, which transfer a methyl group from *S*-adenosyl methionine to the side chains of either lysines or arginines. Methylation of histones is primarily involved in the formation of heterochromatin. Acetylation and methylation not only act as signals to be recognized by other proteins but they also affect the charge of these histone proteins. Acetylation of an amino group on the side chain of lysine removes one positive charge by converting the amino group to an amide. Methylation does not alter the charge, however replacing a hydrogen with a methyl group does lower the pKa making it a better H-bond donor to

DNA. Finally, phosphorylation of serines and threonines within the N-terminal regions of histones also alters the net charge of the protein by introducing negative charge into the NCP. Altering the charge of the histone proteins may play a substantial role in the dynamics of the contacts within the NCP, the histone and DNA and between adjacent nucleosome core particles.

Histone Variants

A number of histone variants are expressed within eukaryotic cells, and each variant may have a distinct functional role in chromatin dynamics (for review, (19, 20)). Histone variants are nonallelic, mRNA poly-adenylated isoforms of the major histones, which are synthesized at various times through out the cell cycle. H2A is the largest family of histone variants, although variants of all other core histones have been identified. To date, there have been five H2A variants identified (21). H2A is the only histone family to contain an extended C-terminal tail, and it is in this region and the C-terminal α-helix where the sequence divergence between variants is greatest. While these variants make up a small percentage (< 15%) of the total H2A protein in a cell, it is becoming clear that these minor variants play a major functional role within the cell. MacroH2A1 and MacroH2A2 contain a large nonhistone fusion on their C-terminus (22, 23) and have been implicated in X-chromosome inactivation (24, 25). H2A-Bbd (Barr Body Deficient) is a recently identified variant, which is preferentially excluded from the inactive X-chromosome (26). The histone variants H2A.X is highly conserved from yeast to humans and is proposed to play a vital role in the repair of DNA double-strand breaks. Since, phosphorylation of a serine residue near its C-terminus is one of the earliest detectable events after induction of a DNA double-strand break (for review, (19, 20)).

The variant most central to this work is H2A.Z. It has approximately 60% sequence identity to the major H2A protein; it is highly conserved from yeast to humans and appears to play a unique functional role within the cell (27). Initially, H2A.Z was thought to be involved in activation of transcription, since in *Tetrahymena*, it was shown to be preferentially associated with the transcriptionally active macronucleus and excluded from the transcriptionally inactive

micronucleus (28). H2A.Z was also shown to be required for the full expression of the inducible genes *PHO5* and *GAL1* in yeast (29). However, a number of recent reports on the function of H2A.Z have implicated it in the formation and maintenance of heterochromatin near telomeres and centromeres. Microarray analysis of a H2A.Z knockout in yeast revealed that many of the H2A.Z activated genes were clustered near the telomeres (30). Upon deletion of H2A.Z, silencing proteins that are normally restricted to the telomeres were now able to spread into the adjacent euchromatic regions, converting them to heterochromatin. This silencing of genes in the absence of H2A.Z was also observed in regions surrounding the *HMR* mating-type locus and the centromere (31). This has led to the hypothesis that H2A.Z acts as a boundary element, preventing the spread of heterochromatin into euchromatic regions.

A number of studies on the biophysical properties of H2A.Z containing nucleosome core particles have been reported. The X-ray crystal structure of a H2A.Z containing nucleosome core particle has been determined, and is very similar to that of the nucleosome core particle containing the major H2A (root mean square deviation <1Å) (32). The major difference is a metal ion binding site on the surface of the NCP containing H2A.Z. Incorporation of H2A.Z appears to affect the folding and stability of the nucleosome core particle. Nucleosome arrays (multiple NCPs formed on a single molecule of DNA with multiple NCP positioning elements) containing H2A.Z were shown to fold to a higher degree of compactness than arrays that contain the major H2A (33). A recent study reported that NCPs containing H2A.Z are more stable then those containing H2A (34). It was observed that a H2A.Z-NCP was more resistant to salt-induced dissociation than H2A-NCP, requiring a higher concentration of NaCl to release the H2A.Z/H2B dimer from the H3/H4-DNA complex. The observations that H2A.Z facilitates higher compaction of DNA and is more stable than the H2A containing NCP supports the hypothesis that H2A.Z plays a key role in heterochromatin formation and maintenance.

The remaining chapters will describe the results of my work in Dr. Lisa Gloss' lab. Chapter Two of this thesis will describe the effects of N-terminal tail removal on the stability of the H2A/H2B heterodimer. It was found that the N-terminal tails have a small, non-additive

effect on the stability. Chapter Three compares the stability of the H2A/H2B dimer to that of the H2A.Z/H2B dimer. The dimer containing H2A.Z is significantly destabilized (~50% decrease) when compared to the H2A/H2B dimer. Chapter Four examines the mechanism of folding for H2A/H2B from two unfolded monomers. The mechanism of folding is a two-step process; involving an initial dimerization reaction followed by a first order reaction to form the native dimer. Finally, in Chapter Five the conclusions of this work are presented along with some future directions.

Figure 1:

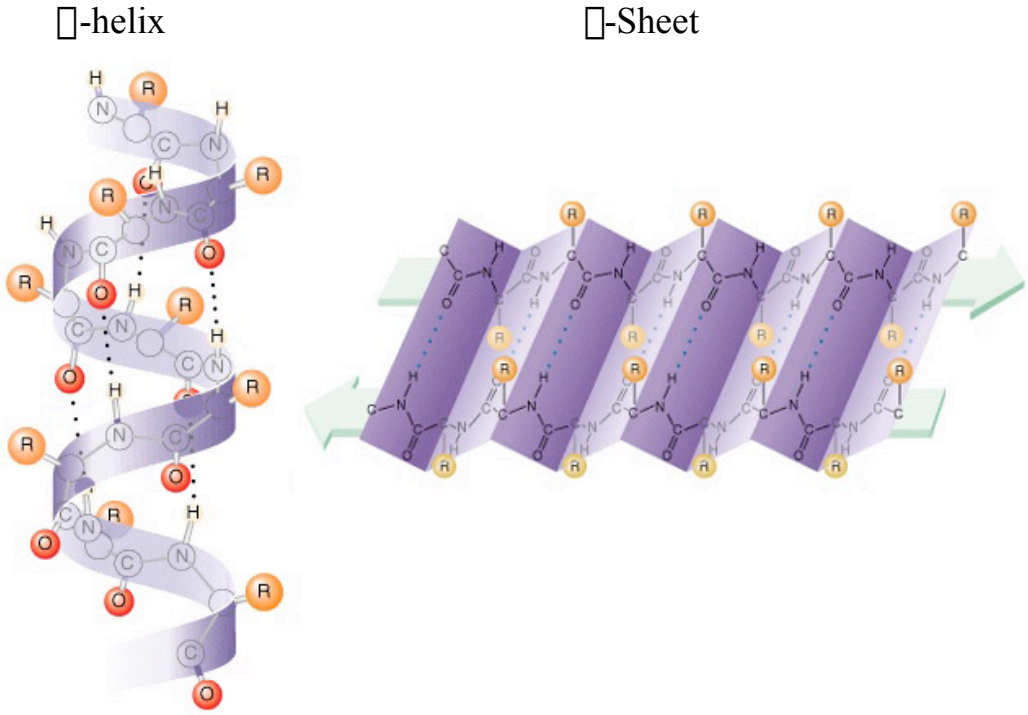

Figure 1: Diagram of the secondary structures α-helix and β-sheet. Showing the hydrogen bonding pattern between the carbonyl group (-C=O) of one residue and the amino group (-N-H) of another. In α-helix these H-bonds occur between every fourth amino acid where as in β-sheet these can involve residues much farther apart in sequence. Structures taken from **www.sbs.utexas.edu/genetics/Supplements/.**

Figure 2:

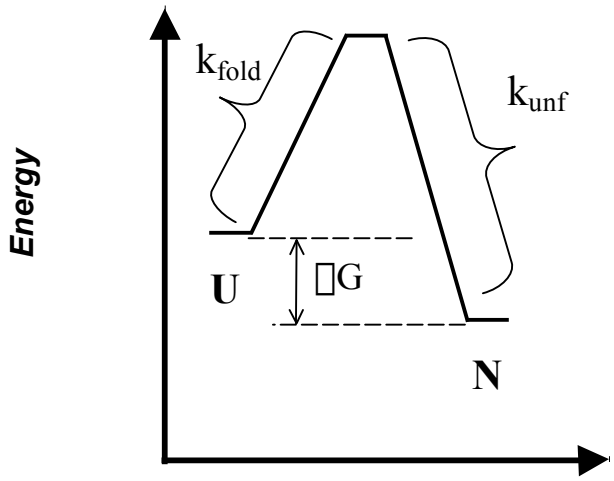

Figure 2: Gibb's free energy diagram indicating the difference in energy between the unfolded (U) and native (N) species.

Figure 3:

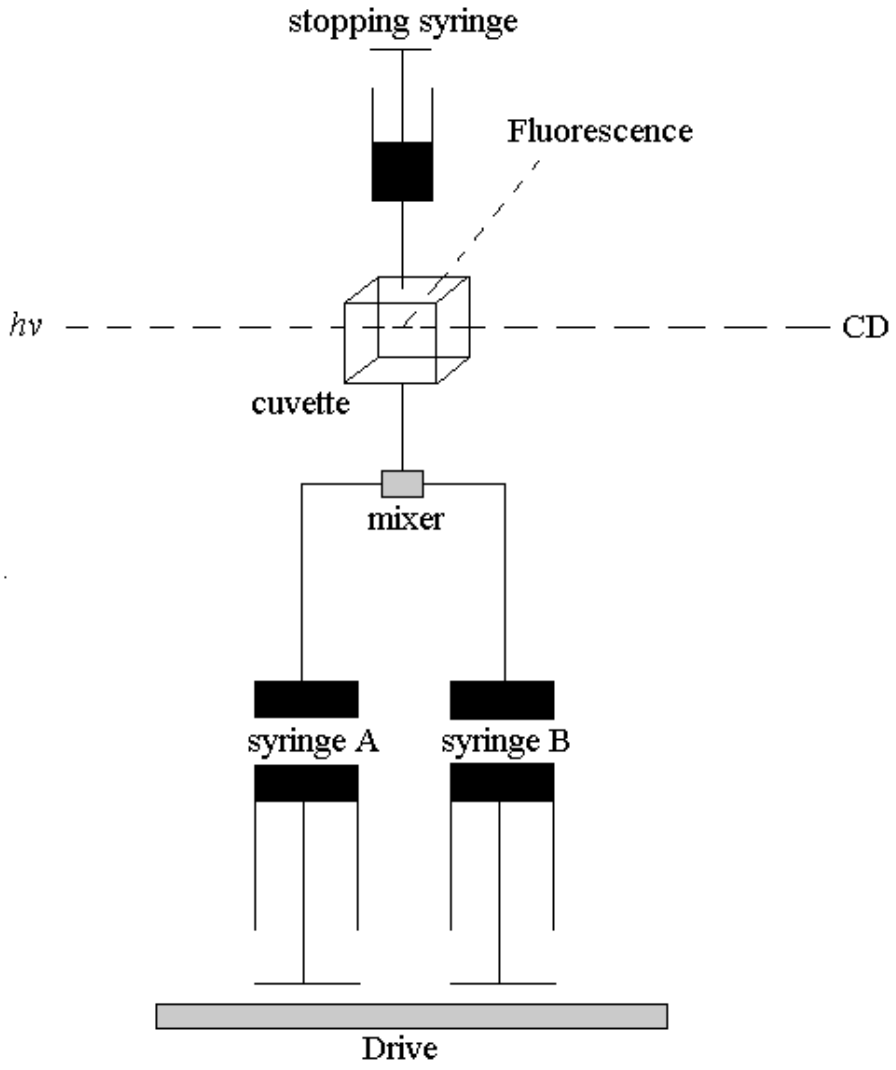

Figure 3: Schematic of a typical stopped flow apparatus. Stopped flow utilizes mechanically driven syringes that push two or more solutions into a mixer where they are rapidly and efficiently mixed. The liquid then enters a cuvette where the spectroscopic signal can be measure in a time dependent manner.

Figure 4:

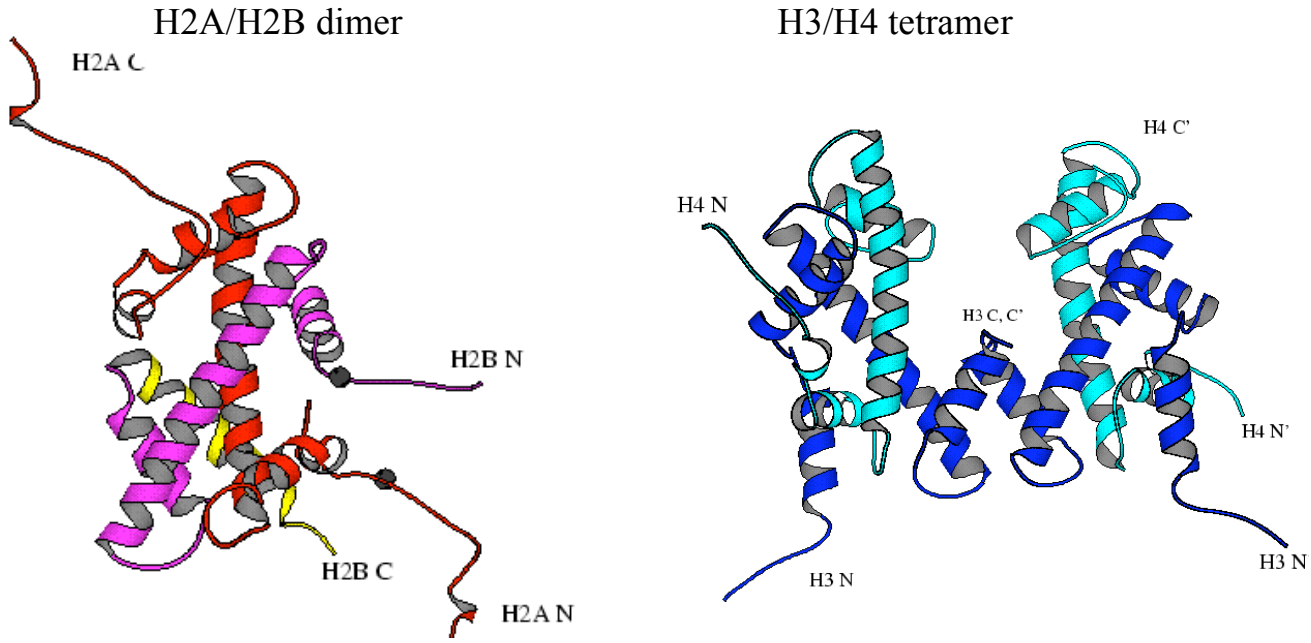

Figure 4: Ribbon diagram of the H2A/H2B dimer and the H3/H4 tetramer, derived from the X-ray crystal structure of the nucleosome core particle. The H2A chain is shown in red, H2B is magenta, H3 is blue and H4 is cyan. Amino acids 4-118 of H2A, 24-122 of H2B, 38-135 of H3 and 20-102 of H4 are shown. These figures were rendered using Molscript v2.1 (35).

REFERENCES

1. Voet, D. and J.G. Voet, Biochemisty. 2 ed. 1995: John Wiley & Sons, Inc. 1361.
2. Garrett, R.H. and C.M. Grisham, Biochemistry. 1995: Saunders College Publishing.
3. Haber, E. and C.B. Anfinsen, Side-chain interactions governing the pairing of half-cystine residues in ribonuclease. J Biol Chem, 1962. **237**: p. 1839-44.
4. Jaenicke, R. and H. Lilie, Folding and association of oligomeric and multimeric proteins. Adv Protein Chem, 2000. **53**: p. 329-401.
5. Matthews, C.R., Pathways of protein folding. Annual Review of Biochemistry, 1993. **62**: p. 653-683.
6. Myers, J.K., C.N. Pace, and J.M. Scholtz, Denaturant m values and heat capacity changes: Relation to changes in accessble surface areas of protein folding. Protein Science, 1995. **4**: p. 2138-2148.
7. Levinthal, C., Are there pathways for protein folding? J. Chim. Phys., 1968. **65**: p. 44-45.
8. Alberts, B., et al., Molecular Biology of the Cell. 4 ed. 2002: Garland Science.
9. McGhee, J.D. and G. Felsenfeld, Nucleosome structure. Annu Rev Biochem, 1980. **49**: p. 1115-56.
10. Wolffe, A. and H. Kurumizaka, The nucleosome: A powerful regulator of transcription. Prog. Nucl. Acid Res. Mol. Biol., 1998. **61**: p. 379-422.
11. Arents, G. and E.N. Moudrianakis, The histone fold: A ubiquitous architectural motif utilized in DNA compaction and protein dimerization. Proc. Natl. Acad. Sci. USA, 1995. **92**: p. 11170-74.
12. Burley, S.K., et al., Histone-like transcription factors in eukaryotes. Curr Opin Struct Biol, 1997. **7**(1): p. 94-102.
13. Oohara, I. and A. Wada, Spectroscopic studies on histone-DNA interactions. II. Three transitions in nucleosomes resolved by salt-titration. J. Mol. Biol., 1987. **196**(2): p. 399-411.

14. Smith, S. and B. Stillman, Stepwise assembly of chromatin during DNA replication in vitro. EMBO J., 1991. **10**: p. 971-980.
15. Hansen, J.C. and A.P. Wolffe, A role for histones H2A/H2B in chromatin folding and transcriptional repression. Proc. Natl. Acad. Sci. U.S.A., 1994. **91**: p. 2339-2343.
16. Goll, M.G. and T.H. Bestor, Histone modification and replacement in chromatin activation. Genes Dev, 2002. **16**(14): p. 1739-42.
17. Grunstein, M., Histone acetylation in chromatin structure and transcription. Nature, 1997. **389**(6649): p. 349-52.
18. Strahl, B.D. and C.D. Allis, The language of covalent histone modifications. Nature, 2000. **403**(6765): p. 41-5.
19. Ausio, J. and D.W. Abbott, The many tales of a tail: carboxyl-terminal tail heterogeneity specializes histone H2A variants for defined chromatin function. Biochemistry, 2002. **41**(19): p. 5945-9.
20. Redon, C., et al., Histone H2A variants H2AX and H2AZ. Curr Opin Genet Dev, 2002. **12**(2): p. 162-9.
21. Sullivan, S.A. and D. Landsman, Characterization of sequence variability in nucleosome core histone folds. Proteins, 2003. **52**(3): p. 454-65.
22. West, M.H. and W.M. Bonner, Histone 2A, a heteromorphous family of eight protein species. Biochemistry, 1980. **19**(14): p. 3238-45.
23. Pehrson, J.R. and V.A. Fried, MacroH2A, a core histone containing a large nonhistone region. Science, 1992. **257**(5075): p. 1398-400.
24. Costanzi, C. and J.R. Pehrson, Histone macroH2A1 is concentrated in the inactive X chromosome of female mammals. Nature, 1998. **393**(6685): p. 599-601.
25. Cohen, D.E. and J.T. Lee, X-chromosome inactivation and the search for chromosome-wide silencers. Curr Opin Genet Dev, 2002. **12**(2): p. 219-24.

26. Chadwick, B.P. and H.F. Willard, A novel chromatin protein, distantly related to histone H2A, is largely excluded from the inactive X chromosome. J Cell Biol, 2001. **152**(2): p. 375-84.

27. Iouzalen, N., J. Moreau, and M. Mechali, H2A.ZI, a new variant histone expressed during Xenopus early development exhibits several distinct features from the core histone H2A. Nucleic Acids Res, 1996. **24**(20): p. 3947-52.

28. Stargell, L.A., et al., Temporal and spatial association of histone H2A variant hv1 with transcriptionally competent chromatin during nuclear development in Tetrahymena thermophila. Genes Dev, 1993. **7**(12B): p. 2641-51.

29. Santisteban, M.S., T. Kalashnikova, and M.M. Smith, Histone H2A.Z regulats transcription and is partially redundant with nucleosome remodeling complexes. Cell, 2000. **103**(3): p. 411-22.

30. Meneghini, M.D., M. Wu, and H.D. Madhani, Conserved histone variant H2A.Z protects euchromatin from the ectopic spread of silent heterochromatin. Cell, 2003. **112**(5): p. 725-36.

31. Rangasamy, D., et al., Pericentric heterochromatin becomes enriched with H2A.Z during early mammalian development. Embo J, 2003. **22**(7): p. 1599-607.

32. Suto, R.K., et al., Crystal structure of a nucleosome core particle containing the variant histone H2A.Z. Nat Struct Biol, 2000. **7**(12): p. 1121-4.

33. Fan, J.Y., et al., The essential histone variant H2A.Z regulates the equilibrium between different chromatin conformational states. Nat Struct Biol, 2002. **9**(3): p. 172-6.

34. Park, Y.J., et al., A new fluorescence resonance energy transfer approach demonstrates that the histone variant H2AZ stabilizes the histone octamer within the nucleosome. J Biol Chem, 2004. **279**(23): p. 24274-82. Epub 2004 Mar 13.

35. Kraulis, P.J., MOLSCRIPT: a program to produce both detailed and schematic plots of protein structures. J. Applied Crystallography, 1991. **24**: p. 946-950.

CHAPTER TWO

THE N-TERMINAL TAILS OF THE H2A-H2B HISTONES AFFECT DIMER STRUCTURE AND STABILITY

This chapter was published in the journal *Biochemistry* in December 2002 (Vol. 41, No. 50, p. 14960-14968.) This chapter therefore differs in format from the remainder of the dissertation. I am the first author of this paper. I performed all of the experiments. I contributed to the writing of this paper but Lisa Gloss wrote the majority of the paper.

[1]**Abbreviations:** CD, circular dichroism; C_M, the urea concentration at which the apparent fraction of unfolded monomer constitutes 50% of the population; ΔN-H2A, N-terminal tail truncation of the H2A, removing residues 2 through 15; ΔN-H2B, N-terminal tail truncation of the H2B, removing residues 2 through 31; ΔG° (H_2O), the free energy of unfolding in the absence of denaturant; F_{app}, apparent fraction of unfolded monomer; FL, fluorescence; KPi, potassium phosphate, pH 7.2; *m* value, parameter describing the sensitivity of the unfolding transition to the [Urea]; MRE, mean residue ellipticity; std. dev., standard deviation; WT, wild-type, full-length H2A and/or H2B.

SUMMARY

The histone proteins of the core nucleosome are highly basic and form heterodimers in a "handshake motif." The N-terminal tails of the histones extend beyond the canonical histone fold of the hand-shake motif and are the sites of post-translational modifications, including lysine acetylations and serine phosphorylations, which influence chromatin structure and activity as well as alter the charge state of the tails. However, it is not well understood if these modifications are signals for recruitment of other cellular factors or if the removal of net positive charge from the N-terminal tail plays a role in the overall structure of chromatin. To elucidate the effects of the N-terminal tails on the structure and stability of histones, the highly charged N-terminal tails were truncated from the H2A and H2B histones. Three mutant dimers were studied: □N-H2A/WT-H2B; WT-H2A/□N-H2B and □N-H2A/□N-H2B. The CD spectra, stabilities to urea-denaturation and the salt-dependent stabilization of the three truncated dimers were compared with that of the wild-type dimer. The data support four conclusions regarding the effects of the N-terminal tails of H2A and H2B: 1) Removal of the N-terminal tails of H2A and H2B enhance the helical structure of the mutant heterodimers. 2) Relative to the full-length, WT heterodimer, the □N-H2A/WT H2B dimer is destabilized while the WT H2A/□N-H2B and □N-H2A/□N-H2B dimers are slightly stabilized. 3) The truncated dimers exhibit decreased *m* values, relative to the WT dimer, supporting the hypothesis that the N-terminal tails in the isolated dimer adopt a collapsed structure. 4) Electrostatic repulsion in the N-terminal tails decreases the stability of the H2A-H2B dimer

INTRODUCTION

The basic packaging unit of DNA in eukaryotic chromatin is the core nucleosome. This structure contains eight histone proteins: two dimers of H2A-H2B that serve as molecular caps for the central $(H3\text{-}H4)_2$ tetramer. Approximately 160 basepairs of DNA are wrapped around the surface of this protein octamer. The nucleosome is no longer considered a simple, static packaging system; rather, the nucleosome is a dynamic regulator of the DNA chemistries in the nucleus, including transcription, replication and repair (*1, 2*). Several post-translational modifications of the core histone oligomers are important modulators of the accessibility of DNA in the nucleosome (*3, 4*). The effects of these modifications are being elucidated as to their "downstream consequences" such as activating transcription or enhancing binding of factors to DNA (for example, (*5*)). However much less is known about the molecular details of the structural and thermodynamic effects of the post-translational modifications of the histone proteins. Biophysical characterization of the stability of the core histones and any alterations caused by post-translational modifications will begin to address such molecular details. In this study, we focus on the N-terminal tails of the H2A-H2B dimer.

The interface of the H2A-H2B dimer is comprised of the "histone-fold motif" common to all of the core histones (*6, 7*) and many other oligomers involved in DNA-protein complexes, such as some of the TAF's (TATA-Binding Protein Associated Factors) (*8, 9*) (Figure 1). The dimerization of two monomers involves some intertwining of the six helices of the histone fold with association in a head-to-tail manner, termed the "hand-shake motif" (*10*).

The eukaryotic core histones contain regions of polypeptide N-terminal to the central, globular helical histone fold. The N-terminal tails of the histones are the sites of the regulatory post-translational modifications, and are the most basic regions of the histones. For example, for the *Xenopus laevis* proteins studied here, the histone fold

motifs contain an excess of 7 and 5 mol% basic residues for H2A and H2B, respectively. The tails contain no acidic residues, and are 38 and 45 mol% basic residues, for H2A and H2B, respectively. The modifications of the N-terminal tails include acetylation of lysine side-chains and methylation of lysine and arginine side-chains; acetylation converts a positively charged amine to an uncharged amide while methylation maintains the positive charge of the modified amino acid. Serine residues in the tails are also sites for phosphorylation, a modification that, like acetylation, alters the charge state of the N-terminal tails. Given that acetylation and phosphorylation decrease the net positive charge of the histones, it is important to determine if electrostatic interactions in the N-terminal tails of H2A and H2B affect the overall stability and structure of the dimer.

To address this question, we measured the urea-induced equilibrium unfolding of three heterodimeric variants of H2A-H2B with N-terminal tail truncations: ΔN-H2A/WT H2B[1]; WT H2A/ΔN-H2B; and ΔN-H2A/ΔN-H2B. The stabilities of these three dimers are compared to the WT H2A-H2B dimer in low salt conditions and as a function of three salts, KCl, KI and KPi. Similar studies have recently been published on the thermal denaturation of trypsin-treated H2A-H2B dimers (*11*). The work presented here has two major differences from this recent study: 1) By the use of site-directed mutagenesis on the histone genes to generate recombinant truncated H2A and H2B variants, we can differentiate between the effects of the H2A and H2B N-terminal tails. 2) By using different salts, we can determine the mechanism(s) by which salt stabilizes the H2A-H2B dimer.

Materials & Methods

Materials

Ultra-pure urea was purchased from ICN Biomedicals (Costa Mesa, CA). CM-Sepharose resin was purchased from Sigma (St. Louis, MO); Sephacryl S-100 and

Heparin resins were purchased from Amersham Pharmacia (Uppsala, Sweden). All other chemicals were of reagent or molecular biology grade.

Methods

Site-directed mutagenesis was performed on the T_7pET vectors containing the *Xenopus laevis* genes that have been described elsewhere (*12*). Truncations of the codons for the N-terminal sequences of the H2A and H2B genes were performed using extra-long PCR (*13*). Codons for residues 2 to 15 and residues 2 to 31 of H2A and H2B, respectively, were deleted from the appropriate genes. The desired truncations and lack of other, undesired mutations in the H2A and H2B genes were confirmed by sequencing the genes in the T_7pET expression plasmids.

Recombinant WT and truncated H2A and H2B histones were over-expressed in *E. coli*, purified and reconstituted into folded dimers as described in the preceding paper (33). The homogeneity of the dimeric state of the reconstituted H2A-H2B dimers were confirmed by HPLC size-exclusion chromatography coupled to a static light scattering detector (Dawn EOS from Wyatt Technologies, Santa Barbara, CA).

Data collection and analyses All of the equilibrium unfolding experiments were performed at 25 °C in a buffer of 20 mM potassium phosphate, pH 7.2 with 0.1 mM EDTA. The details of the equipment and data collection methods are reported in the preceeding manuscript (33). The equilibrium urea-induced unfolding transitions were fitted to a dimeric two-state model, using the global data analysis program, Savuka 5.1; the reported errors represent one standard deviation as determined from rigorous analyses of the error surfaces (33).

The secondary structural content of the proteins were estimated from the far-UV CD spectra using the CDPro package (*14*). Results were compared from two algorithms: Selcon3 (*15*, *16*) and Contin/ll (*17*, *18*).

Results

Design of the truncated H2A and H2B variants. The regions to be truncated in the variants employed in this report were determined from inspection of the X-ray crystal structure of the nucleosome (*7*). N-terminal residues in an extended conformation or unresolved in the X-ray structure were truncated in the variants. The putative N-caps of the N-terminal helices (Thr 16 of H2A and Ser 33 of H2B), as well as the potentially stabilizing carboxylate of H2B's Glu-32 (interaction with the N-terminal helix dipole) were maintained in the truncated variants. After the initiating methionine, the sequences of ΔN-H2A and ΔN-H2B genes begin with the codons for residues Thr-16 and Glu-32, respectively. The ΔN-H2A construct includes an N-terminal turn of helix that proceeds the canonical histone fold motif. The ΔN-H2A and ΔN-H2B variants used in this study have N-terminal truncations that are larger than the common cleavages seen in histones trypsinized in the context of the core nucleosome, at residues 12 and 23 of H2A and H2B, respectively (*19*).

Spectral properties of the H2A-H2B variants. The N-terminal truncations used in this study do not remove any of the 3 and 5 Tyr residues of H2A and H2B, respectively. Therefore, not surprisingly, there is little difference in the intrinsic Tyr fluorescence between the WT and truncated H2A-H2B variants (data not shown).

However, removal of the N-terminal tails does affect the far-UV CD spectra of the H2A-H2B variants, which is indicative of effects on the secondary structural content of the variant dimers. In Figure 2, the CD spectra are presented in two ways: A) the ellipticity values at the same dimer concentrations for all four proteins, reflecting the amount of secondary structure present in each dimer, irrespective of number of residues; and B) the ellipticity values are normalized on a per residue basis (mean residue ellipticity), reflecting the fewer residues present in the ΔN-H2A and ΔN-H2B containing variants. The percentages of α-helix were calculated using the methods of Selcon3 and Continell to analyze the entire spectra. The two methods gave similar results (Table 1). Similar results were also obtained using equations that employ only

the mean residue ellipticity at 220 and 222 nm (data not shown), and have been previously applied to the histone octamer (*20*). The % helix calculated for the WT dimer, ~40%, is reasonably close to that observed in the X-ray structure of the nucleosome, 48%. The X-ray structure includes the H3-H4 tetramer and DNA, which may stabilize additional helical structure compared to the dimer in isolation.

The spectra in Figure 2A clearly demonstrate that the three N-terminal truncations of the H2A-H2B dimer increase the amount of helix on a per dimer basis. This finding is not surprising, as the X-ray crystal structure of the nucleosome (*7*) suggested that the conformations of the tails, to the extent that the residues can be observed, are largely unstructured chains extending away from the helical regions of the dimer (Figure 1). Normalizing the CD spectra to mean residue ellipticity (Figure 2B) corrects for the different number of residues in the WT and truncated dimers. The % helix increases more for the truncated H2A-H2B variants than expected for the removal of the unstructured regions of the N-terminal tails (Table 1). For example, if the 44 N-terminal residues deleted in N-H2A/N-H2B are unstructured, then the % helix of this variant should be ~100 residues of 207 residues, or 48%, relative to the 40% observed for the WT. The far-UV CD spectrum predicts 58 to 63% helix for the tail-less variant. Smaller differences between expected and those predicted from the CD spectra are observed for the single-tail variants.

Stability of the H2A-H2B variants in 200 mM KCl. The equilibrium stability of the H2A-H2B variants were determined under conditions of physiological ionic strength (μ ~ 0.2 M). The urea-induced equilibrium unfolding responses of the H2A-H2B heterodimer variants were monitored by far-UV CD and intrinsic Tyr fluorescence. Like the WT H2A-H2B heterodimer (33), the unfolding of the truncated variants was highly reversible with no hysteresis. For the three truncated dimer variants, reversibility was assessed by comparing the CD and FL spectra of matched, individual samples at several urea concentrations over a range which spanned the unfolding

transition. The matched samples were prepared individually from either an unfolded or a folded protein stock. The spectral intensities of samples derived from unfolding and refolding the two protein stocks agreed to within 90 to 95%. Therefore, removal of the N-terminal tails did not affect the reversibility of the urea-induced equilibrium unfolding.

For all three truncated H2A-H2B dimers, unfolding transitions were collected as a function of dimer concentration: 9 data sets for N-H2A/WT H2B from 1 to 30 μM dimer; 9 data sets for WT H2A/N-H2B from 1 to 20 μM dimer; and 6 data sets for N-H2A/N-H2B from 1 to 10 μM dimer. Most of the data sets are shown as F_{app} curves in Figure 3 (some duplicate data sets were omitted for clarity). Indicative of two-state equilibrium processes, with no populated intermediates: 1) the far-UV CD and FL transitions for a given dimer concentration, were superimposable; and 2) the data as a function of [dimer] were well-described by global fitting to a two-state dimeric model (Figure 3).

In the data analyses, the $\Delta G°(H_2O)$ and *m* values were treated as global parameters describing all of the data sets for a given heterodimer; the pre- and post-transition baselines were treated as local fitting parameters. The resulting fits of the data are illustrated by the solid lines in Figure 3. To improve the certainty of the determination of the *m* value, given the short folded baselines at low dimer concentrations, a second global fit was performed on a larger number of data sets for each H2A-H2B variant that included: the data described above at 200 mM KCl as a function of [dimer], as well as data sets at 5 μM dimer as a function of [KPi] and [KCl] (see below). The *m* value for each dimer was treated as a global parameter for all data sets (29, 28 and 23 titrations for N-H2A/WT H2B, WT H2A/N-H2B and N-H2A/N-H2B, respectively). $\Delta G°(H_2O)$ values were treated as semi-global parameters, linked between data sets collected under the same salt and buffer conditions. The fitted values from this larger global fit for $\Delta G°(H_2O)$ at 200 mM KCl

and *m* values are given in Table 2 with the error estimated at one standard deviation of the variable on the error surface of the global fit. The values in Table 2 are in good agreement with the average value of local fits of the equilibrium data, and less extensive global fits of subsets of data (for example, only data as a function of [dimer] or [salt]). For all three truncated dimers, the fitted *m* values are smaller than that determined for the WT heterodimer.

The removal of the H2A N-terminal tail alone has a small but significant destabilizing effect on the heterodimer, decreasing the free energy of unfolding by 1.1 to 0.7 kcal mol^{-1} relative to the full-length heterodimer, as determined from local and global fits. Truncation of the H2B tail, either alone or with the H2A tail in the double mutant, has no significant effect on the stability, as assessed by the value of $\Delta G°$ (H_2O). The stabilities of the H2A-H2B variants can also be compared by their C_M values, the midpoint of the transition, *i.e.* the concentration of urea at which unfolded monomers constitute 50% of the population. By this measure, the removal of the H2B tail is stabilizing, and this stabilization is not altered by the presence or absence of the H2A tail (Figure 3D, Table 2). The lack of significant change in stability for the double-truncated dimer, relative to the WT H2A/ΔN-H2B dimer, demonstrates a lack of additivity in the effects of tail removal. Non-additivity of mutational effects is generally interpreted as evidence of an interaction between the sites that were mutated (*21*). This interaction of the N-terminal tails need not be via physical contact, but a synergistic, global effect on the electrostatics of the dimer.

Effect of salts on the stability of the H2A-H2B variants. The effects of multiple salts on the stability of WT H2A-H2B suggested a role for electrostatic repulsion in destabilizing the dimer (33). This electrostatic repulsion could arise from the high charge density of the N-terminal tails (~40 mol% basic residues) and/or from interaction of the basic residues in the histone fold motifs (~6 mol% excess basic residues). To address these two possibilities, the stabilities of the truncated H2A-H2B

dimers were determined as a function of KPi, KCl and KI. These salts span the Hofmeister series in their respective abilities to stabilize proteins. The addition of salts, even to molar concentrations, did not alter the two-state, highly reversible unfolding of the variant heterodimers, permitting the determination of accurate thermodynamic parameters as a function of salt.

Local fits of the unfolding transitions as a function of KCl and KPi showed that the *m* values were independent of the [salt], as observed for the WT heterodimer (33). Therefore, the data sets were globally fitted, linking the *m* value across all titrations collected for a given heterodimer as described above; thus, the *m* value was treated as a salt-independent parameter. A linear increase in $\Delta G°$ (H_2O) with increasing concentrations of KPi and KCl was observed for all three H2A-H2B variants, as shown in Figure 4. The slopes of these lines, indicative of the efficacy of the salt in stabilizing the heterodimers, $\delta(\Delta G°)/\Delta C_\mu$, are reported in Table 2.

The effect of increasing concentrations of KI on the stability of the truncated dimer variants (Figure 4) is clearly different than that observed for the WT dimer (33). For WT H2A-H2B, increasing concentrations of KI caused a linear increase in the $\Delta G°$ (H_2O), with a slope of 1.0 kcal $mol^{-1}M^{-1}$, with a salt-independent *m* value. For the truncated dimers, local fits of the unfolding transitions showed that the *m* values varied as a function of [KI]. For ΔN-H2A with truncated or WT H2B, the *m* values increased ~10% from 0.05 to 0.2 M KI; for WT H2A/ΔN-H2B, the *m* values decreased by ~10% over the same range of [KI]. Therefore, in the global fitting of the data, the *m* values were not treated as salt-independent parameters; only $\Delta G°$ (H_2O) was linked between the two or three unfolding transitions collected at the same [KI]. KI has no significant stabilizing effect on WT H2A/ΔN-H2B (Figure 4B), and may be slightly destabilizing at higher concentrations. For ΔN-H2A/WT H2B and ΔN-H2A/ΔN-H2B (Figure 4A and C), KI is stabilizing up to ~0.25 M; the slight increase in the *m* value of these dimers is consistent with a small degree of enhanced folding of the native state induced by KI.

At higher KI concentrations, there is no effect or a slight destabilization. The $\Delta G°$ (H_2O) values for the three truncated variants do not increase linearly as a function of the square root of ionic strength (data not shown).

For the WT dimer, the $\Delta G°$ (H_2O) value for KI extrapolated to the absence of KI is the same, within error, for that observed in similar extrapolatations for other salts (33). For the variant dimers, the extratrapolated $\Delta G°$ (H_2O) values to the absence of salt are similar for the KPi and KCl data, but significantly lower for the KI data, 1 to 2 kcal mol^{-1}. These data demonstrate that KI is destabilizing to the H2A-H2B dimer in the absence of the N-terminal tails.

Discussion

Removal of the N-terminal tails enhances the helical content of the H2A-H2B dimer. Comparison of the far-UV CD spectra of full-length and the ΔN dimers shows that the removal of the N-terminal tails increases the ellipticity and the overall percentage of residues in helical conformation in the heterodimers (Figure 2A). Various prediction methods demonstrate that the increase in % helical content of the truncated variants is greater than expected for simply just removing unstructured, non-helical tails (Figure 2B, Table 1). This increased helicity demonstrates that removal of the tails actually promotes the formation of helical structure in the H2A-H2B dimer, and suggests that the presence of the N-terminal tails destabilizes structure in helical regions of histone proteins, at least in the absence of DNA. The effects on helicity are similar for the H2A tail and the H2B tail, which contains nearly twice the number of residues.

Effects of the N-terminal tails on the stability of the H2A-H2B dimer. Like the heterodimer of full-length H2A-H2B, the ΔN heterodimeric variants unfold under the influence of urea by a highly reversible, two-state process. Similar two-state unfolding was also observed in the thermal denaturation of the H2A-H2B histones (*11*, *22*). The

lack of equilibrium intermediates demonstrates that the monomers are incapable of folding in isolation under conditions that destabilize the native heterodimer.

The values of $\Delta G°$ (H_2O) (Table 2) and C_M (Figure 3D) demonstrate that the ΔN-H2A/WT H2B dimer is destabilized relative to the full-length dimer. Therefore, the H2A N-terminal must stabilize the full-length protein. In contrast, the ΔN-H2A/ΔN-H2B and WT H2A/ΔN-H2B heterodimers have stabilities that are the same as or slightly greater than that of full-length H2A-H2B (Table 2; Figure 3D). The effects of the tail truncations in the double mutant, relative to the two single mutants, are not additive. Any destabilization resulting from truncation of the H2A N-terminal tail is mitigated in the double truncated variant; this may be the result of the enhanced helical structure in the ΔN-H2A/ΔN-H2B variant, 20 to 30 residues relative to the full-length dimer.

The *m* value (Equation 1) describes the sensitivity of the unfolding transition to the denaturant concentration. In proteins that unfold by a two-state equilibrium reaction, this parameter correlates with the change in solvent-accessible surface area between the folded and unfolded species (*23*). The *m* value for the full-length heterodimer is larger than expected if the N-terminal tails are in an extended conformation in the native state (33), and suggested that the N-terminal tails in the isolated, folded heterodimer adopted a collapsed, solvent-excluding structure. This interpretation predicts that removal of the N-terminal tails should decrease the *m* values observed for the ΔN truncated heterodimers. The global fits of the equilibrium unfolding data show that the truncation of the N-terminal tails decreases the observed *m* values beyond the error of the measurement. The magnitude of the decrease in the *m* value for the ΔN dimers may be attenuated by the enhanced helical structure that exist in these H2A-H2B variants (Figure 2B, Table 1).

An alternative explanation for the decreased *m* value of the ΔN H2A-H2B variants is that their unfolding transition is not a cooperative, completely two-state

transition, *i.e.* there is an intermediate populated at equilibrium, but at such low levels that it can not be directly detected by the methods employed. Such an equilibrium intermediate has been detected in this way for RNase H (*24*). For removal of the N-terminal tails to alter the *m* value, the tails must influence the stability of the H2A-H2B dimer, and destabilize a putative equilibrium intermediate, *i.e.* the intermediate is more populated in the absence of the tails. Unstructured, extended N-terminal tails could only influence the stability of the rest of the protein through long distance interactions, such as electrostatic effects. Therefore, this alternative interpretation of the *m* values still suggests that electrostatic repulsion in the N-terminal tails affects the stability of the H2A-H2B dimer.

The ΔC_P is the heat capacity difference between the native and unfolded states determined from thermal denaturation experiments, such as differential scanning calorimetry. This parameter also correlates with change in solvent-accessible surface area between the native and unfolded species, like the *m* value from denaturant-induced unfolding experiments (*23*). When compared at similar solvent conditions, (pH 6.0 to 6.5 and 25 to 50 mM NaCl), the full-length H2A-H2B dimer exhibited a higher ΔC_p value, 1.3 to 1.4 kcal $K^{-1}mol^{-1}$, than that of the trypsinized, tail-less dimer, 1.1 kcal $K^{-1}mol^{-1}$ (*11*, *22*). This trend is consistent with the findings of this report on the decreased *m* values of the ΔN H2A-H2B variants.

The salt-induced stabilization of the ΔN and WT H2A-H2B variants were determined (Figure 4, Table 2). A discussion of the different stabilizing mechanisms of salts is presented in the preceding paper (33). For full-length H2A-H2B, the predominant stabilizing effect of salts was via a preferential hydration/Hofmeister effect mechanism (for review, (*25-28*)). However, electrostatic repulsion plays a role in destabilizing the WT heterodimer. The following discussion supports this interpretation and suggests that the electrostatic repulsion arises from residues in the N-terminal tails.

KPi is a potent stabilizer of the full-length H2A-H2B dimer, doubling the free energy of unfolding across a concentration range of 20 to 700 mM (33). The efficacy of KPi to stabilize the heterodimers, $\partial(\Delta G°)/\partial C_\mu$ values, for the truncated variants are 1.2 to 1.8 kcal $mol^{-1}M^{-1}$ greater than that exhibited by the full-length heterodimer (Table 2). If the KPi stabilization of the H2A-H2B dimers is solely the result of a preferential hydration mechanism (*27*, *28*), removal of the N-terminal tails should have no effect on or decrease the efficacy of KPi to stabilize the truncated variants. The magnitude of stabilization by preferential hydration can be considered in terms of a thermodynamic cycle of free energies: the free energy of transfer for the native and unfolded states from water to the solution containing the excluded cosolute, and free energies of unfolding in water and in the presence of the excluded cosolute (*27*, *29*). Stabilization arises from the increase in the free energy of the denatured state, relative to the native state, in the presence of the cosolute because the surfaces exposed upon denaturation enhance the preferential exclusion of the cosolute. If the solvent-accessible surface area of a region of the protein does not change upon unfolding, then that region of the protein will not contribute to stabilization by preferential hydration. The expected effects on the $\partial(\Delta G°)/\partial C_\mu$ values are considered below for two scenarios regarding the N-terminal tails IF preferential hydration is the only mechanism of action of KPi.

1) The N-terminal tails are in an unfolded conformation in the native state: There will be no significant difference in hydrophobic surface area exposed to water and excluded cosolute upon protein unfolding in the presence or absence of the N-terminal tails. Therefore, removal of the tails should have no effect on stabilization by a Hofmeister ion; the $\partial(\Delta G°)/\partial C_\mu$ values should be the same for the WT and truncated dimers.

2) The N-terminal tails are in a collapsed, solvent-excluding structure in the native state and undergo an unfolding reaction: (Data in this report suggests this is the case; see above discussion of the *m* value.) Additional surface is exposed to solvent

upon unfolding of the WT dimer, compared to the truncated dimers. Thus, removal of the tails should decrease the amount of surface that is affected by the presence of the Hofmeister ion. Therefore, the efficacy of the ion to stabilize the protein to denaturation, $\partial(\Delta G°)/\partial C_\mu$, should be decreased.

The observed effect of removal of the N-terminal tails, an <u>enhanced</u> efficacy of KPi stabilization, is not consistent with stabilization solely by preferential hydration or the Hofmeister effect. The results in Table 2 can be explained by stabilization of the full-length H2A-H2B dimer by both preferential hydration and screening of electrostatic repulsion that arises from the basic residues in the N-terminal tails.

Favorable interactions between protein side-chains and a preferentially-excluded cosolute such as KPi will attenuate the stabilization by a preferential hydration mechanism (*29, 30*). If the regions that interact favorably with the cosolute are removed, then the efficacy of the cosolute to stabilize the protein by exclusion from the surface of the protein and promoting preferential hydration should be enhanced. The greater values of $\partial(\Delta G°)/\partial C_\mu$ for the truncated H2A-H2B dimers, relative to WT, demonstrate that KPi interacts with these tails. Two related types of electrostatic interactions could be at work: ion binding or screening of electrostatic repulsion from the high positive charge density of the side-chains. If phosphate anions bind the the tails, the affinity must be very low. The apparent dissociation constant must exceed 500 mM, as the plots of $\Delta G°$ (H_2O) (Figure 4) and C_M (data not shown) as a function of [KPi] show no curvature that would indicate an approach to saturation of the binding site(s), as seen for phosphate binding stabilizing the Ribonuclease P protein (*31*).

An estimate of the stabilization from screening electrostatic repulsion was made by extrapolating the $\Delta G°(H_2O)$ values to 0 M, to estimate the stability in the absence of preferential hydration. Relative to WT H2A-H2B, the stabilities of ΔN-H2A/WT H2B, WT H2A/ΔN-H2B and ΔN-H2A/ΔN-H2B are increased by 0.8, 2.0 and 1.3 kcal mol^{-1} (with errors of 0.06 to 0.1 kcal mol^{-1}), respectively. Similar, but slightly smaller

estimates, were obtained from the KCl data sets. These differences in free energy suggest that electrostatic repulsion decreases the stability of the dimers by ~7 to 15% at a standard state of 1 M dimer. The value of $\partial(\Delta G°)/\partial C_{\mu}$ is independent of dimer concentration. At more physiological dimer concentrations, such as those employed in these experiments, the contribution of electrostatic interactions is higher. For example, at 10 μM dimer, the contribution of electrostatic repulsion decreases the stability of the dimers by 20 to 40%. As shown previously by thermal denaturation (*11*), the tails are not the major contributor to the stability of the H2A-H2B dimer. However, electrostatic repulsion from the N-terminal tails plays a significant role in the stability of the dimer.

A similar trend of enhanced efficacy is seen for the KCl stabilization of the ΔN H2A-H2B dimers relative to the full-length dimer. However, the effect is smaller, with $\partial(\Delta G°)/\partial C_{\mu}$ values only ~0.3 kcal $mol^{-1}M^{-1}$ greater for the truncated dimers relative to the full-length dimer (Table 2). KCl is lower on the Hofmeister scale than KPi. Accordingly, KCl should be less preferentially excluded from the surface of proteins than is KPi. Therefore, the attenuation of stabilization by a preferential hydration mechanism should be less for KCl than for KPi.

KI is generally considered to be a mild protein denaturant. However, as a salt, KI can stabilize a protein by screening electrostatic repulsion. This favorable effect is observed in the mild KI stabilization of full-length H2A-H2B, resulting in a linear increase in $\Delta G°$ (H_2O) of 1 kcal $mol^{-1}M^{-1}$ (33). The data for the H2A-H2B variants suggests that the stabilization of WT by KI is the result of screening electrostatic repulsion primarily within the N-terminal tails. Therefore, when the tails are truncated, the stabilizing effects of increasing [KI] are largely mitigated, and destabilization is apparent when $\Delta G°$ (H_2O) values are extrapolated to the absence of salt. However, there appears to be some stabilization by KI from interactions with the histone fold motif, indicated by the effects on the ΔN-H2A containing dimers (Figures

4A and C). However, this stabilization is largely complete by ~0.2 M KI, whereas KI continues to stabilize full-length H2A-H2B up to 0.8 M KI.

Comparison to previous reports on the stability of the H2A-H2B dimer. Thermal denaturation, using differential scanning calorimetry and far-UV CD, of WT and trypsinized H2A-H2B dimers (removing the N termini of both histones and the C-terminal tail of H2A) have been reported previously (*11, 22*). Thermal denaturation, in general, may have an advantage over chemical denaturants in studies that address the role of cosolutes on the stability of proteins. Over the concentration range employed in an equilibrium urea denaturation experiment, the concentration of cosolutes is drastically changed. Therefore, with a background of 0 to 7 M urea, the effects of submolar salt concentrations may not be as dramatic as in a thermal denaturation experiment where the concentrations of cosolutes are not varied across the unfolding transition. However, in the case of the H2A-H2B histones, thermal denaturation has a strong disadvantage in that the unfolding is less reversible and is hampered by aggregation at higher temperatures (*11, 22*); this aggregation is exacerbated by increased ionic strength and/or removal of the histone tails--precisely the alterations to the system that are of interest in this report. The high reversibility of the urea denaturation of the H2A-H2B dimers was not affected by increased ionic strength or removal of the N-terminal tails. This advantage of urea denaturation permits the determination of more accurate and precise thermodynamic parameters to allow the elucidation of the subtle effects of salts and N-terminal tail deletions.

Thermal denaturation studies comparing full-length and trypsinized H2A-H2B dimers showed that the truncated dimer is slightly more stable below 20 mM NaCl, as evidenced by a slightly higher T_M, the midpoint of the unfolding transition (*11*). At higher NaCl concentrations, the full-length dimer was slightly more stable. The authors suggested that the tails may acquire a partially ordered conformation at higher ionic strengths that contributed minor stabilization to the full-length dimer. The

results of this paper show that the H2A tail is stabilizing, but that the H2B tail is slightly destabilizing. Urea denaturation results support the conclusion from the thermal denaturation data that the histone tails have a relatively small effect on the stability of the heterodimer, and that the structured domains of the histones play the central role in the thermodynamics of histone stability. However, the effects of electrostatic repulsion in the N-terminal tails, as indicated by the results of this paper, may have an important impact on nucleosome dynamics (see below).

The mechanism of stabilization of the H2A-H2B dimer by NaCl was not addressed in the thermal denaturation of the full-length (*22*) or trypsinized (*11*) dimers. The T_M values for the full-length and trypsinized dimers do not increase linearly with [NaCl] (Figure 2b of (*11*)). If the T_M data are plotted as a function of the square root of [NaCl] (data not shown), to examine electrostatic components of the stabilization, the full-length H2A-H2B displays a biphasic increase in T_M with increasing [NaCl]. From 0.01 to 0.05 M NaCl, the T_M is very sensitive to [NaCl]. From 0.1 to 1.0 M NaCl, the linear slope of T_M with increasing [NaCl] is much shallower. The increase in the T_M values of the trypsinized H2A-H2B with increasing [NaCl] is a single linear response, with a slope similar to the shallower transition observed for the full-length dimer data. The thermal denaturation data suggest that: 1) electrostatic repulsion, screened by increasing concentrations of NaCl, destabilizes the full-length dimer; 2) the repulsion arises from two regions of the protein; and 3) the tail regions removed by the action of trypsin are responsible for the most sensitive region observed in the full-length dimer. This interpretation of the thermal denaturation data is consistent with the findings of this report based on urea denaturation data.

Conclusions and implications for function of the H2A-H2B dimer in the nucleosome. The data in this report support four conclusions regarding the N-terminal tails of the H2A and H2B monomers of the histone heterodimer. 1) The removal of the N-terminal tails of the H2A and H2B dimer enhances the helical content of the

heterodimer (Figure 2; Table 1). 2) Removal of the H2A N-terminal tail destabilizes the ΔN-H2A/WT H2B dimer; removal of the H2B tail, alone or in the absence of the H2A tail, slightly stabilizes the heterodimers (Figure 3, Table 2). The stability effects of the single tail truncations are not additive in the effects on the ΔN-H2A/ΔN-H2B variant. 3) The decreased *m* values of the truncated heterodimers (Table 2) are consistent with the N-terminal tails adopting collapsed, solvent-excluding structures, unlike the extended conformations seen in the X-ray structures of the nucleosome (7). 4) There are two mechanisms operating in the H2A-H2B stabilization by potassium salts (Figure 4, Table 2). The predominant mechanism is through the preferential hydration and the Hofmeister effect. The salts also stabilize by screening electrostatic repulsion, which arises largely from the N-terminal tails of the dimer.

These data and conclusions help elucidate biophysical features that may play an important role in the dynamics of the nucleosome. To understand the equilibria and kinetics of nucleosome folding and unfolding, the stability and structure of the isolated proteins must be taken into account (33). During transcription (and perhaps other DNA processes in the cell such as replication and repair), there is an important equilibrium between the intact histone octamer and a partially unfolded nucleosome in which the H2A-H2B dimers are more weakly bound, and perhaps partially or completely dissociated from the nucleosome. Stabilization of the isolated H2A-H2B dimer will favor a more unfolded, dissociated state of the nucleosome. A potential mechanism to stabilize the histones is to reduce electrostatic repulsion on these highly charged oligomers. Acetylation of Lys residues and phosphorylation of adjacent Ser residues in the N-terminal tails should serve to reduce electrostatic repulsion, stabilize the H2A-H2B dimer and alter the equilibrium between an intact and partially unfolded nucleosome. The data in this and the preceding paper (33) also suggest that the N-terminal tails of H2A-H2B adopt a collapsed structure in the isolated dimer. This structure should be similarly stabilized by post-translational modifications to the tails

that reduce electrostatic repulsion. Hyperacetylation has been reported to enhance helical structure in the N-terminal tail of H4 (*20*). To fully understand the equilibria involved in the folding and unfolding of the nucleosome, the presence and alteration of folded conformations in the N-terminal tails of the isolated histone oligomers should be determined and considered.

Acknowledgments

We dedicate this paper to the memory of our late colleague, Jeremy N.S. Evans, in appreciation for his friendship and scientific insights and guidance. Douglas D. Banks assistedin determining the molecular weight of the dimers by HPLC size-exclusion chromatography coupled to light-scattering. Helpful discussions and critical review of the manuscript by Traci Topping and Dr. Michael J. Smerdon are appreciated. The pET over-expression vectors for the wild-type histone genes were kindly provided by Drs. Karolin Luger (currently at Colorado State University) and Timothy Richmond of the Instititute for Molecular Biology and Biophysics at the ETHZ, Zurich, Switzerland.

Table 1. Analysis of the CD spectra of WT and N-terminal truncated H2A-H2B variants.

Parameter	WT H2A WT H2B	ΔN-H2A WT H2B	WT H2A ΔN-H2B	ΔN-H2A ΔN-H2B
MRE x 10^{-3}, 220 nm (deg cm^2 $dmol^{-1}$)[a]	-12.6	-14.8	-15.4	-20.2
# residues in dimer[b]	251	237	221	207
% α-helix[c]	40/39	48/48	50/49	58/63
% α-helix expected[d]	--	42	45	48
# residues helical by CD[e]	100	114	110	120/130

[a]CD signal, corrected to mean residue ellipticity, for the H2A-H2B variants are shown in Figure 2B.
[b]The number of residues assumes the removal of the N-terminal Met, as seen for the WT histones (*12*).
[c]The % α-helix for each H2A-H2B variant was calculated from the spectra using two methods Selcon3 and Contin/ll; the results are given as the first and second values, respectively.
[d]Amount of helix expected, relative to the WT H2A-H2B dimer with 40% helix, if the N-terminal deleted regions contained no helical structure and their removal did not induce formation of helical structure.
[e]% helix determined from deconvolution of the CD spectra multiplied by number of residues in the dimer.

Table 2. Parameters describing the urea induced equilibrium transitions of the H2A-H2B variants.[a]

Parameter	WT H2A WT H2B[b]	ΔN-H2A WT H2B	WT H2A ΔN-H2B	ΔN-H2A ΔN-H2B
$\Delta G°(H_2O)$[c] (kcal mol^{-1})	11.8 (0.3)	11.1 (0.1)	12.2 (0.1)	11.8 (0.1)
C_M (M) [c]	1.4 (0.1)	1.2 (0.1)	1.6 (0.1)	1.6 (0.1)
m value[d] (kcal $mol^{-1}M^{-1}$)	2.9 (0.1)	2.7 (0.1)	2.8 (0.1)	2.6 (0.1)
$\partial(\Delta G°)/\partial C_\mu$[e] (kcal $mol^{-1}M^{-1}$)				
KI	1.0 (0.1)	N/A	N/A	N/A
KCl	5.9 (0.3)	6.2 (0.2)	6.1 (0.3)	6.3 (0.3)
KPi	9.7 (0.3)	11.0 (0.5)	10.9 (0.3)	11.5 (0.2)

[a]Conditions: 20 mM potassium phosphate buffer, 0.1 mM EDTA, pH 7.2, 25 °C. The values in parenthesis represent the error of one standard deviation from rigorous error analysis of global fits of the data. For $\partial(\Delta G°)/\partial C_\mu$, the standard deviation is for linear fits of the data weighted by the errors determined from the global fits that determined the $\Delta G°(H_2O)$ and *m* values.
[b]Data from Gloss & Placek, (33).
[c]Free energy of unfolding for transitions at relatively low ionic strength, 200 mM KCl, globally fit as a function of dimer concentration, at a standard state of 1 M dimer. Data are shown in Figure 3. The C_M, urea concentration where the unfolded monomers constitute 50% of the population, is reported for transitions at 1 μM dimer (Figure 3D).
[d]Determined from global fits of transitions as a function of protein concentration (Figure 3) and transitions as a function of [KPi] and [KCl]; globally fit, salt-independent values.
[e]Slope of linear fit of $\Delta G°(H_2O)$ *vs* ionic strength. Data are shown in Figure 4. For KI, a linear fit is not applicable to describe the data.

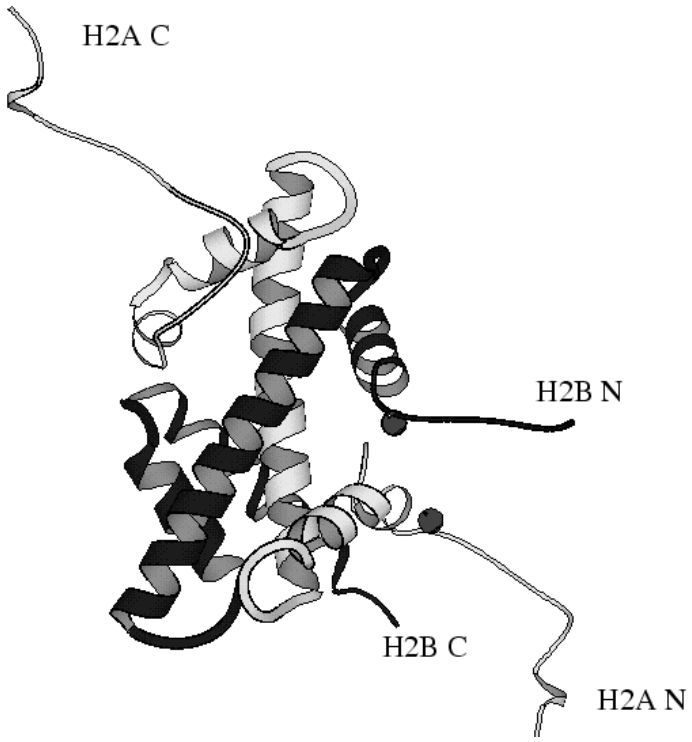

Figure 1. Ribbon diagram of the H2A-H2B dimer, derived from the X-ray crystal structure of the core nucleosome (*7*). The H2A monomer is shown as the lighter colored chain. The □-helices of the histone-fold motif are represented as wider ribbons. The H2A ribbon includes residues 4 to 118 (of 129 residues), and that of H2B, residues 24 to 122 (of 122 residues). Residue 16 of H2A and residue 32 of H2B are the residues after the N-terminal methionine residue in the □N-H2A and □N-H2B constructs, respectively; the □-carbons of these residues are denoted by a sphere. The figure was rendered using Molscript v2.1 (*32*).

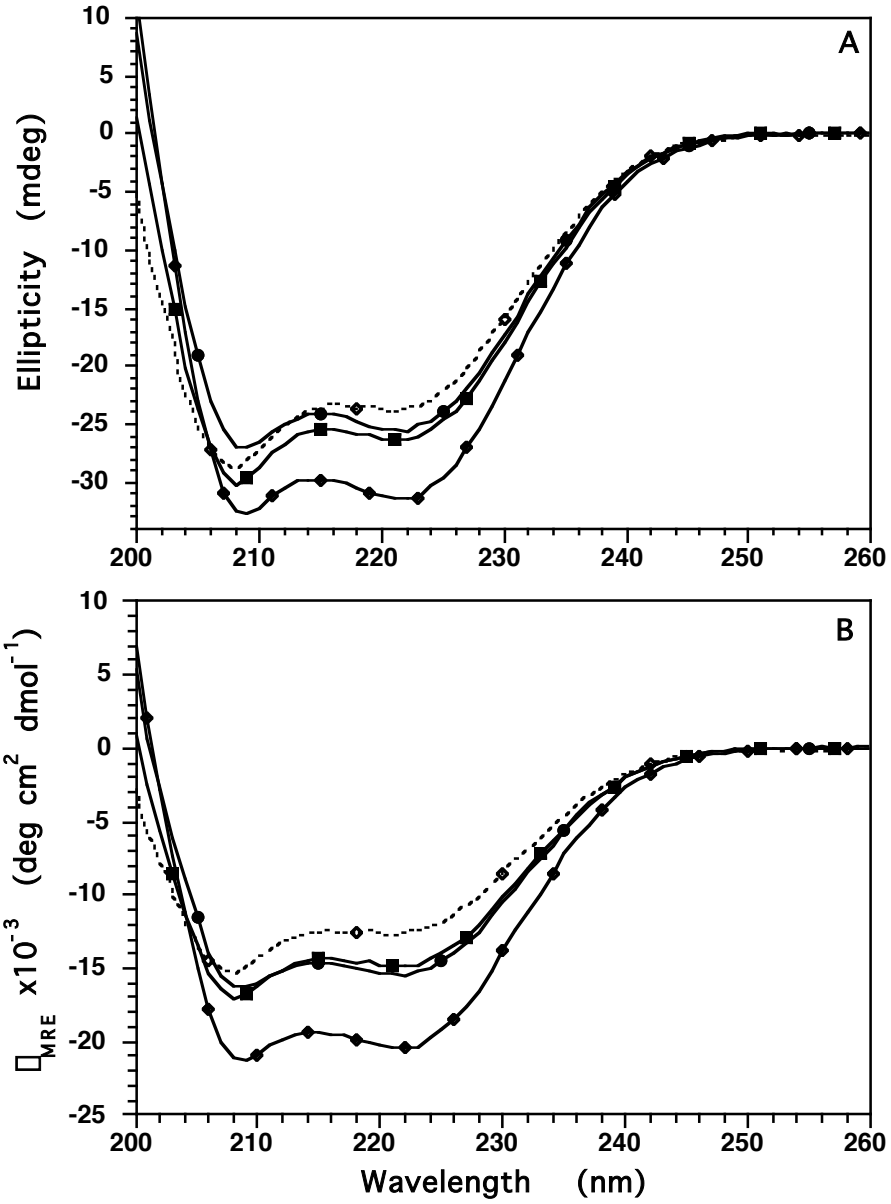

Figure 2. Far-UV CD spectra of WT and truncated H2A-H2B dimers. For both panels: WT H2A-H2B, ◊, dotted line; □N-H2A/WT-H2B, ■; WT-H2A/□N-H2B, ●; □N-H2A/□N-H2B, ♦. A) Spectra at 5 μM dimer, and not corrected for differences in the number of the residues in the variant dimers. B) Spectra in units of mean residue ellipticity (MRE), and thus normalized for number of residues in the polypeptide chains. Conditions: 20 mM potassium phosphate, 0.1 mM EDTA, pH 7.2, 25 °C.

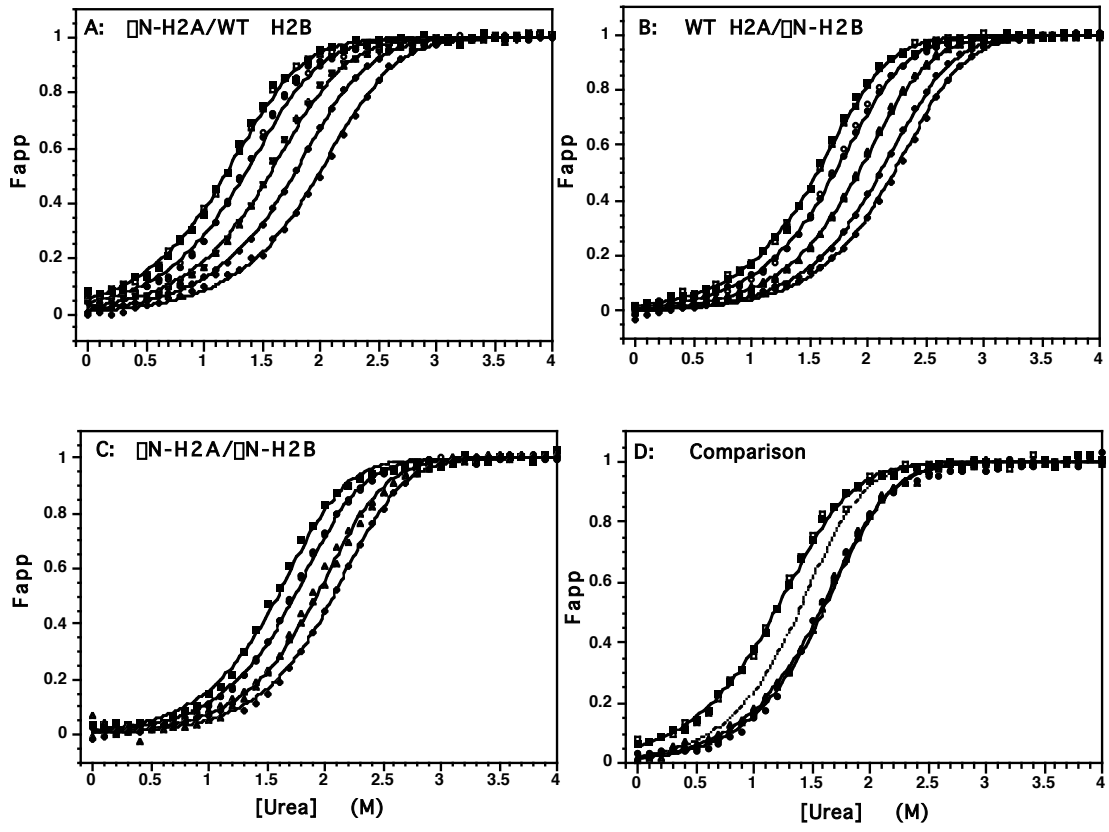

Figure 3. Representative urea-induced equilibrium denaturation transitions at several dimer concentrations for the N-terminal-truncated H2A-H2B variants. Data for the CD and FL titrations were collected to urea concentrations higher than shown (generally 5 to 6 M), but the region of the unfolding transition has been expanded for clarity. The lines represent the global fits of multiple equilibrium data sets for each dimer variant. A) □N-H2A/WT-H2B at: 1 μM CD, ■, and FL, □; 2 μM CD, ●, and FL, ○; 5 μM FL, ▲and □; 12 μM FL, ♦; 30 μM FL, ◊. B) WT-H2A/□N-H2B at: 1 μM CD, ■, and FL, □; 2 M CD, ●, and FL, ○; 5 μM CD, ▲, and FL, □; 12 μM FL, ♦; 20 μM FL, ◊. C) □N-H2A/□N-H2B at: 1 μM CD, ■; 2 μM CD, ●, and FL, ○; 5 μM CD, ▲, and FL, □; 10 μM FL, ♦. D) Overlay of the three H2A-H2B variants at 1 μM dimer: □N-H2A/WT-H2B, squares; WT-H2A/□N-H2B, triangles; □N-H2A/□N-H2B, circles. For comparison, the fit of the full-length H2A-H2B dimer is represented by the dotted line [Gloss, 2002 #293]. The size of the data points are equal to or larger than the error in the measurement. Conditions: 20 mM potassium phosphate, 0.1 mM EDTA, pH 7.2, 25 °C.

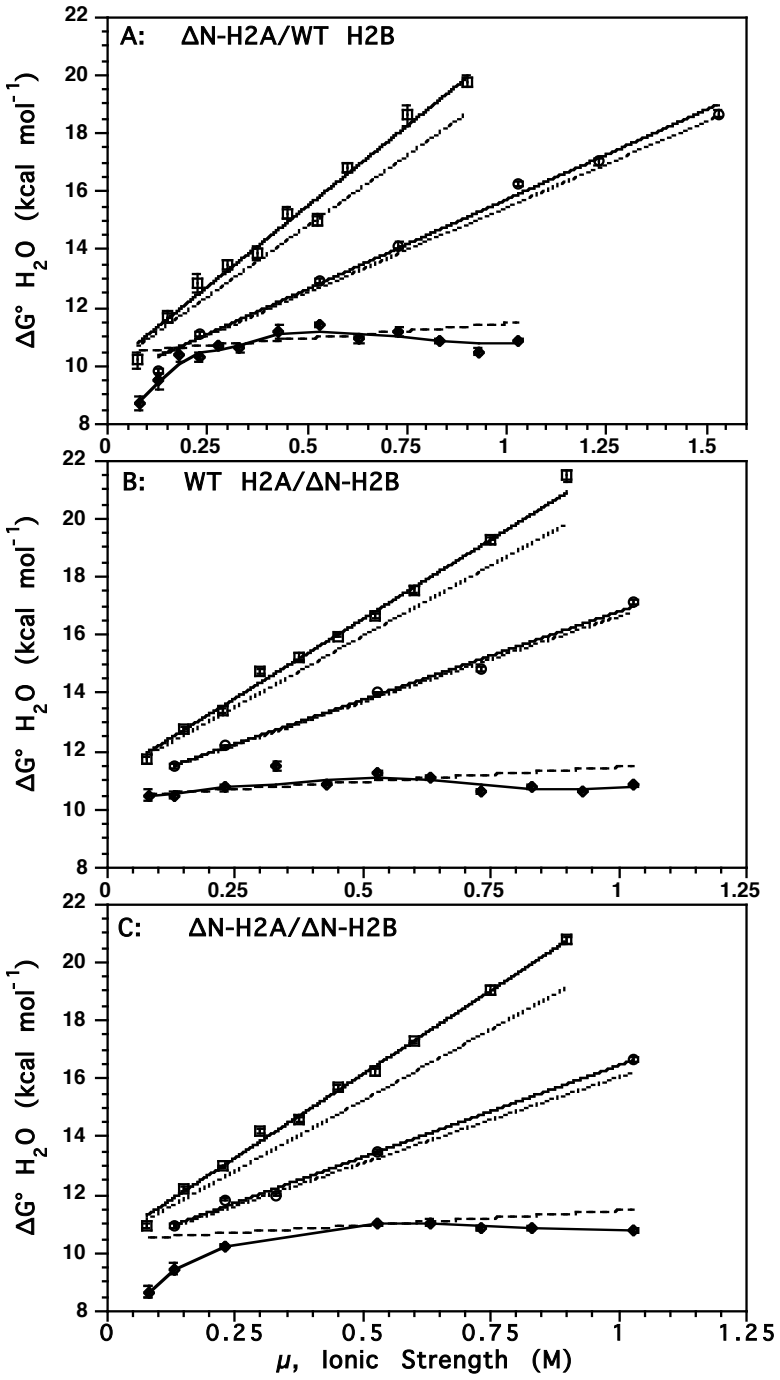

Figure 4. Dependence of the free energy of unfolding, □G°(H_2O), of the H2A-H2B variants on ionic strength with three potassium salts: KPi, ; KCl, ; KI, ◊. A) □N-H2A/WT-H2B. B) WT-H2A/□N-H2B. C) □N-H2A/□N-H2B. An error of one standard deviation on the error surface for the global fits is shown or is less than the size of the data points. The solid lines for the KPi and KCl data represent a linear fit of the data plotted as a function of ionic strength; the line for the KI data does not represent a fit, but is drawn to guide the eye. For comparison, the slopes of the WT data (33) are shown as dotted lines. For clarity, the slopes for the WT KCl and KPi data are normalized to the □G°(H_2O) in the absence of salt of the mutant data (Y-

intercept of the linear fit), to emphasize the difference in slopes. Conditions: 5 μM dimer, at least 20 mM potassium phosphate, pH 7.2, 0.1 mM EDTA, 25 °C.

References

1. Workman, J. L., and Kingston, R. E. (1998) Alteration of nucleosome structure as a mechanism of transcriptional regulation. Ann. Rev. Biochem. 67, 545-79.
2. Wolffe, A. P., and Guschin, D. (2000) Chromatin structural features and targets that regulate transcription. J. Structural Biology 129, 102-122.
3. Cheung, P., Allis, C. D., and Sassone-Corsi, P. (2000) Signaling to chromatin through histone modifications. Cell 103, 263-71.
4. Strahl, B. D., and Allis, C. D. (2000) The language of covalent histone modifications. Nature 403, 41-5.
5. Anderson, J. D., Lowary, P. T., and Widom, J. (2001) Effects of histone acetylation on the equilibrium accessibility of nucleosomal DNA target sites. J Mol Biol 307, 977-85.
6. Arents, G., and Moudrianakis, E. N. (1993) Topography of the histone octamer surface: Repeating structural motifs utilized in the docking of nucleosomal DNA. Proc. Natl. Acad. Sci. USA 90, 10489-93.

7. Luger, K., Mader, A. W., Richmond, R. K., Sargent, D. F., and Richmond, T. J. (1997) Crystal structure of the nucleosome core particle at 2.8 A resolution. Nature 389, 251-60.
8. Xie, X., Kokubo, T., Cohen, S. L., Mirza, U., Hoffmann, A., Chait, B. T., Roeder, R. G., Nakatani, Y., and Burley, S. K. (1996) Structural similarity between TAFs and the heterotetrameric core of the histone octamer. Nature 380, 316-322.
9. Birck, C., Poch, O., Romier, C., Ruff, M., Mengus, G., Lavigne, A. C., Davidson, I., and Moras, D. (1998) Human TAFII28 and TAFII18 interact through a histone fold encoded by atypical evolutionary conserved motifs also found in the SPT3 family. Cell 94, 239-49.
10. Arents, G., Burlingame, R. W., Wang, B. C., Love, W. E., and Moudrianakis, E. N. (1991) The nucleosomal core histone octamer at 3.1 Å resolution: a tripartite protein assembly and a left-handed superhelix. Proc. Natl. Acad. Sci. U.S.A. 88, 10148-52.
11. Karantza, V., Freire, E., and Moudrianakis, E. N. (2001) Thermodynamic studies of the core histones: Stability of the octamer subunits is not altered by removal of their terminal domains. Biochemistry 40, 13114-123.

12. Luger, K., Rechsteiner, T. J., Flaus, A. J., Waye, M. M., and Richmond, T. J. (1997) Characterization of nucleosome core particles containing histone proteins made in bacteria. J. Mol. Biol. 272, 301-311.
13. Sang, N., Condorelli, G., De Luca, A., MacLachlan, T. K., and Giordano, A. (1996) Generation of site-directed mutagenesis by extralong, high fidelity polymerase chain reaction. Anal. Biochem. 233, 142-144.
14. Sreerama, N., and Woody, R. W. (2000) Estimation of protein secondary structure from circular dichroism spectra: comparison of CONTIN, SELCON, and CDSSTR methods with an expanded reference set. Anal Biochem 287, 252-60.
15. Johnson, W. C. (1999) Analyzing protein circular dichroism spectra for accurate secondary structures. Proteins 35, 307-12.
16. Sreerama, N., and Woody, R. W. (1994) Protein secondary structure from circular dichroism spectroscopy. Combining variable selection principle and cluster analysis with neural network, ridge regression and self-consistent methods. J Mol Biol 242, 497-507.
17. Provencher, S. W., and Glockner, J. (1981) Estimation of globular protein secondary structure from circular dichroism. Biochemistry 20, 33-7.

18. Sreerama, N., Venyaminov, S. Y., and Woody, R. W. (1999) Estimation of the number of alpha-helical and beta-strand segments in proteins using circular dichroism spectroscopy. Protein Sci 8, 370-80.
19. Hansen, J. C., Tse, C., and Wolffe, A. P. (1998) Structure and function of the core histone N-termini: More than meest the eye. Biochemistry 37, 17637-17641.
20. Wang, X., Moore, S. C., Laszckzak, M., and Ausió, J. (2000) Acetylation increases the α-helical content of the histone tails of the nucleosome. J. Biol. Chem. 275, 35013-35020.
21. Wells, J. A. (1990) Additivity of mutational effects in proteins. Biochemistry 29, 8509-17.
22. Karantza, V., Baxevanis, A. D., Freire, E., and Moudrianakis, E. N. (1995) Thermodynamic studies of the core histones: Ionic strength and pH dependence of H2A-H2B dimer stability. Biochemistry 34, 5988-96.
23. Myers, J. K., Pace, C. N., and Scholtz, J. M. (1995) Denaturant m values and heat capacity changes: Relation to changes in accessble surface areas of protein folding. Protein Science 4, 2138-2148.
24. Spudich, G., and Marqusee, S. (2000) A change in the apparent m value reveals a populated intermediate under equilibrium conditions in Escherichia coli ribonuclease HI. Biochemistry 39, 11677-83.

25. Baldwin, R. L. (1996) How Hofmeister ion interactions affect protein stability. Biophys. J. 71, 2056-63.
26. Record, M. T., Jr., Zhang, W., and Anderson, C. F. (1998) Analysis of effects of salts and uncharged solutes on protein and nucleic acid equilibria and processes: A practical guide to recognizing and interpreting polyelectrolyte effects, Hofmeister effects and osmotic effects of salts. Advances in Protein Chemistry 51, 282-355.
27. Timasheff, S. N. (1993) The control of protein stability and association by weak interactions with water: How do solvents affect these processes? Annu. Rev. Biophys. Biomol. Struct. 22, 67-97.
28. Timasheff, S. N. (1998) Control of protein stability and reactions by weakly interacting cosolvents: The simplicity of the complicated. Advances in Protein Chemistry 51.
29. Bolen, D. W., and Baskakov, I. V. (2001) The osmophobic effect: Natural selection of a thermodynamic force in protein folding. J. Mol. Biol. 310, 955-963.
30. Saunders, A. J., Davis-Searles, P. R., Allen, D. L., Pielak, G. J., and Erie, D. A. (2000) Osmolyte-induced changes in protein conformational equilibria. Biopolymers 53, 293-307.

31. Henkels, C. H., Kurz, J. C., Fierke, C. A., and Oas, T. G. (2001) Linked folding and anion binding of the Bacillus subtilis ribonuclease P protein. Biochemistry 40, 2777-89.
32. Kraulis, P. J. (1991) MOLSCRIPT: a program to produce both detailed and schematic plots of protein structures. J. Applied Crystallography 24, 946-950.
33. Gloss, L. M. and Placek B. J. (2002) The Effect of Salts on the Stability of the H2A-H2B Histone Dimer. Biochemistry 41, 14951-14959.

CHAPTER THREE

The H2A.Z-H2B dimer is unstable compared to the dimer containg the major H2A isoform

This chapter was prepared for submission to the journal *Protein Science* and therefore differs in format from the remainder of the dissertation. I am the first author of this paper. I performed the majority of the work contained in this paper. L. Nicole Harrison created the H2A_C mutant and determined the stability of the H2A_C/H2B dimer under my supervision. Ms. Harrison will be listed as second author. Brooke M. Villers participated in the determination of the stability of the H2A.Z/H2B dimer in 1 M TMAO. Ms. Villers will be listed as third author. I contributed to the writing of this paper but Lisa Gloss wrote the majority of the paper.

Abbreviations: CD, circular dichroism; FL, fluorescence; Fapp, apparent fraction of unfolded monomer; $\Delta G^{\circ}(H_2O)$, the free energy of unfolding in the absence of denaturant; GdmCl, guanidinium chloride; H2A, major isoform encoded by the *Xenopus laevis* gene; H2A.Z, H2A variant encoded by the mouse gene ; H2A-ΔC, C-terminal tail truncation, after Arg99, of the *Xenopus laevis* major H2A isoform; KP_i, potassium phosphate *m*-value, parameter describing the sensitivity of the unfolding transition to the [Urea]; MRE, mean residue ellipticity; NCP, nucleosome core particle; TMAO, trimethylamine-N-oxide; SVD, singular value decomposition.

SUMMARY

To further the understanding of the thermodynamics of the nucleosome core particle, the stability of the H2A.Z/H2B heterodimer was determined and compared to the stability of the H2A/H2B heterodimer. The equilibrium stabilities of the H2A.Z/H2B dimer and the H2A/H2B dimer were determined by urea-induced denaturing, using fluorescence, anisotropy and circular dichroism. The H2A.Z/H2B dimer is unstable in mild ionic conditions (~ 0.2 M). To facilitate the determination of the equilibrium stability for H2A.Z/H2B the know protein stabilizer TMAO (trimethylamine-N-oxide) was utilized, the stability of H2A/H2B was determined under identical conditions. The unfolding of both dimers was best described by a two-state equilibrium model, with no detectable equilibrium intermediates populated. When the stabilities of the two dimers were compared, the H2A.Z/H2B dimer is substantially destabilized as compared to the H2A/H2B dimer. The equilibrium stabilities of H2A.Z/H2B and H2A/H2B in the absence of denaturant are 7.3 kcal mol^{-1} and 15.5 kcal mol^{-1}, respectively, in 1 M TMAO.

INTRODUCTION

Within the nucleus of eukaryotic cells, DNA is compacted by the nucleoprotein complex chromatin. The fundamental repeating unit of chromatin is the nucleosome core particle (NCP). The NCP consists of two copies each of the histone proteins, H2A, H2B, H3 and H4, and ~150 bp of DNA, which is wrapped 1.65 times around the central protein octamer. Each of these proteins fold into a structural motif termed the "histone fold", which contains a long central α helix flanked on each end by a loop and shorter α helix (Arents and Moudrianakis 1993; Luger et al. 1997a). H2A and H2B heterodimerize in a head to tail manner called the "handshake motif" (Figure 1A). H3 and H4 heterodimerize in a similar structure; two H3/H4 dimers then form the H3/H4 tetramer via a four-helix bundle of the C-termini of two H3 proteins.

The compaction of DNA afforded by the NCP also restricts the access of cellular machinery to the DNA, and nucleosomal structures are often repressive to the DNA-based chemistries of the cell. During processes such as replication, transcription, repair and recombination, the structure of chromatin must be altered to provide access to the DNA. Cells have developed several ways in which to modulate chromatin structure and NCP dynamics: 1) post-translational modifications; 2) ATP-dependent chromatin remodeling complexes and 3) incorporation of histone variants. Post-translational modifications, primarily of the histone-tail domains, have been extensively studied (for review, (Strahl and Allis 2000; Jenuwein and Allis 2001)). Modifications such as acetylation, methylation and phosphorylation alter the properties of chromatin and influence accessibility of the DNA as well as act as signals for the recruitment of nuclear factors. Secondly, ATP-dependent chromatin remodeling complexes utilize the energy from ATP hydrolysis to rearrange both histone-DNA and histone-histone interactions. (for review, (Lusser and Kadonaga 2003)). Generally, the function of these complexes is to increase NCP mobility and may enable the translocation of the histone octamer along the DNA. Finally, the proteins constituting the NCP can be varied by the incorporation of alternate histones.

The structural and functional properties of NCPs can be altered by incorporation of variant histones with different biochemical properties than the major histone isoform. Variants have been identified for each of the four core histones, but the H2A family contains the most members. The major site of sequence divergence between the H2A family members is in the C-terminal regions of the proteins (Ausio and Abbott 2002). The various H2A isoforms appear to be involved in specific cellular functions. H2A.X, for example, is involved in the response to DNA double-strand breaks, and phosphorylation of a serine residue in the C-terminal tail of the protein is one of the earliest events after induction of DNA double-strand breaks (Rogakou et al. 1998). MacroH2A is thought to play a pivotal role in the inactivation of one copy of the X chromosome and contains a large non-histone fold C-terminal domain (Costanzi and Pehrson 1998).

This report focuses on the variant H2A.Z, an isoform found in most eukaryotes. It is required for survival in *Drosphila melanogaster* (van Daal and Elgin 1992), *Tetrahymena thermophila* (Liu et al. 1996) and mice (Faast et al. 2001). H2A.Z is highly conserved across species, ~90%, but shares only ~60% sequence identity with the major H2A protein (Iouzalen et al. 1996). In *D. melanogaster,* the region of H2A.Z essential for survival is in the C-terminus (Clarkson et al. 1999). Initially, H2A.Z was thought to be involved in transcription activiation, because in *T. thermophila,* H2A.Z is found only in the transcriptionally active macronucleus and not in the inactive micronucleus (Stargell et al. 1993). In *Saccharomyces cerevisiae*, H2A.Z is required for normal induction of the *GAL1* and *PHO5* genes; the requirement for H2A.Z is enhanced in strains deficient for chromatin remodeling complexes (Santisteban et al. 2000). More recent studies have implicated H2A.Z in the maintenance of pericentrimeric heterochromatin and telomeric heterochromatin (Meneghini et al. 2003; Rangasamy et al. 2003).

The X-ray crystal structure of a NCP containing H2A.Z (Suto et al. 2000) reveals an overall structure very similar to that of an NCP containing the major H2A (RMSD <1Å) (Luger et al. 1997a). The subtle structural differences between two NCPs are in the interface between the H2A/H2B dimer and H3/H4 tetramer and a metal ion binding site in the H2A.Z NCP.

These differences appear to have effects within an individual NCP and between nucleosomes in higher order chromatin structures. A recent report showed that H2A.Z NCPs are more stable than H2A NCPs (Park et al. 2004). Additionally, H2A.Z incorporation facilitates the folding of individual nucleosomal arrays while inhibiting the formation of higher order interactions between the arrays (Fan et al. 2002).

The properties of the histone oligomers are key determinants of the dynamic properties of the nucleosome which regulate the DNA accessibility. To provide biophysical insights into NCP dynamics as influenced by the incorporation of histone variants, we have compared the stability of H2B dimers containing the major H2A isoform and the H2A.Z variant. Previously, we have shown that the H2A/H2B dimer is a moderately stable protein (Gloss and Placek 2002). In this report, we demonstrate that, in contrast, the H2A.Z/H2B dimer is quite unstable.

Results

The histones used in these studies were purified from a recombinant *E. coli* expression system (see Methods). Unlike histones purified from eukaryotic sources, the recombinant histones were homogenous in lacking post-translational modifications, as shown by mass spectrometry. The *Xenopus laevis* genes for the major H2A and H2B isoforms were used for recombinant expression (Luger et al. 1997b); however, the overexpression plasmid for H2A.Z contains the gene from mouse (Suto et al. 2000). This H2A.Z was reconstituted with *Xenopus laevis* H2B by the methods used for the major H2A (Placek and Gloss 2002). The heterodimer of mouse H2A.Z/*Xenopus* H2B is the construct that has been used in previous biophysical studies of the effect of H2A.Z on the properties of the nucleosome, including X-ray crystallography (Suto et al. 2000), analytical ultracentrifugation (Fan et al. 2002) and equilibrium assembly and dissociation (Park et al. 2004). Although, the histone monomers in this complex are from different organisms, this is not anticipated to have any significant effect on the folding

properties of the heterodimer. Mouse and *Xenopus* H2A.Z are 90% identical overall (Figure 1B). In the globlular, helical, histone fold, domain of ~70 residues, there are six amino acid differences. Five of the substitutions are conservative: two Ser/Thr substitutions; Ser replaced with either Ala or Asn, and an Ala/Gly exchange. The sixth difference is very solvent accessible, exchanging the *Xenopus* Leu for a His in mouse. Only one of the differences, a Ser/Thr substitution in the long α2 helix, is significantly excluded from solvent and makes intermonomer contacts.

The stability of the variant H2A/H2B dimers were determined from urea-induced unfolding transitions. The extent of native structure as a function of [Urea] was monitored by far-UV circular dichroism (CD) at 222 nm and intrinsic Tyr fluorescence (FL) at 305 nm. Far-UV CD provides a global measure of the secondary structure of the protein. Tyr FL provides information on the tertiary and quaternary structure of the heterodimers. The major *Xenopus laevis* H2A contains three tyrosine residues at positions 39, 50 and 57. These Tyr residues are largely excluded from solvent in the folded dimer by both intra and inter-monomer contacts. The most solvent accessible Tyr at position 39, is not conserved in the H2A.Z sequences, and is a Ser in the *Xenopus* and mouse proteins. The *X. laevis* H2B monomer contains five Tyr, three of which are also largely excluded from solvent by tertiary and quaternary structure.

Cosolute stabilization of H2A.Z/H2B. In the absence of denaturant, the mean residue ellipiticty at 222 nm of the H2A.Z/H2B dimer is 50% less than that of the dimer containing the major H2A isoform (Figure 2). Given the very similar structures of the two heterodimers, in the context of the nucleosome (Suto et al. 2000), the diminished CD signal of the H2A.Z/H2B dimer suggested that perhaps this heterodimer is less well folded than the dimer comprised of the two major isoforms. Comparison of HPLC size-exclusion chromatograms of H2A/H2B and

H2A.Z/H2B dimers showed that the H2A.Z-containing species was a mixture of dimer and monomeric species. Glutaraldehyde cross-linking, performed as described previously (Banks and Gloss 2003), confirmed that the dimer was a heterotypic association of H2A.Z and H2B. Furthmore, the urea-induced unfolding transitions of the two heterodimers confirmed that the H2A.Z/H2B dimer was only partially folded. Much lower urea concentrations were required to unfold the H2A.Z/H2B heterodimer (data not shown). The unfolding transitions exhibited high reversibility, 90 to 95%. However, the H2A.Z/H2B unfolding transitions could not be fit to an equilibrium model to determine a free energy of unfolding in the absence of denaturant, $\Delta G°$ (H_2O), because of a lack of a native baseline to determine the spectral properties of the fully folded native dimer. Therefore, cosolutes were used to stabilize the H2A.Z/H2B dimer.

Initially, high salt concentrations, 0.3 M KP_i or 1 M KCl, were employed to stabilize the H2A.Z/H2B dimer; these conditions had been shown to greatly stabilize the H2A/H2B dimer (Gloss and Placek 2002). While the addition of salts did stabilize H2A.Z/H2B, as evidenced by requiring higher urea concentrations to unfold the dimer, these conditions did not sufficienlty stabilize the dimer such that a native baseline could be discerned. The high salt conditions also had the additional complication of reducing the reversibility of the unfolding reaction, probably because of aggregation as detected in HPLC size exclusion chromatograms.

Trimethylamine-N-oxide (TMAO) has been shown to be a potent cosolute for stabilizing partially folded proteins, and extending the native baseline region (Henkels et al. 2001; Mello and Barrick 2003). TMAO is an organic osmolyte that stabilizes proteins through the osmophobic effect because of unfavorable interactions with the peptide backbone (Wang and Bolen 1997; Bolen 2001) and preferential hydration of the native species (Timasheff 1998). The FL and far-UV CD signals of the H2A.Z/H2B dimer increased with increasing TMAO

concentrations, reaching a plateau above 3 M TMAO (Figure 2). These data suggest that 3 to 4 M TMAO is required to induce complete folding of the H2A.Z/H2B dimer. HPLC size-exclusion chromotrography of the dimer in 1 M TMAO confirmed that the population was predominately dimeric, with no detectable aggregate. Note, TMAO does not significantly affect the CD and FL properties of H2A/H2B. However, it is not practical to study the urea-induced unfolding of the histones in such high concentrations of TMAO because it is not possible to make urea solutions of high enough concentration, in the presence of 3 M TMAO, to completely unfold the histone dimers. Therefore, further studies were performed in 1 M TMAO; the various methods used to determine the native baseline are described below.

Equilibrium stability of H2A.Z/H2B. A data set of 10 urea equilibrium unfolding transitions in 1 M TMAO were collected over a range of dimer concentrations from 2 to 17.3 μM. The data set included unfolding transitions monitored by both far-UV CD and Tyr FL; FL data included both FL intensity and FL anisotropy as a function of [Urea]. Representative transitions are shown in Figures 3A and 3B for far-UV CD and FL intensity, respectively. As expected for a dimeric protein, the unfolding transition is protein concentration dependent; as the dimer concentration increases, the transition between folded and unfolded species shifts to higher urea concentrations. At the lowest dimer concentrations, no native baseline is observed. The data were globally fitted to a two-state equilibrium model for the unfolding of a dimer to two unfolded monomers, with no populated intermediates (as described by Equations 1 and 2, Methods section). In all global fits, the $\Delta G°$ (H_2O) and *m* values were treated as global parameters, linked across the entire data set. The well-defined unfolded baselines were treated as local fitted parameters, and not linked between the various titrations in the data set.

In the global fitting of the data set, several methods were used to constrain the poorly defined native baselines. 1) The intercept of the native baselines (the signal at 0 M urea) were fixed to the values of the spectral signals observed at 3 to 4 M TMAO. The slopes of the native baselines were treated as fitted parameters, either globally linked between titrations monitoring the same spectral signal or treated as local parameters. 2) The far-UV CD data were normalized to mean residue ellipticity, and the parameters for the native baselines were linked between all of the CD titrations. 3) The slopes of all native baselines were fixed at 0 for all titrations, and the intercept treated as a local parameter or linked between titrations monitoring the same spectral signal. 4) The data set was fit with the slopes and intercepts of the native baselines treated as local adjustable parameters, without any additional constraints to define the native baseline. The latter method, having the largest number of fitted parameters, and thus the most degrees of freedom, gave the best fit of the data, as assessed by reduced Chi-squared values and the agreement between the fit and the data points. The $\Delta G°$ (H_2O) and *m* values for this fit are given in Table 1, and the results are shown as the solid lines in Figures 3 and 4. The fitted values of $\Delta G°$ (H_2O) from the various methods of constraining the native baseline ranged from 7.3 to 7.8 kcal mol^{-1}; the *m* values ranged from 1.0 to 1.3 kcal $mol^{-1}M^{-1}$. These ranges are within the errors reported in Table 1 for the least constrained fit. Therefore, the $\Delta G°$ (H_2O) and *m* values reported in Table 1 for the H2A.Z/H2B dimer are reasonably accurate, despite the poor definition of the native baseline in 1 M TMAO.

The data from the different spectral probes can be compared by converting the spectral data to F_{app} transitions, the apparent fraction of unfolded monomers as a function of [Urea] (see Equation 1, Methods section). The far-UV CD and Tyr FL F_{app} curves are coincident (Figure 4A), demonstrating a concerted loss of secondary, tertiary and quaternary structure. This

coincidence suggests that the H2A.Z/H2B dimer unfolds by a two-state equilibrium mechanism. Further support is provided by the agreement between the data and the global fit as a function of dimer concentration (Figures 3 and 4)

Equilibrium stability of H2A/H2B in 1 M TMAO. To compare the stability of heterodimers containing the H2A.Z and major H2A isoforms under similar solvent conditions, the stability of the H2A/H2B was determined from equilibrium urea unfolding studies in 1 M TMAO. A data set of 11 unfolding transitions at several dimer concentrations was collected, spanning a dimer concentration range of 1 to 8 μM; the data set contained transitions monitored by both far-UV CD and intrinsic Tyr FL data. The presence of TMAO did not decrease the high reversiblity, ≥ 95%, of the H2A/H2B unfolding reported previously in the absence of TMAO (Gloss and Placek 2002). The data set was globally fit to a two-state equilibrium mechanism, which has been shown previously to adequately describe the equilibrium unfolding in the absence of TMAO (Gloss and Placek 2002). The $\Delta G°$ (H_2O) and *m* values were treated as global parameters (Table 1), linked across the entire data set, while the native and unfolded baselines were treated as local parameters. The coincidence of unfolding transitions monitored by CD and FL data and the agreement between the data and the global fit at various dimer concentrations (Figure 4B) demonstrate that the unfolding of the H2A/H2B dimer is a two state process in the presence of 1 M TMAO.

Equilibrium stability of H2A_C/H2B. The greatest sequence diversity between the H2A variants is in the extended C-terminal tail region of the protein. To assess the contribution of this region to the stability of the H2A/H2B dimer, a C-terminal truncated mutant of the major H2A isoform was generated. The H2A-ΔC mutation terminated the polypeptide after residue 99 by insertion of a stop codon. The truncaton site was chosen to remove all of the C-terminal

residues which were in an extended conformation or unresolved in the X-ray crystal structure (Luger et al. 1997a). The urea-induced unfolding of the H2A-ΔC/H2B dimer is ≥ 95% reversible. A data set of nine equilbrium transitions were collected, spanning a range of dimer concentrations from 1 to 20 μM dimer, with unfolding monitored by both CD at 222 nm and FL intensity at 305 nm. The data set was globally fitted to a two-state equilibrium model (described by Equations 1 and 2, Methods section). Representative data and fits are shown in Figure 5, and the globally fitted $\Delta G°$ (H_2O) and *m* values are given in Table 1.

Discussion

Stability differences between histone fold dimers. Previous chemical denaturant studies have shown that the H2A/H2B dimer is a relatively stable dimer for its size (Gloss and Placek 2002). For the histones, it is difficult to compare stabilities, as quantified by the $\Delta G°$ (H_2O) values, between studies using urea and guanidinium chloride (GdmCl); for example, H2A/H2B exhibits higher stability to GdmCl denaturation than to urea denaturation (Gloss and Placek 2002; Banks and Gloss 2003), apparently because of the ionic nature of the GdmCl salt and the highly basic histone sequence. The stability to GdmCl denaturation of other histone-fold-containing dimers have been reported and can be directly compared to that reported for H2A/H2B in GdmCl. Of the eukaryotic NCP heterodimers, the H3/H4 dimer exhibits only 60% of the stability of H2A/H2B (Banks and Gloss 2003). Surprisingly, H2A/H2B exhibits greater stability than even the histone homodimers of thermophilic and hyperthermophilic archae, hMfB (20% greater) and hPyA1 (5% greater) (Topping and Gloss 2004).

In contrast, the H2A.Z/H2B dimer is strikingly unstable, and is the least stable of the histone folds characterized to date. This instability is apparent without detailed analyses of the

chemical denaturation data. The mesophilic archael homodimeric archael histone, hFoB, and the H3-H4 dimer require cosolutes such as TMAO to promote folding to the native state (Banks and Gloss 2003; Topping and Gloss 2004). However, for both of these histone dimers, 1 M TMAO is sufficient to induce complete folding, and results in a native baseline in the presence of denaturants. However, concentrations of TMAO greater than 1 M are required to promote complete folding of the H2A.Z/H2B dimer (Figure 2). Fits of the H2A.Z/H2B data indicate that in 1 M TMAO, at most ~20% of the monomers are unfolded at concentrations less than 20 μM (Figures 3 and 4A). In 1 M TMAO, H2A.Z/H2B exhibits only 47% of the stability to urea denaturation of the H2A/H2B dimer (Table 1).

Fitting of chemical denaturation data provides the stability, quantified by the $\Delta G°$ (H_2O) parameter, and also the *m* value, which describes the steepness of the unfolding transition, *i.e.* the sensitivity to the denaturant concentration (Equation 2, Methods). For the relatively stable dimers, H2A/H2B, and the archael histones, hMfB and hPyA1, the *m* value correlates quite well with that expected for that calculated from the change in solvent accessible surface area between the unfolded monomers and native dimer (Myers et al. 1995). However, for the unstable H2A.Z/H2B and H3/H4 dimers, and to a lesser extent, the archael hFoB homodimer, the *m* values are significantly less than expected for proteins of their size (Banks and Gloss 2003; Topping and Gloss 2004). This suggests that a low *m* value may be a common feature of poorly folded histones, particularly in TMAO. For example, the *m* value of H2A/H2B decreases from 6.4 to 5.4 kcal $mol^{-1}M^{-1}$ in 0 and 1 M TMAO, respectively (Banks and Gloss 2003). Lower than expected *m* values can also be an indication of the presence of an equilibrium intermediate, for example (Spudich and Marqusee 2000). However, the folding of H2A.Z/H2B appears to be a two-state process based on: 1) the coincidence of transitions

monitoring multiple spectorscopic probes (Figure 4A); and 2) the quality of the global fits to a two state model as a function of protein concentration (Figures 3 and 4A). The poorly defined native baseline of H2A.Z/H2B makes it difficult to differentiate between the quality of fits to a two-state model or a model with additional states, and thus additional fitting parameters.

The regions required for the function of H2A.Z are the C-terminal residues 92 to 102, the C-terminal α-helix beyond the canonical histone fold, and residues 106 to 119, the distal end of the extended C-terminal tail (Figure 1) (Clarkson et al. 1999). To ascertain the effect of this region on the stability of H2A/H2B dimers, the C-terminal residues 100 to 119 were truncated in the mutant H2A-ΔC/H2B. The presence of the C-terminal tail does confer some additional stability to the H2A/H2B dimer, 1.6 kcal mol^{-1} (Table 1; Figure 5) The destabilization resulting from removal of the C-terminal tail is greater than that observed for removing the 15 amino acids of the H2A N-terminal tail, 0.9 kcal mol^{-1} (Placek and Gloss 2002). However, the truncation of the functionally important C-terminal tail does not account for the difference in stability between dimers containing H2A and H2A.Z, 8.2 kcal mol^{-1} (Table 1). Therefore, the sequence differences that encode the stability differences between the two histone heterodimers must lay within the globular, helical histone fold region.

Sequence differences that may impact the relative stability of H2A/H2B and H2A.Z/H2B dimers. The relative instability of H2A.Z/H2B occurs despite ~70% identity in the helical, globular regions of the two H2A sequences (between residues 16 and 97; Figure 1B) and very similar structures, in the context of the nucleosome. While there is sequence divergence in the extended N- and C terminal tails, and these regions can modulate dimer stability, the histone fold domain is the major determinants of dimer stability. There are three clusters of sequence differences between H2A and H2A.Z that may, individually or in combination, encode the

stability difference between the heterodimers formed by these proteins: 1) the loop region between α1 and α2 of the histone fold (X.l.A residues 37 to 41); 2) the N-terminus of α2, particularly the Pro to Ala substitution at X.l.A residue 48 and the completely buried Leu to Ser or Thr change at X.l.A. residue 51; and 3) the C-terminus of α2 and the loop connecting to α3 (X.l.A residues 69 to 78). The α1 to α2 loop is one residue shorter in the major H2A structure, and also contains a Tyr that is absent in H2A.Z; one face of Tyr residue is packed against the protein surface through hydrophobic interactions. The substitution of a Leu for an Asn (C-terminus of α2, X.l.A. residue 73) removes the hydrogen bond C-capping interaction of the Asn. The clusters of mutations in the helix termini and loop regions connecting the shorter helices to the long central helix of the histone fold may serve to alter the packing and interactions between the three helices of the histone fold, as well as how the H2A and H2A.Z monomers interact with the H2B monomer. Further mutational studies will be required to identify the exact determinants of the stability difference between H2A and H2A.Z containing heterodimers.

Implications for nucleosome function. The nucleosome core particle is a highly dynamic structure that must be restructured to allow access to the DNA during cellular processes such replication, transcription and repair. The incorporation histone variants is one means to alter the dynamics of the NCP and chromatin structure. Histone variants introduce new recognition sites for the recruitment of other nuclear proteins that facilitate the downstream actions. Additionally, the biophysical properties of the histone variant may directly alter the stability and dynamics of the NCP. A recent report has demonstrated that incorporation of H2A.Z/H2B dimer does affect NCP stability (Park et al. 2004). NCPs containing H2A.Z/H2B dimers are more stable to the NaCl-induced dissociation of the H2A/H2B dimers than H2A

containing NCPs. The instability of the H2A.Z/H2B dimer reported in this paper provides new insights into NCP stability.

The association of the H2A/H2B dimers with the NCP has been shown to be a dynamic process. Several studies have demonstrated that the H2A/H2B dimer can readily exchange between nuclesosomes both i*n vivo* and *in vitro* (Louters and Chalkley 1984; 1985; Kimura and Cook 2001). Furthermore, transcriptionally active chromatin is often depleted in H2A/H2B dimers (Louters and Chalkley 1985; Jackson 1990), and it has been shown that RNA pol II can displace H2A/H2B dimers during transcription (Kireeva et al. 2002). Therefore, there is an important equilibrium between the mature, fully assembled NCP and partially unfolded NCPs in which the H2A/H2B dimers are less tightly bound or completely dissociated. Histone variants or histone post-translational modifications can impact this equilibrium by altering the free energy of the mature NCP OR by altering the free energy of the dissociated dimer (Gloss and Placek 2002). Therefore, the stability of the free dimer will impact this equilibrium, and the state of nucleosome assembly is intimately linked to histone stability. A more stable H2A/H2B dimer should favor a more unfolded, dissociated state of the NCP. We have previously shown that the highly basic N-terminal tails destabilize the H2A/H2B dimer by electrostatic repulsion (Gloss and Placek 2002; Placek and Gloss 2002). The charge state of the tails are modulated by post-translational modifications such as Ser phosphorylation and Lys acetylation, which should stabilize the free H2A/H2B dimer, and certainly hyperacetylation correlates with transcriptional activity and depletion of the H2A/H2B dimer. In this report, we have shown that the free H2A.Z/H2B dimer is unstable, and this instability correlates with a shift of the equilibrium toward a more stable, assembled NCP, making the dimers less likely to dissociate under conditions that lead to dissociation of the H2A/H2B dimer (Park et al. 2004).

Materials and Methods

Materials. Ultrapure urea was purchased from ICN Biomedicals (Costa Mesa, CA). TMAO, from Sigma (St. Louis, MO), was dissolved in H_2O and deionized in batch mode with AG 11A8 mixed-bed resin purchased from BioRad (Richmond, CA). The TMAO concentration was determined from its refractive index as described elsewhere (Bolen 2001).

Methods. Production of recombinant histones. Recombinant H2A, H2A-ΔC and H2B were overexpressed and purified as described previously (Gloss and Placek 2002). The C-terminal truncation of H2A was generated by introducing a stop codon after the codon for Arg99, using extra long PCR as described previously (Placek and Gloss 2002). H2A.Z was overexpressed and purified by the same methods as the other histones, using a pET vector containing the mouse H2A.Z gene under the control of a T_7 promoter (Suto et al. 2000). The H2A.Z and H2A-ΔC monomers were reconstituted with the H2B monomer to the native heterodimer and further purified as described previously (Placek and Gloss 2002).

Urea Equilibrium Unfolding Titrations. The standard buffer conditions were 1 M TMAO, 20 mM potassium phosphate, 0.2 M KCl, 0.1 mM EDTA, pH 7.2, 25 ˚C. CD and FL data were collected on an AVIV 202SF spectrophotometer and an AVIV Model ATF-105/305 differential/ratio spectrofluoremeter, respectively. Both instruments were interfaced with Hamilton Model 500 automated titrators. Automated CD unfolding titrations were monitored at 222 nm in a 1 cm cell. At the highest H2A.Z monomer concentrations, sample absorbance was too high to use the 1 cm cell necessary for the automated titrations. Therefore, the unfolding transitions were monitored by preparing individual samples at each [Urea] and collecting wavelength spectra between 260 and 210 nm in a 0.2 cm cell. The spectra were analyzed by singular value decomposition (SVD) (Henry and Hofrichter 1992; Ionescu et al. 2000). SVD analyses have two advantages: 1) better signal to noise relative to data collected at a single wavelength; and 2) the ability to analyze data at multiple wavelengths to enhance either the detection of or confirm the absence of equilibrium intermediates. Automated FL titration data

were collected using an excitation wavelength of 280 nm and emission wavelength of 305 nm, with 2 nm bandwidths. The equilibration time for each titration was 3-5 minutes; this time interval was significantly longer than the time required to complete the slowest kinetic step for both folding and unfolding reactions for both histone dimers. The reversiblity of the urea-induced unfolding reactions of the heterodimers were quantified by comparing the CD and FL spectra of matched, individual samples prepared from folded protein stocks and urea unfolded stocks; samples were prepared with final urea concentrations that spanned the unfolding transitions to demonstrate a lack of hysteresis in the folding/unfolding transitions.

Data Analysis. The equilibrium unfolding titrations were fitted to a two-state model for a dimeric system (described in detail elsewhere, (Gittelman and Matthews 1990)). For a two-state dimeric system, F_{app} (the apparent fraction unfolded monomer) is related to the equilibrium constant, K_{eq}, and total monomer concentration, P_T, as well as the observed spectral properties, by the following equations:

$$F_{app} = \frac{\sqrt{K_{eq}^2 + 8K_{eq}P_T} - K_{eq}}{4P_T} = \frac{Y_i - Y_N}{Y_U - Y_N} \quad (1)$$

where Y_i is the CD signal measured at $[Urea]_i$, and Y_N and Y_U are the spectral properties of the folded and unfolded species. A linear extrapolation between the free energy of unfolding, ΔG°, and the urea concentration was used (Pace 1986).

$$\Delta G^\circ = \Delta G^\circ_{(H_2O)} - m[Urea] \quad (2)$$

where $\Delta G^\circ(H_2O)$ is the free energy of unfolding in the absence of denaturant at a standard state of 1 M dimer and the *m* value reflects the sensitivity of the transition to urea concentration. Data collected with different probes and at varied monomer concentrations were fitted globally with the program Savuka 5.1 (Zitzewitz et al. 1995; Gualfetti et al. 1999). In global fits, the

$\Delta G^{\circ}(H_2O)$ and *m* values were linked across the multiple data sets; the native and unfolded baselines were treated as either local parameters or linked across selected data sets.

Acknowledgements

This work was supported by a grant to L.M.G. from the National Science Foundation (MCB-9983831). B.J.P. was partially supported by an NIH Biotechnology training grant (GM08336-13). The pET over-expression vectors for the H2A.Z histone were kindly provided by Karolin Luger (Colorado State University) David J. Tremethick (Australian National University).

References

Arents, G., and Moudrianakis, E.N. 1993. Topography of the histone octamer surface: Repeating structural motifs utilized in the docking of nucleosomal DNA. *Proc. Natl. Acad. Sci. USA* **90:** 10489-10493.

Ausio, J., and Abbott, D.W. 2002. The many tales of a tail: carboxyl-terminal tail heterogeneity specializes histone H2A variants for defined chromatin function. *Biochemistry* **41:** 5945-5949.

Banks, D.D., and Gloss, L.M. 2003. Equilibrium folding of the core histones: the H3-H4 tetramer is less stable than the H2A-H2B dimer. *Biochemistry* **42:** 6827-6839.

Beechem, J.M. 1992. Global analysis of biochemical and biophysical data. *Methods in Enzymology* **210:** 37-54.

Bolen, D.W. 2001. Protein stabilization by naturally occurring osmolytes. *Methods Mol Biol* **168:** 17-36.

Clarkson, M.J., Wells, J.R., Gibson, F., Saint, R., and Tremethick, D.J. 1999. Regions of variant histone His2AvD required for Drosophila development. *Nature* **399:** 694-697.

Costanzi, C., and Pehrson, J.R. 1998. Histone macroH2A1 is concentrated in the inactive X chromosome of female mammals. *Nature* **393:** 599-601.

Faast, R., Thonglairoam, V., Schulz, T.C., Beall, J., Wells, J.R., Taylor, H., Matthaei, K., Rathjen, P.D., Tremethick, D.J., and Lyons, I. 2001. Histone variant H2A.Z is required for early mammalian development. *Curr Biol* **11:** 1183-1187.

Fan, J.Y., Gordon, F., Luger, K., Hansen, J.C., and Tremethick, D.J. 2002. The essential histone variant H2A.Z regulates the equilibrium between different chromatin conformational states. *Nat Struct Biol* **9:** 172-176.

Gittelman, M.S., and Matthews, C.R. 1990. Folding and stability of trp aporepressor from Escherichia coli. *Biochemistry* **29:** 7011-7020.

Gloss, L.M., and Placek, B.J. 2002. The Effect of Salts on the Stability of the H2A-H2B Histone Dimer. *Biochemistry* **41:** 14951-14959.

Gualfetti, P.J., Bilsel, O., and Matthews, C.R. 1999. The progressive development of structure and stability during the equilibrium folding of the alpha subunit of tryptophan synthase from Escherichia coli. *Protein Sci* **8:** 1623-1635.

Henkels, C.H., Kurz, J.C., Fierke, C.A., and Oas, T.G. 2001. Linked folding and anion binding of the Bacillus subtilis ribonuclease P protein. *Biochemistry* **40:** 2777-2789.

Henry, E.R., and Hofrichter, J. 1992. Singular value decomposition: Application of analysis of experimental data. *Methods Enzymol.* **210:** 129-192.

Ionescu, R.M., Smith, V.F., O'Neill, J.C., Jr., and Matthews, C.R. 2000. Multistate equilibrium unfolding of Escherichia coli dihydrofolate reductase: thermodynamic and spectroscopic description of the native, intermediate, and unfolded ensembles. *Biochemistry* **39:** 9540-9550.

Iouzalen, N., Moreau, J., and Mechali, M. 1996. H2A.ZI, a new variant histone expressed during Xenopus early development exhibits several distinct features from the core histone H2A. *Nucleic Acids Res* **24:** 3947-3952.

Jackson, V. 1990. In vivo studies on the dynamics of histone-DNA interaction: evidence for nucleosome dissolution during replication and transcription and a low level of dissolution independent of both. *Biochemistry* **29:** 719-731.

Jenuwein, T., and Allis, C.D. 2001. Translating the histone code. *Science* **293:** 1074-1080.

Kimura, H., and Cook, P.R. 2001. Kinetics of core histones in living human cells: little exchange of H3 and H4 and some rapid exchange of H2B. *J Cell Biol* **153:** 1341-1353.

Kireeva, M.L., Walter, W., Tchernajenko, V., Bondarenko, V., Kashlev, M., and Studitsky, V.M. 2002. Nucleosome Remodeling Induced by RNA Polymerase II. Loss of the H2A/H2B Dimer during Transcription. *Mol Cell* **9:** 541-552.

Kraulis, P.J. 1991. MOLSCRIPT: a program to produce both detailed and schematic plots of protein structures. *J. Applied Crystallography* **24:** 946-950.

Liu, X., Li, B., and GorovskyMa. 1996. Essential and nonessential histone H2A variants in Tetrahymena thermophila. *Mol Cell Biol* **16:** 4305-4311.

Louters, L., and Chalkley, R. 1984. In vitro exchange of nucleosomal histones H2a and H2b. *Biochemistry* **23:** 547-552.

Louters, L., and Chalkley, R. 1985. Exchange of histones H1, H2A, and H2B in vivo. *Biochemistry* **24:** 3080-3085.

Luger, K., Mader, A.W., Richmond, R.K., Sargent, D.F., and Richmond, T.J. 1997a. Crystal structure of the nucleosome core particle at 2.8 A resolution. *Nature* **389:** 251-260.

Luger, K., Rechsteiner, T.J., Flaus, A.J., Waye, M.M., and Richmond, T.J. 1997b. Characterization of nucleosome core particles containing histone proteins made in bacteria. *J. Mol. Biol.* **272:** 301-311.

Lusser, A., and Kadonaga, J.T. 2003. Chromatin remodeling by ATP-dependent molecular machines. *Bioessays* **25:** 1192-1200.

Mello, C.C., and Barrick, D. 2003. Measuring the stability of partly folded proteins using TMAO. *Protein Sci* **12:** 1522-1529.

Meneghini, M.D., Wu, M., and Madhani, H.D. 2003. Conserved histone variant H2A.Z protects euchromatin from the ectopic spread of silent heterochromatin. *Cell* **112:** 725-736.

Myers, J.K., Pace, C.N., and Scholtz, J.M. 1995. Denaturant *m* values and heat capacity changes: Relation to changes in accessble surface areas of protein folding. *Protein Science* **4:** 2138-2148.

Pace, C.N. 1986. Determination and analysis of urea and guanidine hydrochloride denaturation curves. *Methods Enzymol.* **131:** 266-280.

Park, Y.J., Dyer, P.N., Tremethick, D.J., and Luger, K. 2004. A new fluorescence resonance energy transfer approach demonstrates that the histone variant H2AZ stabilizes the histone octamer within the nucleosome. *J Biol Chem* **279:** 24274-24282. Epub 22004 Mar 24213.

Placek, B.J., and Gloss, L.M. 2002. The N-terminal tails of the H2A-H2B histones affect dimer structure and stability. *Biochemistry* **41:** 14960-14968.

Rangasamy, D., Berven, L., Ridgway, P., and Tremethick, D.J. 2003. Pericentric heterochromatin becomes enriched with H2A.Z during early mammalian development. *Embo J* **22:** 1599-1607.

Rogakou, E.P., Pilch, D.R., Orr, A.H., Ivanova, V.S., and Bonner, W.M. 1998. DNA double-stranded breaks induce histone H2AX phosphorylation on serine 139. *J Biol Chem* **273:** 5858-5868.

Santisteban, M.S., Kalashnikova, T., and Smith, M.M. 2000. Histone H2A.Z regulats transcription and is partially redundant with nucleosome remodeling complexes. *Cell* **103:** 411-422.

Spudich, G., and Marqusee, S. 2000. A change in the apparent m value reveals a populated intermediate under equilibrium conditions in Escherichia coli ribonuclease HI. *Biochemistry* **39:** 11677-11683.

Stargell, L.A., Bowen, J., Dadd, C.A., Dedon, P.C., Davis, M., Cook, R.G., Allis, C.D., and Gorovsky, M.A. 1993. Temporal and spatial association of histone H2A variant hv1 with transcriptionally competent chromatin during nuclear development in Tetrahymena thermophila. *Genes Dev* **7:** 2641-2651.

Strahl, B.D., and Allis, C.D. 2000. The language of covalent histone modifications. *Nature* **403:** 41-45.

Suto, R.K., Clarkson, M.J., Tremethick, D.J., and Luger, K. 2000. Crystal structure of a nucleosome core particle containing the variant histone H2A.Z. *Nat Struct Biol* **7:** 1121-1124.

Timasheff, S.N. 1998. Control of protein stability and reactions by weakly interacting cosolvents: the simplicity of the complicated. *Adv Protein Chem* **51:** 355-432.

Topping, T.B., and Gloss, L.M. 2004. Stability and folding mechanism of mesophilic, thermophilic and hyperthermophilic archael histones: The importance of folding intermediates. *J. Mol. Biol.***:** in press.

van Daal, A., and Elgin, S.C. 1992. A histone variant, H2AvD, is essential in Drosophila melanogaster. *Mol Biol Cell* **3:** 593-602.

Wang, A., and Bolen, D.W. 1997. A naturally occurring protective system in urea-rich cells: mechanism of osmolyte protection of proteins against urea denaturation. *Biochemistry* **36:** 9101-9108.

Zitzewitz, J.A., Bilsel, O., Luo, J., Jones, B.E., and Matthews, C.R. 1995. Probing the folding mechanism of a leucine zipper peptide by stopped-flow circular dichroism spectroscopy. *Biochemistry* **34:** 12812-12819.

Table 1. Parameters describing the equilibrium stability of the H2A/H2B and H2A.Z/H2B dimers.[a]

Histone dimer	[TMAO] (M)	$\Delta G°$ (H_2O) (kcal mol^{-1})	*m* value (kcal mol^{-1} M^{-1})
H2A/H2B[b]	0	11.8 (0.3)	2.9 (0.1)
H2A/H2B	1	15.5 (0.4)	2.7 (0.1)
H2A.Z/H2B	1	7.3 (0.5)	1.1 (0.2)
H2A-ΔC/H2B	0	10.2 (0.2)	2.5 (0.1)

[a]Conditions: 20 mM potassium phosphate, 0.2 M KCl, 0.1 mM EDTA, pH 7.2, 25 ˚C and 1M TMAO where indicated. The values in parentheses represent one standard deviation on the error surfaces of the global fits as determined by rigorous error analysis (Beechem 1992).

[b] From (Gloss and Placek 2002)

1A.

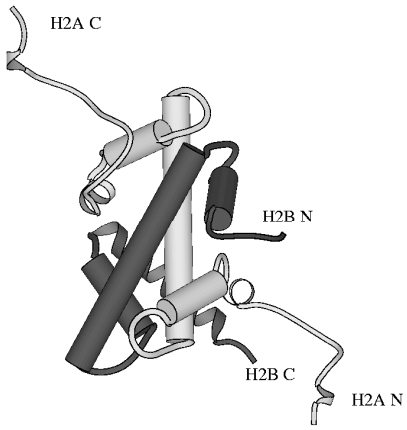

1B.

```
            1                N                1
X.l.A         SG--RGKQGGKT RAKAKTRSSR AGLQFPVGRV HRLLRKGNYA-
X.l.A.Z       AGGKAGKDTGKA KATSITRSSR AGLQFPVGRI HRLLKNRTTSH
M.m.A.Z       AGGKAGKDSGKA KTKAVSRSQR AGLQFPVGRI HRHLKSRTTSH
                       *     *****  *           x   *  *xxx x

           41 2                                          1
X.l.A         ERVGAGAPVY LAAVLEYLTA EILELAGNAA RDNKKTRIIP RHLQLAVRND
X.l.A.Z       GRVGGTAAVY TAAILEYLTA EVLELAGNAS KDLKVKRISP RHLQLAIRGD
M.m.A.Z       GRVGATAAVY SAAILEYLTA EVLELAGNAS KDLKVKRITP RHLQLAIRGD
              x   *x x   *  x        x       x x x xx   *

           91          C
X.l.A         EELNKLLGRV TIAQGGVLPN IQSVLLPKKT ESSKSTKSK
X.l.A.Z       EELDALIK-A TIAGGGVIPH IHKSLIGKKG Q-QKTV
M.m.A.Z       EELDSLIK-A TIAGGGVIPH IHKSLIGKKG Q-QKTV
                 x*
```

Figure 1. Placek *et al.*

Figure 1. A) Ribbon diagram of the H2A/H2B dimer, derived from the X-ray crystal structure of the core nucleosome containing H2A.Z (Luger et al. 1997a). H2A is shown in the lighter gray and H2B is shown in black. The three helices of the canonical histone fold are shown as cylinders. The figure was rendered using Molscript v2.1 (Kraulis 1991). B) Alignment of the protein sequences of the major H2A from *X. laevis* (X.l.A) and the H2A.Z sequences from *X. laevis* and mouse (X.l.A.Z and M.m.A.Z, respectively). Numbering refers to the X.l.A sequence. The regions of helical structure, as observed in the X-ray crystal structures of the NCP, are indicated by the bars above the alignment. Sequence differences between the mouse and *X. laevis* H2A.Z are indicated below the alignment (*). Residues in structured regions that are conserved in several vertebrate major H2A isoforms but are different in the two H2A.Z sequences are underlined; those differences that are conserved between several H2A.Z sequences are indicated by an x below the sequences.

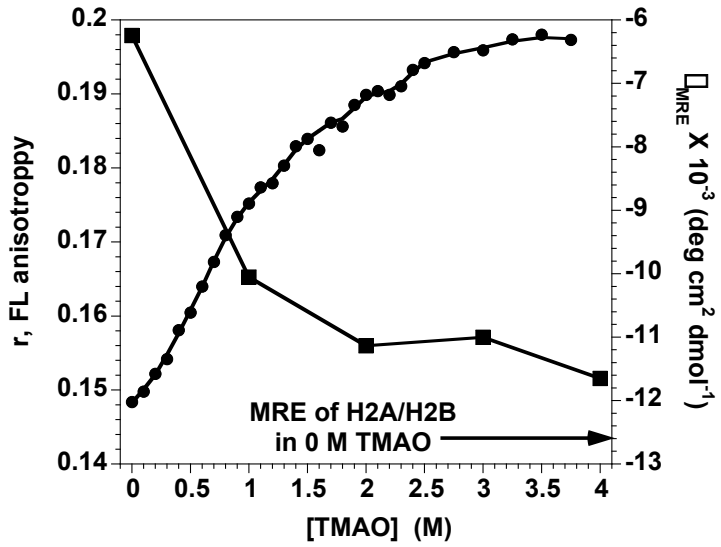

Figure 2: TMAO dependence of the Tyr FL anisotropy (●) and far-UV CD at 222 nm (■)) of the H2A.Z/H2B dimer. The lines are drawn to guide the eye and do represent fits of the data. Conditions: 5 μM dimer, 20 mM KP_i, 0.2 M KCl, 0.1 mM EDTA, pH 7.2, 25 ˚C.

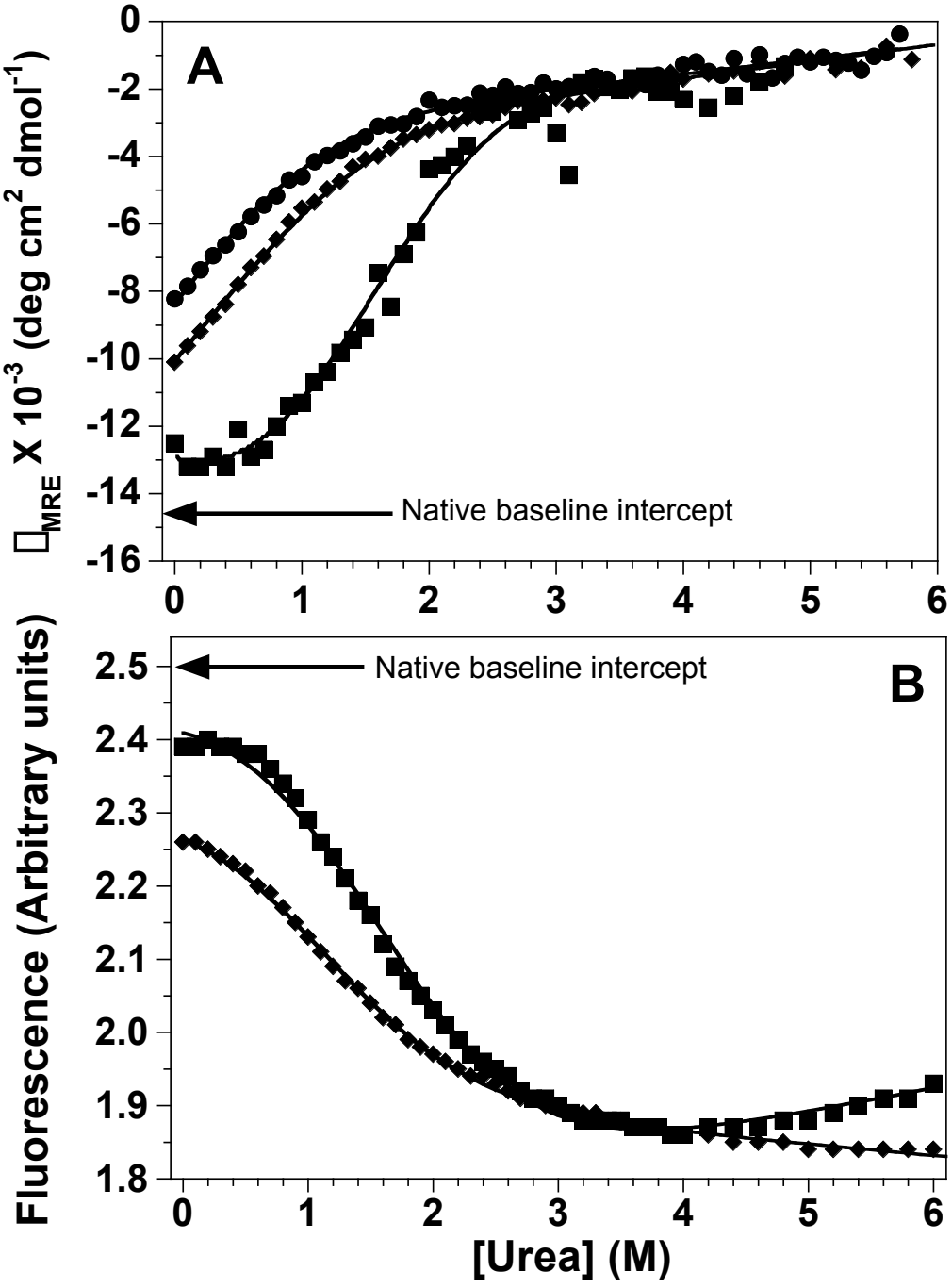

Figure 3. Placek *et al.*

Figure 3: Equilibrium urea unfolding transitions of H2A.Z/H2B in 1 M TMAO. A) Unfolding monitored by CD at 222 nm: 2 μM dimer, ●; 5 μM dimer, ♦; 12 μM dimer, ■. B) Unfolding monitored by intrinsic Tyr FL at 305 nm: 5 μM dimer, ♦; 17.3 μM dimer, ■. The solid lines in both panels represent global fits of multiple data sets. Conditions: 20 mM KP_i, 0.2 M KCl, 0.1 mM EDTA, pH 7.2, 25 ˚C.

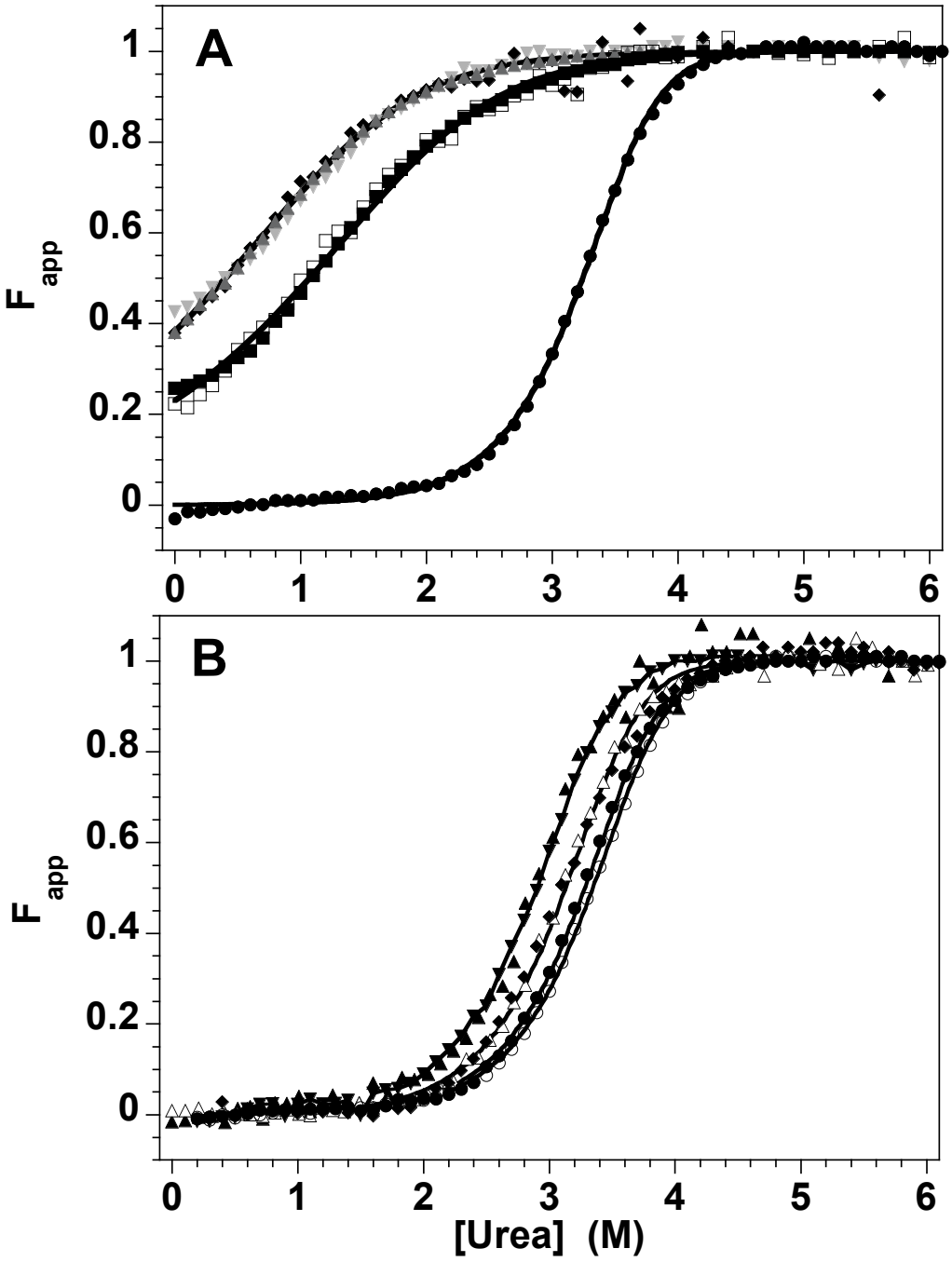

Figure 4. Placek *et al*.

Figure 4: Representative F_{app} curves for the equilibrium urea unfolding of the H2A/H2B heterodimer variants in 1 M TMAO. CD data were collected at 222 nm and FL data at 305 nm. A) H2A.Z/H2B unfolding transitions. 5 µM dimer: CD, ♦; FL intensity, ▲; FL anisotropy, ▼. 17.3 µM dimer: FL intensity, ■; FL anisotropy, □. The unfolding of major H2A/H2B at 5 µM dimer, monitored by FL intensity (●), is shown for comparison. B) Unfolding transitions of the major H2A/H2B. 1 µM dimer: CD, ▲; FL intensity, ▼. 3 µM dimer, CD, □; FL, ♦. 6 µM dimer, FL, ●. 8 µM dimer, FL, ○. For both panels, the solid lines represent global fits of multiple data sets. Conditions are given in the legend of Figure 3.

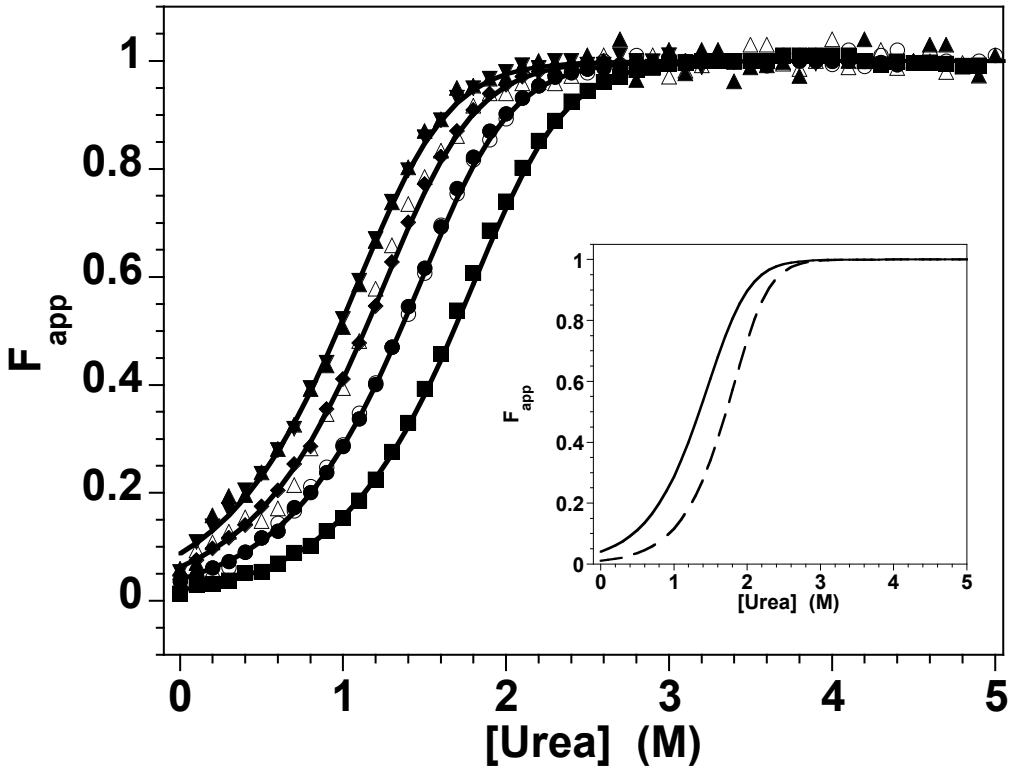

Figure 5. Representative F_{app} curves for the equilibrium urea unfolding of the H2A-ΔC/H2B heterodimer. CD data were collected at 222 nm, and FL intensity data at 305 nm. 1 μM dimer: CD, ▲; FL, ▼. 2 μM dimer: CD, □; FL, ♦. 5 μM dimer: CD, ●; FL, ○. 20 μM, FL, ■. The solid lines represent global fits of multiple data sets. Inset: Comparison of the F_{app} curves of the H2A-ΔC/H2B (solid line) and full length H2A/H2B dimers (dashed line), at 5 μM dimer. Conditions: 0 M TMAO, 20 mM KP_i, 0.2 M KCl, 0.1 mM EDTA, pH 7.2, 25 ˚C.

CHAPTER FOUR

THREE-STATE KINETIC FOLDING MECHANISM OF THE H2A/H2B HETERODIMER: THE INFLUENCE OF THE N-TERMINAL TAILS ON THE TRANSITION STATE BETWEEN A DIMERIC INTERMEDIATE AND THE NATIVE DIMER

This chapter was prepared for submission to the *Journal of Molecular Biology* and therefore differs in format from the remainder of the thesis. I am the first author of this paper. I performed all of the experiments. I contributed to the writing of this paper but Lisa Gloss wrote the majority of the paper.

Abbreviations: BP, burst-phase; CD, circular dichroism; C_M, urea concentration of the midpoint of the equilibrium unfolding transition; FL, intrinsic Tyr fluorescence; $\Delta G°$ (H_2O), the free energy of unfolding in the absence of denaturant; ΔN-H2A, N-terminal tail truncation of the H2A, removing residues 2 through 15; ΔN-H2B, N-terminal tail truncation of the H2B, removing residues 2 through 31; I_2, dimeric folding intermediate; KPi, potassium phosphate; *m* value and $m^{\ddagger}$, the denaturant dependence of the equilibrium unfolding transition and the folding and unfolding rates respectively; MRE, mean residue ellipticity; NCP, nucleosome core particle; N_2, native dimer; SF, stopped-flow; 2U, two unfolded, disassociated monomers.

SUMMARY

The kinetic folding mechanism for the H2A/H2B dimer has been determined by stopped-flow circular dichroism and fluorescence techniques. H2A/H2B heterodimer is a constituent of the nucleosome core particle, which is the basic repeating unit of chromatin in all eukaryotic cells. The kinetic data are consistent with a two-step folding reaction where the two unfolded monomers associate to form a dimeric intermediate with in the dead-time of the instrument (<5 ms), the intermediate is converted to the native dimer by a slower, first order reaction. Analysis of the burst-phase amplitudes as a function of denaturant indicates that the majority of the free energy for the native protein is formed in the intermediate, 9.5 kcal mol^{-1}. Folding-to-unfolding double jump experiments were performed to monitor the formation of the native dimer as a function of folding delay times. The data demonstrates that the dimeric intermediate is on-pathway and obligatory. The formation of a dimeric intermediate in the folding mechanism for H2A/H2B, is seen for a number of other intertwined, α-helical dimers, segment-swapped dimers, and may be a common feature of this class of proteins.

INTRODUCTION

All of the information required for a protein's native structure, the stability of that structure and how this structure is achieved from the unfolded state, is encoded within protein's primary amino acid sequence. The majority of protein folding efforts have focused on monomeric proteins (for review, (Fersht, 1994; Matthews, 1993)) which have provided many insights into the mechanisms of protein folding. Relatively small (usually less than 75 residues), single domain monomers often fold by kinetic two-state mechanism, with no transient intermediates (for review, (Jackson, 1998; Plaxco et al., 2000)). Larger monomers, with multiple domains, often fold through more complicated pathways, including transient kinetic intermediates and potentially parallel pathways (for review, (Kim & Baldwin, 1990; Matthews, 1993; Wallace & Matthews, 2002)). Monomeric systems have provided many insights that have guided efforts to predict protein structure, stability and folding mechanism. However, the current state of these predictive abilities is still imperfect. Furthermore, less headway has been made on applying such predictive methods to oligomer protein folding, particularly with respect to stability and folding mechanism, where the formation and stability of secondary and tertiary structures must be coordinated with the development of quaternary structure.

The smallest dimeric model folding systems, for example, single domain systems such as *Arc* repressor and GCN4 leucine zipper peptides, exhibit two state folding kinetics.(Milla & Sauer, 1994; Zitzewitz et al., 1995) However, larger model systems, particularly those that can be dissected into multiple domains, fold through multiple kinetic steps and sometimes, multiple pathways; examples include bacterial luciferase,(Clark et al., 1997; Noland & Baldwin, 2003) ketosteroid isomerase,(Kim et al., 2001a; Kim et al., 2001b) glutathione S-transferases.(Wallace & Dirr, 1999; Wallace et al., 1998) We have focused on a group of DNA-binding dimers with intertwined, segment-swapped, □-helical interfaces, including the *E. coli* proteins, *Trp* repressor(Gloss & Matthews, 1998a; Gloss & Matthews, 1998b; Gloss et al., 2001) and FIS(Topping et al., 2004) (Factor for Inversion Stimulation) as well as the histone fold contained in homodimeric archael histones(Topping & Gloss, 2004) and the hetero-oligomeric histones of

the eukaryotic core nucleosome. The folding mechanism of the H3/H4 dimer-tetramer system has been reported previously.(Banks & Gloss, 2003; Banks & Gloss, 2004)

Two H2A/H2B heterodimers and a dimer of H3/H4 dimers (the H3/H4 tetramer) comprise the histone protein core of the nucleosome, around which ~150 bp of DNA is wrapped. This nucleosome core particle, NCP, is the basic repeating structural unit of chromatin, which facilitates the packaging of DNA within the nucleus of eukaryotic cells. The core histone proteins contain a highly conserved structural motif that has been termed the histone fold.(Arents & Moudrianakis, 1993; Luger et al., 1997) This fold is defined by a long central α-helix, which is flanked on the N and C termini by a loop and a a shorter α-helix (Figure 1). Two monomers form a heterodimer by docking in a head to tail arrangement, termed the hand-shake motif,(Arents & Moudrianakis, 1995) with intertwining of the helices from each monomer. All of the core histones contain an N-terminal tail that is highly basic and poorly resolved in the X-ray crystal structure of the NCP.(Luger et al., 1997) These N-terminal tails are also the major sites of post-translational modifications that regulate the dynamics of chromatin structure in response to a variety of nuclear processes, including replication, transcription, gene silencing and repair.(Strahl & Allis, 2000) These post-translational modifications include methylation of lysines and arginines, acetylation of lysines and phosphorylation of serines; the latter two modifications clearly alter the charge state of the N-terminal tails.

We have previously reported on the equilibrium stability of the H2A/H2B heterodimer(Gloss & Placek, 2002) and N-terminal tail truncated variants of this heterodimer.(Placek & Gloss, 2002) The N-terminal tails of H2A and H2B have a small, but significant effect on the stability of the dimer, and the salt-dependence of the stabilities of the full-length and truncated H2A/H2B dimers demonstrated the importance of electrostatic repulsion in destabilizing the heterodimer. This report focuses on the kinetic folding mechanism of the H2A/H2B heterodimer, and how the N-terminal tails alter the transistion state between the folded dimer and the oligatory dimeric intermediate.

Results

To determine the kinetic mechanism of folding and assembly of the H2A/H2B histone dimer, the kinetics of the unfolding and folding reactions were examined as a function of final urea concentration. Stopped-flow mixing methods were used, and the kinetic responses detected by far-UV CD at 222 nm to monitor helical structure and intrinsic Tyr FL to monitor tertiatry and quaternary structure (representative kinetic traces are shown in Figure 2). H2A and H2B contain three and five Tyr residues, respectively, which are partially to completely buried in the native dimer, forming intra- and inter-chain interactions. For both folding and unfolding, relaxation times determined from SF-FL and SF-CD were very similar. The unfolding and folding kinetic responses of the ΔN-H2A/H2B and H2A/ΔN-H2B heterodimers were also examined, to ascertain the impact of electrostatic repulsion on the development of native structure.

Unfolding reaction. Unfolding kinetic traces were collected for the three H2A/H2B variants by SF jumps from 0 M urea to various final urea concentrations and 7.5 μM monomer. At all urea concentrations, from 1.6 M to 3.6 M, the kinetic traces were well-described by fits to a single, first-order exponential phase (Eq. 3, data not shown). The average relaxation times obtained from local fits are shown in Figures 3A-C. The fitted initial and final signals agreed well with those expected from equilibrium data for the conversion of native dimer to unfolded monomers. These data suggest that there is no kinetic unfolding intermediate formed in the SF deadtime of ~5 ms. There is a significant urea dependence of the unfolding relaxation times, a log linear decrease in relaxation time with increasing [Urea]. Kinetic traces under strongly unfolding conditions, $\geq$ 1.8 M urea, were globally fit to Equation 4 (Methods) to determine the urea dependence of the unfolding kinetics of the three H2A/H2B variants. The global fits yield two paramters, k_u (H_2O), the unfolding rate in the absence of denaturant, and the $m^{\ddagger}$ value, which reflects the sensitivity of the reaction to the denaturant concentration. This latter parameter is usually considered to be proportional to the change in solvent accessible surface area between the initial species and the transition state. The results of the global fits are shown in Figure 3;

the fitted parameters are summarized in Table 1. The global fits are in excellent agreement with the locally fitted data (Figures 3A-C).

Folding reaction—first order kinetic phase. Folding reactions were initiated by SF dilution of an equimolar mixture of the H2A and H2B monomers in 4 M urea. Final urea concentrations of 0.5 to 1.8 M were obtained, and a final [Monomer] of 7.5 μM. SF-Fl and SF-CD kinetic traces were well fit by a single, first-order exponential equation (Eq. 3, Figure 2). Second order kinetic traces are generally not well fit by a single exponential. Furthermore, the observed relaxation times did not depend significantly on protein concentration (data not shown). Under strongly refolding conditions, the relaxation time at 1 μM dimer was 2.7-fold greater than at 12 μM dimer. The expected difference in relaxation times for a second-order, monomer association reaction would be ~12-fold. Therefore, it is clear that the kinetic folding phase observed on the SF time-scale is not a second order process involving monomer association.

The locally fitted folding relaxation times exhibit a significant urea dependence, increasing with increasing urea concentrations, as typical for a protein folding reaction. The kinetic data from 0.5 to 1.6 M urea were globally fittted to Eq. 4 to determine the urea dependence of the folding kinetics. The results are shown in Figure 3 and summarized in Table 1. As observed for the unfolding kinetics, there is good agreement between the local and global fits for all three H2A/H2B variants. For the full-length H2A/H2B dimer, folding kinetics as a function of [Urea] were also collected at a final [Monomer] of 3.75 μM (Figure 3A). The $m^{\ddagger}$ value was very similar, 1.03 kcal $mol^{-1}M^{-1}$, to that determined from the fits of the data at 7.5 μM monomer. The k_f (H_2O) value was 1.9-fold greater than that determined for the 7.5 μM monomer data—again, a difference that is less than expected for a second-order process, 4-fold. The folding leg of the "Chevron" in Figure 3A appears to be shifted to lower [Urea] for the lower monomer concentration. This is expected for a first order step in an overall second order equilibrium process, such as folding of a dimeric protein. The small effect of monomer concentration on the observed relaxation times is consistent with the protein concentration dependence of the stability, as reflected by the different final equilibrium position (or F_{app},

apparent fraction unfolded) of the dimer at different protein concentrations. Thus, the shift of the Chevron mimics the shift of the F_{app} curves and C_M values in equilibrium data collected as a function of [dimer].(Gloss & Placek, 2002; Placek & Gloss, 2002)

The observed folding relaxation times converge with the unfolding relaxation times near the midpoint of the equilibrium transition, ~1.6 to 2 M urea, for all three H2A/H2B variants. This convergence is expected if the two reactions are the reverse of each other, *i.e.* the folding reaction leads to the native dimer from which the unfolding reaction is intiated. Therefore, the convergence strongly suggests that the first-order folding reaction converts the folding ensembe to the native dimer. If a first-order kinetic phase leads to the native dimer in the observed folding reaction, the association of the monomers must occur in a faster, preceding reaction, such as a burst-phase reaction occuring in the ~5 ms dead time of the stopped-flow instrument.

Folding reaction—burst phase dimerization phase. SF-CD amplitudes can be compared to equilibrium transistions monitored at 222 nm. (However, such a comparison is difficult for FL data; SF-FL was collected at all wavelengths above a 295 nm cut-off filter, and equilibrium FL data was collected at a 2 nm bandwidth around the wavelength of 305 nm.) The SF-CD signal detected after the 5 ms SF dead time is significantly greater than that expected for the unfolded monomers (Figure 2A). The fitted SF-CD amplitude for the observed kinetic phase is far less than that expected for the conversion of unfolded monomers to the native dimer, as determined from equilibrium experiments. These signal/ampliude comparisons indicate that a burst phase reaction has occurred in the SF dead time which proceeds with a significant development of secondary structure. The urea dependence of the SF-CD signals were examined (Figure 4). The final ellipticities for both folding and unfolding SF-CD kinetics agree well with the urea dependence of the equilibrium data. The burst phase signal exhibits a protein concentration dependence, increasing with monomer concentration, that is consistent with a second order association reaction. Furthermore, the BP amplitudes decrease with increasing urea concentration as expected for a transient kinetic intermediate.

To determine the stability of this apparent BP intermediate, the BP signal of full-length H2A/H2B, at two monomer concentrations, 3.75 and 7.5 μM monomer, were globally fit to a two state monomer-to-dimer model as described elsewhere for other apparently dimeric burst phase intermediates.(Topping et al., 2004) In the fit, the unfolded baseline was fixed at values the determined from the final signal of SF-CD unfolding kinetics, in agreement with equilibrium data. The slope of the folded baseline was fixed at that determined for the final SF-CD equilibrium signal. The intercept of the folded baseline for the kinetic intermediate was not fixed, but was linked between the two monomer concentrations. The results of the global fit are shown in the solid lines in Figure 4. The fitted $\Delta G°$ (H_2O) and *m* values for the BP reaction were 9.5 kcal mol^{-1} and 1.6 kcal $mol^{-1}M^{-1}$, respectively. These values are a significant proportion of those reported for the equilibrium stability of the H2A/H2B dimer: $\Delta G°$ (H_2O) of 11.8 kcal mol^{-1} and an *m* value of 2.9 kcal $mol^{-1}M^{-1}$.(Gloss & Placek, 2002)

Folding → unfolding double jump study. The SF-CD amplitude data (Figure 4) demonstrates that a substantial portion of the secondary structure of the native ensemble, N_2, is formed in the 5 ms SF dead time; at the lowest urea concentrations, the BP CD signal is ~50% of that of the final N_2 signal. Furthermore, the BP signal is protein concentration dependent as expected for a transient dimeric kinetic intermediate, I_2. The folding and unfolding kinetic responses also suggest that dimerization occurs in the burst-phase for at least some of the folding monomers which are then converted to the native dimer by a subsequent first-order reaction observable on the SF time scale. However, it is possible that the BP I_2 species is not an obligatory, on-pathway intermediate, and that some fraction of the monomers can fold directly the native heterodimer in the 5 ms SF dead time. To address this possibility, it is necessary to directly assay the time-dependent population of the native state. The detection method of the assay must be on a time scale that is comensurate with or exceeds the observed rates of folding, such as the spectroscopic detection of specific ligand binding. Unfortunately, no such assay has been developed for the histone proteins. However, double jump experiments are able to assay

the development of the native species by virtue of the slower rate of unfolding of N_2, relative to any transient kinetic intermediates.

In a typical folding-unfolding double-jump experiment, unfolded protein is diluted in the stopped flow such that the denaturant concentration is reduced to a range where folding is favored. The protein ensemble is allowed to fold for varying lengths of time, after which the protein solution is then injected into buffer with a higher urea concentration that favors the unfolding reaction (specific conditions are given in the legend of Figure 5). This unfolding reaction is then monitored by SF-FL or SF-CD; in this report, SF-FL was used because of the higher sensitivity of this spectroscopic probe. The unfolding reactions after the folding delay exhibited a single kinetic phase, with relaxation times that were not dependent on delay time. Therefore, the unfolding double jump data set was globally fit to a single exponential, with the relaxation time linked across all kinetic traces. The unfolding relaxation time for the double jump data was 1.0 s, in good agreement with that measured by SF-FL for the direct unfolding under these conditions, 1.3 s.

The unfolding amplitudes as a function of folding delay time are shown in Figure 5. At the shortest accessible delay times, 8 to 12 ms, very little unfolding amplitude was detected, demonstrating that virtually no N_2 dimer is populated in the BP reaction. As the folding delay time increases, the detected unfolding amplitude increases with a relaxation time of 1.0 ± 0.2 s (fitted line in Figure 5), in excellent agreement with the relaxation time measured for direct folding to these conditions, 1.1 s. This agreement demonstrates that the observed kinetic phase in SF-CD and SF-FL does lead to the native dimer. Furthermore, the fitted change in amplitude as a function of delay time constitutes 98% of the total unfolding amplitude after the longest refolding delays, confirming that the virtually all of the folding proceeds through the dimeric BP I_2 species. The results of the double jump data demonstrate that the structure detected in the SF BP constitutes an obligatory, on-pathway kinetic intermediate in the folding of the H2A/H2B dimer.

Discussion

Folding mechanism of H2A/H2B. The kinetic folding mechanism of the histone dimer H2A/H2B involves two discernable kinetic steps: 1) development of a significant amount of secondary structure in intermediate ensemble that is formed in the 5 ms SF dead time; and 2) a first order folding reaction that leads to the formation of the native H2A/H2B dimer. In combination, four results demonstrate that the BP intermediate is an obligatory dimeric kinetic intermediate, I_2, that is subsequently converted to the native heterodimer. First, the kinetic response observed by SF-FL and SF-CD was well described by a single exponential (Figure 2) and exhibited very little protein concentration dependence, consistent with a first order reaction, not a process involving monomer association. Second, the convergence of the folding relaxation times with those of the unfolding reaction near the midpoint of the equilibrium transition demonstrates that this first order process leads to the formation of the native dimer in the rate-determining step of folding (Figure 3). Third, the double-jump experiments demonstrate that formation of the native dimer is constrained by the observed first order folding reaction, with no native dimer formed in the BP reaction (Figure 5). Therefore, dimerization must precede the observed first order step. Fourth, the BP SF-CD signal increases with increasing protein concentration dependence in a manner that is consistent with formation of a dimeric intermediate in the SF dead time (Figure 4). Therefore, the proposed mechanism for the folding of the H2A/H2B dimer is shown in Scheme 1: the H2A and H2B monomers rapidly associate in a burst phase reaction to form a dimeric intermediate that then folds to the native dimer in a subsequent first order folding reaction. The apparent relaxation time for dimerization must be less than 5 ms, given that the formation of I_2 is complete in the SF deadtime, even at final dimer concentrations of 1 to 2 μM. Therefore, the second order rate constant, $k_{assoc} \geq 10^8\ M^{-1}s^{-1}$, approaching the diffusion limit. Scheme 1 represents a minimal mechanism; because the dimerization reaction is not directly detected, but occurs in the SF dead time, it is not known if the monomers are unfolded or have undergone a partial folding reaction before association.

Another possible two step mechanism is one in which I_2 is an off-pathway intermediate: $I_2 \leftarrow 2U \rightarrow N_2$ where protein that folds to I_2 or N_2 in burst-phase reactions, but I_2 must then unfold by the observed, rate-limiting first order process in order to reach the native state. A potential I_2 species might be an unproductive homo-typic dimerization. Computational studies (for review, (Plotkin & Onuchic, 2002a; Plotkin & Onuchic, 2002b)) and the growing number of small, monomeric proteins that fold rapidly without kinetic intermediates (for review, (Jackson, 1998; Plaxco et al., 2000)), have suggested that intermediates can be kinetic traps that hinder productive folding. Therefore, it is important to consider such an off-pathway mechanism. However, two lines of evidence make it implausible that I_2 is an unproductive, off-pathway intermediate. First, as stated above, the convergence of the observed folding and unfolding relaxation times shows that I_2 can proceed to N_2. Second, the off-pathway model would require that the first order reaction is actually an unfolding reaction to convert I_2 back to the unfolded monomers. Such an unfolding reaction would predict $m^{\ddagger}$ value < 0, as seen for the unfolding reaction starting from folded dimer (Figure 3, Table 1), but not the first order reaction observed under folding conditions.

Properties of the SF-CD burst phase intermediate, I_2, and the transition state between I_2 and N_2. At 0.5 to 0.75 M urea, the XXXFitting of the BP CD signal as a function permits an assessment of the stability of the I_2 ensemble. The fitted $\Delta G°$ (H_2O) value is 9.5 kcal mol^{-1}, at a standard state of 1 M dimer, which is 80% of the stability of the native dimer. Fitting of the data also provides an estimate of the *m* value for the conversion between unfolded monomers and the I_2 ensemble—a value of 1.6 kcal $mol^{-1}M^{-1}$. This parameter often correlates with the change in accessible surface area between the unfolded and folded states. The magnitude of the *m* value for the 2U to I_2 reaction suggests that the transient kinetic intermediate has buried 55% of the total surface area buried in the equilibrium transition to the native heterodimer. Thus, the I_2 species has significant stability, relative to the native dimer, but lacks certain elements of structure in the formation of helices and burial of surface area.

The stabilization associated with the conversion of I_2 to the native dimer can be determined from the observed folding and unfolding kinetic data in the Chevron plots in Figure 3, using the following relationships:

$$\Delta G^{\circ}_{I_2 \rightarrow N_2}(H_2O) = RT \ln\left[\frac{k_u(H_2O)}{k_f(H_2O)}\right] \qquad (1a)$$

$$m_{I_2 \rightarrow N_2} = m^{\ddagger}_{\mathrm{f}} - m^{\ddagger}_{\mathrm{u}} \qquad (1b)$$

The calculated values are given in Table 1. The parameters describing the conversion of unfolded monomers to folded dimer, as determined from kinetic experiments, can be compared to those published previously for the equilibrium properties of the full-length H2A/H2B dimer.(Gloss & Placek, 2002) The summation of properties determined from the BP analyes and the Chevron plots yield $\Delta G°$ (H_2O) and *m* values of 12.2 kcal mol^{-1} and 3.2 kcal $mol^{-1}M^{-1}$, respectively for the conversion of 2U to N_2. Thus, the stability based on the kinetic mechanism shown in Scheme 1 is in good agreement with the stability determined by equilibrium methods, $\Delta G°$ (H_2O) of 11.8 kcal mol^{-1} and an *m* value of 2.9 kcal $mol^{-1}M^{-1}$. This agreement is further support for the proposed kinetic mechanism for the folding of the H2A/H2B dimer.

The deletion of the N-terminal tails of H2A and H2B appear to have little effect on the overall folding mechanism, as judged by similar urea dependence of the BP CD signal (data not shown) and the stability determined from the observed folding/unfolding kinetics (Table 1). This lack of an effect is not surprising given the subtle differences in stability between the full-length and N-terminal truncated H2A/H2B variants.(Placek & Gloss, 2002) However, the N-terminal tails do affect the transition state between I_2 and N_2. Removal of either N-terminal tail has minimal effects on the folding kinetics. However, the unfolding kinetics are significantly impacted, with changes in the rates as well as the urea-dependence of the rates (Figure 3D). Removal of the H2A N-terminal tail decreases the k_u (H_2O) value by nearly a factor of 2, with an

increase in the $m^{\ddagger}_{u}$ value. Removal of the H2B N-terminal tail has little effect on the k_u (H_2O) value, but decreases the $m^{\ddagger}_{u}$ value. The net result is an apparent movement of the transition state. The position of the transition state, or its similarity to the native state, can be quantified by the Φ value:

$$\Phi = \frac{m^{\ddagger}_{f}}{m^{\ddagger}_{f} - m^{\ddagger}_{u}} \qquad 2$$

The Φ value generally varies from 0, a very I_2-like transition state, to 1, a very native-like transition state. The Φ value for the full-length H2A/H2B, 0.67 (Table 1), suggests that the transition state has a fairly native-like burial of surface area. The removal of the H2A N-terminal tail, which results in a less stable ΔN-H2A/H2B, decreases the Φ value, implying a less native-like transition state. Conversely, removal of the H2B N-terminal tail, which makes a more stable H2A/ΔN-H2B, increases the Φ value, making the transition state more native like. This movement along the reaction coordinate is consistent with the Hammond postulate (for review, (Fersht, 1999))

Comparison of H2A/H2B folding mechanism to other dimers containing the histone fold. The histone fold is an intertwined, segment-swapped, α-helical dimerization interface. The structure is found not only in H2A/H2B, but also in the H3/H4 dimer/tetramer of the core nucleosome and the homodimeric archael histones. Both eukaryotic core heterodimers fold by the mechanism shown in Scheme 1, with a association rate that approaches the diffusion limit to form a transient dimeric I_2 ensemble in the SF dead time. This conservation of mechanism is accompanied by a conservation of structure, with little conservation of sequence. The archael histones appear to fold directly to the native dimer, with no dimeric intermediate.(Topping & Gloss, 2004) However, the association rate for the archael histones are much slower, on the order of 10^6 $M^{-1}s^{-1}$. This rapid folding, with near diffusion limited association reactions to form

a I_2 kinetic species has been observed for the other two intertwined, segment-swapped, α-helical DNA-binding dimers whose folding mechanisms have been elucidated, FIS(Topping et al., 2004) (Factor for Inversion Stimulation) and *Trp* repressor(Gloss & Matthews, 1998a; Gloss & Matthews, 1998b; Gloss et al., 2001). These comparisons strongly suggests that kinetic folding intermediates serve to accelerate protein folding by breaking down the cooperativity of the folding event into multiple steps with lower individual transition state energies between the steps.

Materials and Methods

Materials. Ultrapure urea was purchased from ICN Biomedicals (Costa Mesa, CA). All other chemicals were of reagent or molecular biology grade. The *E. coli* recombinant overexpression, purification and reconstitution of the wild-type and N-terminal truncation mutants of the H2A and H2B proteins have been described previously.(Gloss & Placek, 2002; Placek & Gloss, 2002)

Methods.

CD and FL data collection. The buffer conditions for all experiments were 20 mM KPi, 200 mM KCl, 0.1 mM K_2EDTA, pH 7.2 and 25 ºC. Stopped-flow kinetic data were collected with an AVIV Instruments stopped-flow tower interfaced with an AVIV 202SF CD spectrometer. Stopped-flow CD data were collected at 222 nm. Stopped-flow FL data were collected with an excitation wavelength of 280 nm and monitoring the fluorescence at 90° relative to the incoming light after a 295 nm cutoff filter. The dead time of the stopped-flow instrument is ~5 ms for a typical push velocity of 2 ml/s. For SF-CD and SF-FL ~40 and 20 traces were averaged, respectively, to improve the signal to noise ratio.

Data analyses. Individual kinetic traces were fit locally using the KaleidaGraph 3.5 software (Synergy Software, Reading, PA) to the equation:

$$Y(t) = Y_{\infty} + \Delta Y_i \exp\left(\frac{-t}{\tau_i}\right) \quad (3)$$

where ΔY_t is the amplitude associated with the kinetic phase, τ is equal to the relaxation time and Y_∞ is the final equilibrium signal of the reaction. The folding and unfolding data were well described by fits to a single, first-order exponential.

Global analyses of the kinetic data were performed with the Savuka 5.1 software. This software allows the simultaneous fitting of multiple data sets collected under different conditions or with different spectral probes, such as CD and FL. The urea dependencies of the relaxation times were fit to the equation:

$$\frac{1}{\tau_i} = k_{(H_2O)} \exp\left(\frac{m^{\ddagger}[Urea]}{RT}\right) \quad (4)$$

where k (H_2O) is the rate constant of the folding or unfolding reaction in the absence of denaturant and $m^{\ddagger}$ reflects the sensitivity of the reaction to denaturant. In global fits of the data sets at multiple monomer concentrations, the values of $m^{\ddagger}$ and k (H_2O) were linked over all kinetic traces for a given dimer at a given protein concentration. The values of ΔY_i and Y_∞ were treated as local parameters and not linked between data sets. The burst-phase CD signals determined from the global fits of the data were fitted to a two-state equilibrium model for the unfolding of a dimer to two unfolded monomer, using equations described elsewhere.(Gittelman & Matthews, 1990; Gloss & Placek, 2002; Topping et al., 2004) In the global fitting of the BP data, the $\Delta G^{o}(H_2O)$ and *m* values were treated as global parameters.

Double-jump Experiments. Stopped-flow double jump experiments were performed using an AVIV Instruments three syringe mixer, with a delay line between the first and second mixers. Unfolded protein was mixed with refolding buffer in the first mixer, and this sample was allowed to age in the delay line for varying lengths of time. The solution was then mixed with unfolding buffer in the second mixer, and the unfolding reaction was monitored by intrinsic Tyr FL. For delay times of less than 12 ms, a 11 μL delay line was used; for longer delay

times, a 198 μL delay line was used. With the 11 μL delay line, different delay times were achieved by varying the push velocity.

Acknowledgements

This work was supported by grants to L.M.G. from the National Science Foundation (MCB-9983831) and the American Cancer Society (RPG-00-085-01-GMC). B.J.P. was partially supported by an NIH Biotechnology training grant (GM08336-13). The pET over-expression vectors for the wild-type histone genes were kindly provided by Drs. Karolin Luger (Department of Biochemistry & Molecular Biology, Colorado State University) and Timothy Richmond (Instititute for Molecular Biology and Biophysics at the ETHZ, Zurich, Switzerland).

Table 1. Kinetic parameters describing the folding and unfolding reactions of full-length and N-terminal truncated H2A/H2B variants.[a]

Parameter	H2A/H2B	□N-H2A/ H2B	H2A/□N-H2B
Folding			
k_f (H_2O) (s^{-1})	5.7 (0.3)	4.2 (0.1)	6.3 (0.1)
$m^{\ddagger}_f$ (kcal $mol^{-1}M^{-1}$)	1.08 (0.03)	0.86 (0.01)	1.06 (0.01)
# kinetic traces	53	40	47
Unfolding			
k_u (H_2O) (s^{-1})	0.060 (0.003)	0.035 (0.002)	0.062 (0.002)
$m^{\ddagger}_u$ (kcal $mol^{-1}M^{-1}$)	-0.52 (0.01)	-0.74 (0.01)	-0.40 (0.01)
# kinetic traces	57	48	71
I_2 to N_2 values[b]			
ΔG° (H_2O) (kcal mol^{-1})	2.70	2.83	2.74
m value (kcal $mol^{-1}M^{-1}$)	1.60	1.60	1.46
□ value[c]	0.67	0.54	0.73

[a]Conditions: final monomer concentration of 7.5 μM; 200 mM KCl, 0.1 mM EDTA, 20 mM KPi, pH 7.2, 25 °C. Parameters are the result of global fitting of the kinetic data to Equation 4. The numbers in parentheses are the error at one standard deviation.

[b]The values for the I_2 to N_2 reaction were calculated from Equations 1a and 1b.

[c]Calculated from Equation 2.

Figure and Scheme legends

Figure 1. Ribbon diagram of the H2A-H2B dimer, derived from the X-ray crystal structure of the core nucleosome (Luger et al., 1997). The H2A monomer is shown as the red chain, H2B in magenta with the C-terminal helix beyond the histone fold shown in yellow. The H2A monomer shows residues 4 to 118 (of 129 residues), and the H2B monomer shows residues 24 to 122 (of 122 residues). The Cα atoms of H2A-15 and H2B-32 are highlighted as spheres; these are the residues after the N-terminal methionine residue in the ΔN constructs. The figure was rendered using Molscript v2.1 (Kraulis, 1991).

Figure 2. Representative folding kinetic traces for the full-length H2A/H2B. In both panels, the heavy dark lines represent a global fit of the data to a single first order exponential (Equations 3 and 4). A) SF-FL. B) SF-CD. The expected CD signal of unfolded H2A/H2B under these conditions, as extrapolated from the linear unfolded baseline observed in equilibrium experiments and the final amplitudes of SF-CD unfolding kinetics, is indicated. Conditions: Final [monomer] of 7.5 μM, final [Urea] of 0.5 M, 200 mM KCl, 0.1 mM EDTA, 20 mM KPi, pH 7.2, 25 °C.

Figure 3. Urea dependence of the folding and unfolding kinetic phases. Local fits of SF-CD and SF-FL kinetic traces are shown as points; the data points approximate the error obtained from replicate kinetic traces at each [Urea]. The global fits of the data to Equation 4 are shown as lines, and the fitted parameters are given in Table 1. A) full-length H2A/H2B: final monomer concentrations of 7.5 μM, folding, ●; unfolding, ◆; and 3.75 μM folding, ■. B) H2A/ΔN-H2B: folding, ●, and unfolding, ◆, to 7.5 μM monomer. C) ΔN-H2A/H2B: folding, ●, and unfolding, ◆, to 7.5 μM monomer. D) Overlay of the folding and unfolding global fits for the three dimers: H2A/H2B, solid lines; H2A/ΔN-H2B, dashed lines; ΔN-H2A/H2B, dotted lines. Buffer conditions are given in the legend of Figure 2.

Figure 4. Stopped-flow ellipticities of full-length H2A/H2B as a function of urea concentration. The data have been normalized for differences in cuvette/buffer contributions and monomer concentrations. Burst phase signals at 3.75 μM monomer, ■, and 7.5 μM monomer, ●. For clarity, the final signals are only shown for the 7.5 μM data: folding, ○, and unfolding, ❑. The folded and unfolded baselines for the native state (dotted lines) were determined from equilibrium transitions and the final amplitudes of SF-CD unfolding data. Representative equilibrium transitions and fits of the burst-phase data to a two-state equilibrium model are shown as solid lines. The native baseline of the burst-phase intermediate is shown as a dashed line. Buffer conditions are given in the legend of Figure 2.

Figure 5. Folding → unfolding double jump experiment for full-length H2A/H2B dimer. The unfolding amplitude, as detected by SF-FL, is plotted as a function of folding delay time. The solid line represents the fit of the data to a single exponential, with a relaxation time of 1.0 s; this value is in excellent agreement with the value obtained for direct folding under these conditions, 1.1 s. The fitted change in amplitude as a function of delay time is 98% of the fitted total signal change. Conditions: 26 □M dimer unfolded in 3.5 M urea was refolded by SF dilution to 1 M urea and 7.5 □M dimer, and allowed to refold for 4 ms to 10 s. After the folding delay, a second SF jump was made to the unfolding conditions of 3 M urea, and a final monomer concentration of 7.5 μM monomer. Buffer conditions were as described in the legend of Figure 2.

Scheme 1. Kinetic mechanism for the folding of the H2A/H2B heterodimer.

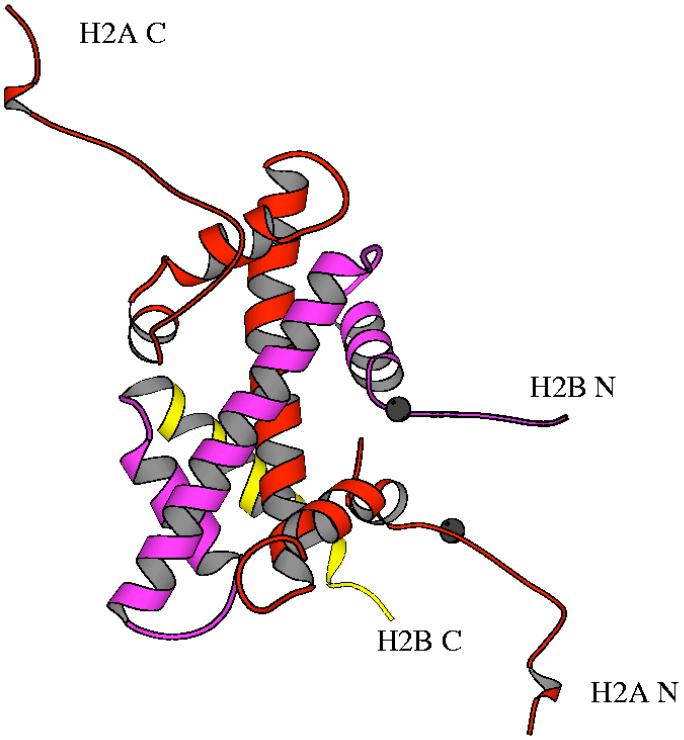

Figure 1. Placek & Gloss

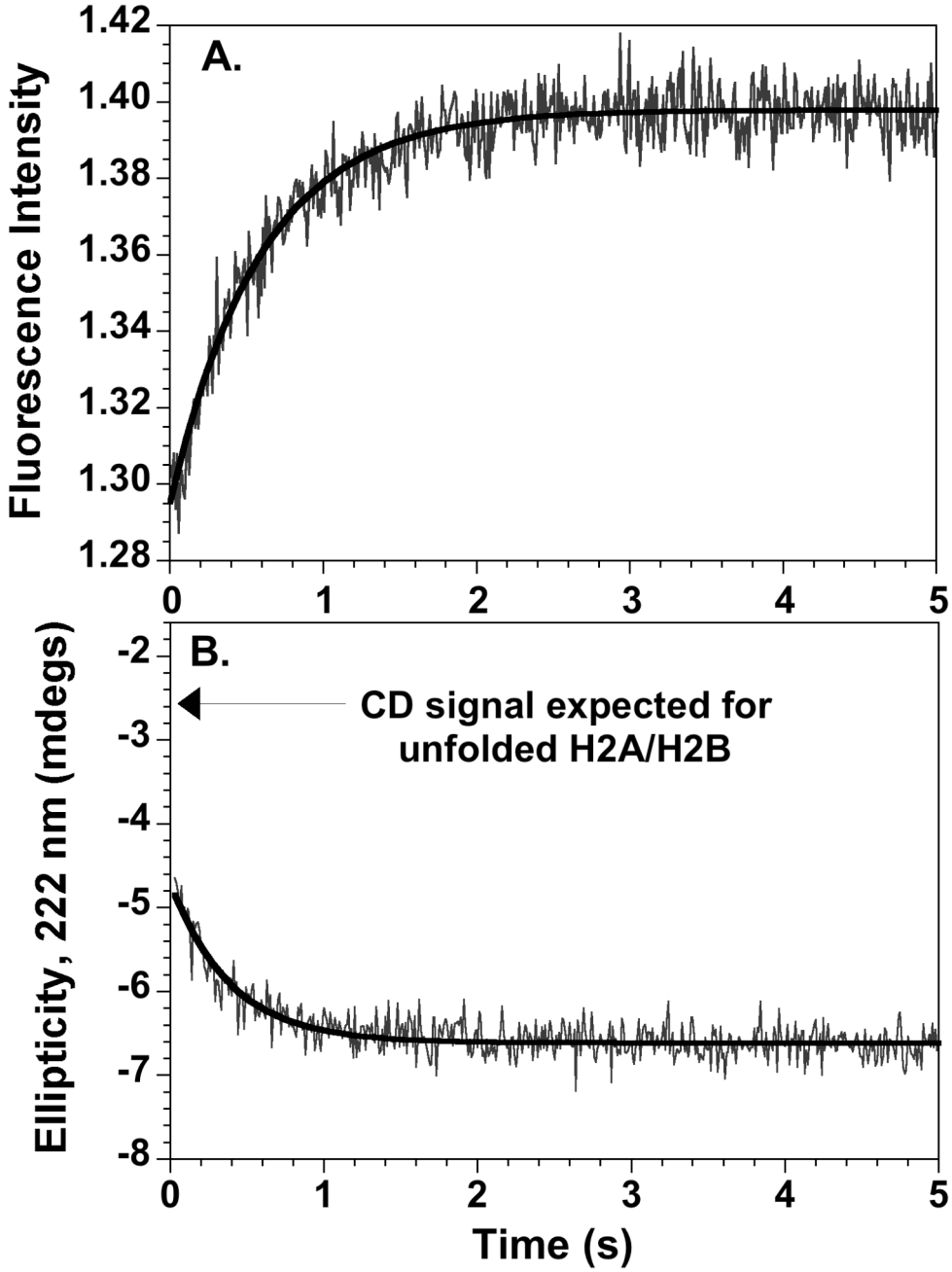

Figure 2. Placek & Gloss

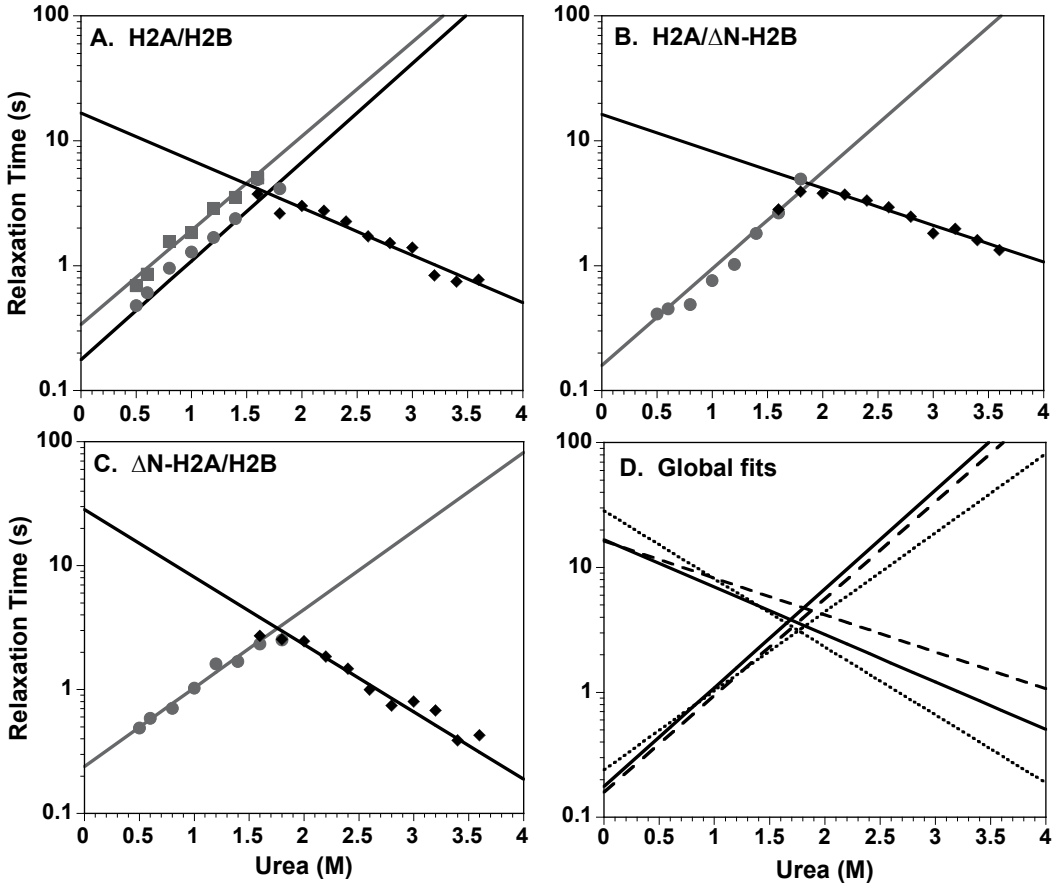

Figure 3. Placek & Gloss

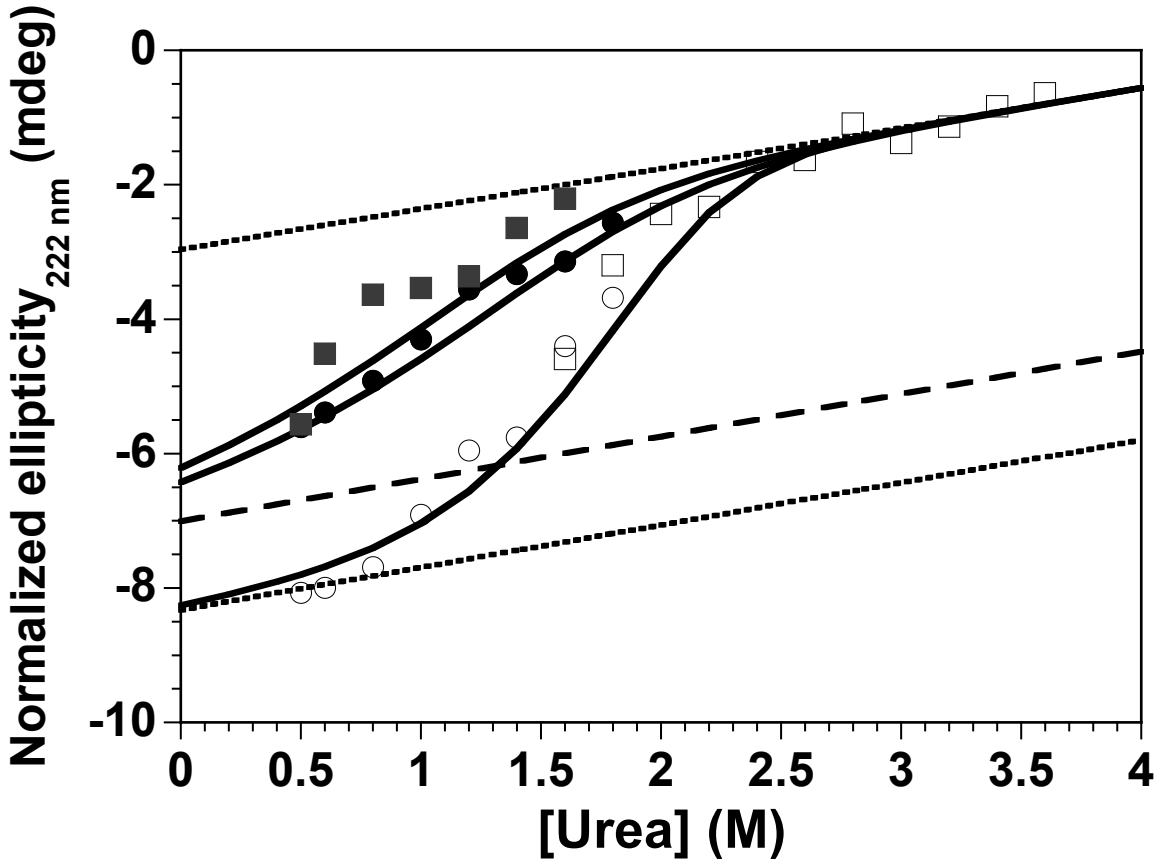

Figure 4. Placek & Gloss

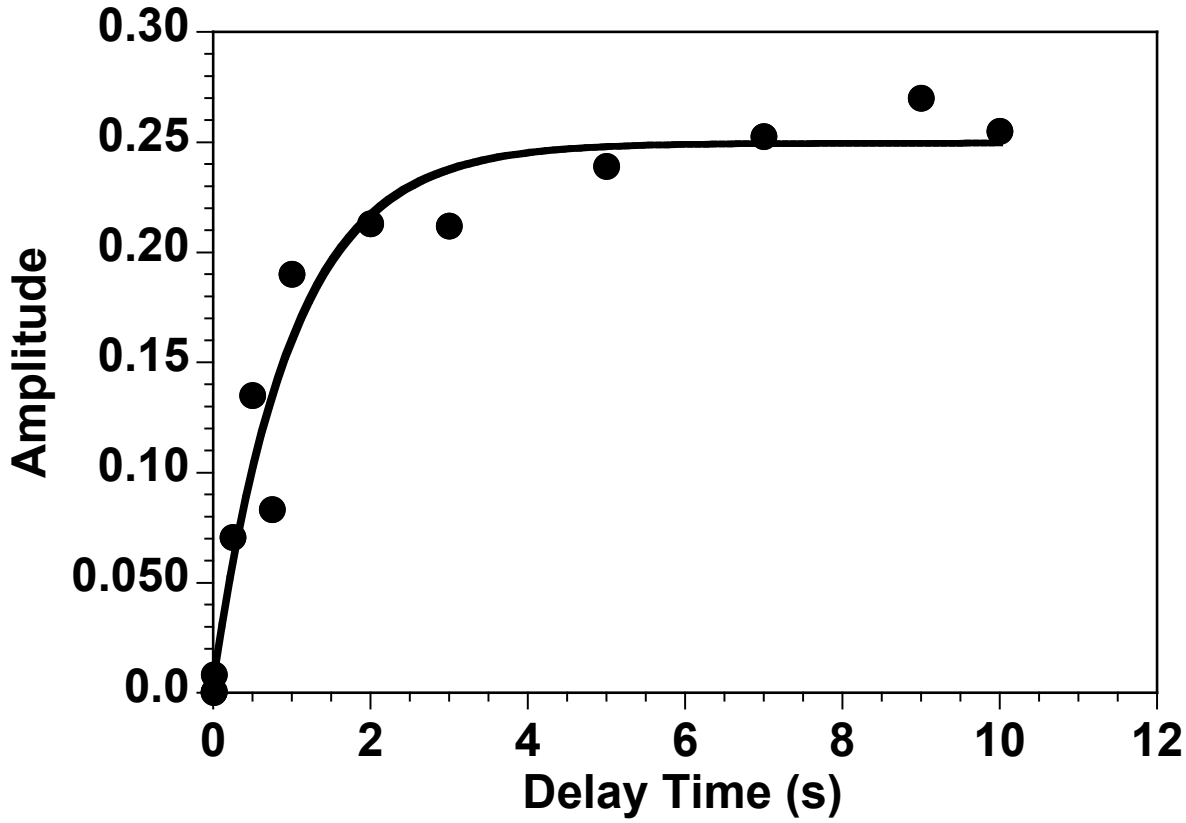

Figure 5. Placek & Gloss

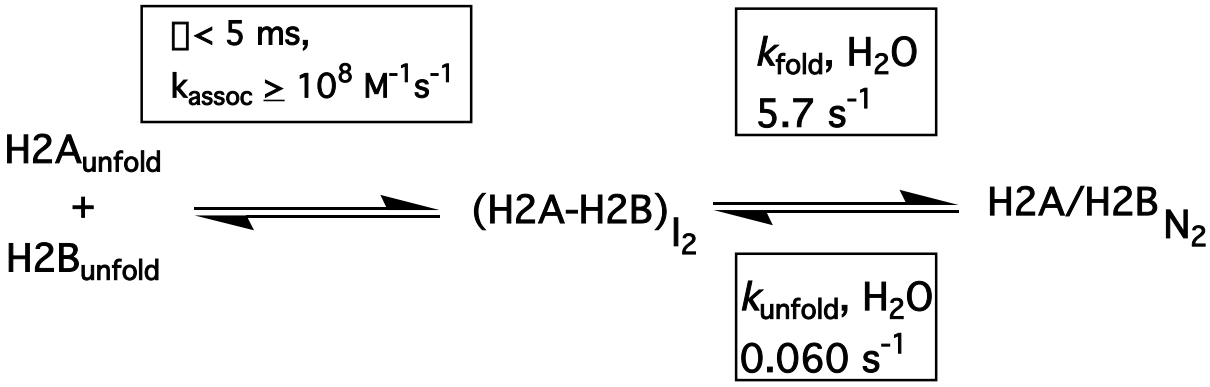

Scheme 1. Placek & Gloss

Reference:

Arents, G. & Moudrianakis, E. N. (1993). Topography of the histone octamer surface: Repeating structural motifs utilized in the docking of nucleosomal DNA. *Proc. Natl. Acad. Sci. USA* **90**, 10489-93.

Arents, G. & Moudrianakis, E. N. (1995). The histone fold: A ubiquitous architectural motif utilized in DNA compaction and protein dimerization. *Proc. Natl. Acad. Sci. USA* **92**, 11170-74.

Banks, D. D. & Gloss, L. M. (2003). Equilibrium folding of the core histones: the H3-H4 tetramer is less stable than the H2A-H2B dimer. *Biochemistry* **42**(22), 6827-39.

Banks, D. D. & Gloss, L. M. (2004). Folding mechanism of the $(H3\text{-}H4)_2$ histone tetramer of the core nucleosome. *Protein Sci* **13**(5), in press.

Clark, A. C., Raso, S. W., Sinclair, J. F., Ziegler, M. M., Chaffotte, A. F. & Baldwin, T. O. (1997). Kinetic mechanism of luciferase subunit folding and assembly. *Biochemistry* **36**(7), 1891-9.

Fersht, A. (1999). *Structure and Mechanism in Protein Structure: A Guide to Enzyme Catalysis and Protein Folding*. 1 edit, 1. 1 vols, W. H. Freeman and Company.

Fersht, A. R. (1994). Pathway and stability of protein folding. *Biochem. Soc. Trans.* **22**(2), 267-73.

Gittelman, M. S. & Matthews, C. R. (1990). Folding and stability of trp aporepressor from Escherichia coli. *Biochemistry* **29**(30), 7011-7020.

Gloss, L. M. & Matthews, C. R. (1998a). The barriers in the biomolecular and unimolecular folding reaction of the dimeric core domain of *Escherichia coli Trp* repressor are dominated by enthalpic contributions. *Biochemistry* **37**, 16000-16010.

Gloss, L. M. & Matthews, C. R. (1998b). Mechanism of folding of the dimeric core domain of *Escherichia coli Trp* repressor: A nearly diffusion-limited reaction leads to the formation of an on-pathway dimeric intermediate. *Biochemistry* **37**, 15990-15999.

Gloss, L. M. & Placek, B. J. (2002). The Effect of Salts on the Stability of the H2A-H2B Histone Dimer. *Biochemistry* **41**, 14951-14959.

Gloss, L. M., Simler, B. R. & Matthews, C. R. (2001). Rough energy landscapes in protein folding: Dimeric E. coli Trp repressor folds through three parallel channels. *J. Mol. Biol.* **312**, 1121-1134.

Jackson, S. E. (1998). How do small single-domain proteins fold? *Fold Des* **3**(4), R81-91.

Kim, D. H., Jang, D. S., Nam, G. H. & Choi, K. Y. (2001a). Folding mechanism of ketosteroid isomerase from Comamonas testosteroni. *Biochemistry* **40**(16), 5011-7.

Kim, D. H., Nam, G. H., Jang, D. S., Yun, S., Choi, G., Lee, H. C. & Choi, K. Y. (2001b). Roles of dimerization in folding and stability of ketosteroid isomerase from Pseudomonas putida biotype B. *Protein Sci* **10**(4), 741-52.

Kim, P. S. & Baldwin, R. L. (1990). Intermediates in the folding reactions of small proteins. *Annu. Rev. Biochem.* **59**, 631-660.

Kraulis, P. J. (1991). MOLSCRIPT: a program to produce both detailed and schematic plots of protein structures. *J. Applied Crystallography* **24**, 946-950.

Luger, K., Mader, A. W., Richmond, R. K., Sargent, D. F. & Richmond, T. J. (1997). Crystal structure of the nucleosome core particle at 2.8 A resolution. *Nature* **389**(6648), 251-60.

Matthews, C. R. (1993). Pathways of protein folding. *Annual Review of Biochemistry* **62**, 653-683.

Milla, M. E. & Sauer, R. T. (1994). P22 Arc repressor: folding kinetics of a single-domain, dimeric protein. *Biochemistry* **33**, 1125-1133.

Noland, B. W. & Baldwin, T. O. (2003). Demonstration of two independently folding domains in the alpha subunit of bacterial luciferase by preferential ligand binding-induced stabilization. *Biochemistry* **42**(10), 3105-12.

Placek, B. J. & Gloss, L. M. (2002). The N-terminal Tails of the H2A-H2B Histones Affect Dimer Structure and Stability. *Biochemistry* **41**, 14960-14968.

Plaxco, K. W., Simons, K. T., Ruczinski, I. & Baker, D. (2000). Topology, stability, sequence, and length: defining the determinants of two-state protein folding kinetics. *Biochemistry* **39**(37), 11177-83.

Plotkin, S. S. & Onuchic, J. N. (2002a). Understanding protein folding with energy landscape theory. Part I: Basic concepts. *Q Rev Biophys* **35**(2), 111-67.

Plotkin, S. S. & Onuchic, J. N. (2002b). Understanding protein folding with energy landscape theory. Part II: Quantitative aspects. *Q Rev Biophys* **35**(3), 205-86.

Strahl, B. D. & Allis, C. D. (2000). The language of covalent histone modifications. *Nature* **403**(6765), 41-5.

Topping, T. B. & Gloss, L. M. (2004). Stability and folding mechanism of mesophilic, thermophilic and hyperthermophilic archael histones: The importance of folding intermediates. *J. Mol. Biol.*, in press.

Topping, T. B., Hoch, D. A. & Gloss, L. M. (2004). Folding mechanism of FIS, the intertwined, dimeric factor for inversion stimulation. *J Mol Biol* **335**(4), 1065-81.

Wallace, L. A. & Dirr, H. W. (1999). Folding and assembly of dimeric human glutathione transferase A1-1. *Biochemistry* **38**(50), 16686-94.

Wallace, L. A. & Matthews, C. R. (2002). Sequential vs. parallel protein-folding mechanisms: experimental tests for complex folding reactions. *Biophys Chem* **101-102**, 113-31.

Wallace, L. A., Sluis-Cremer, N. & Dirr, H. W. (1998). Equilibrium and kinetic unfolding properties of dimeric human glutathione transferase A1-1. *Biochemistry* **37**(15), 5320-8.

Zitzewitz, J. A., Bilsel, O., Luo, J., Jones, B. E. & Matthews, C. R. (1995). Probing the folding mechanism of a leucine zipper peptide by stopped-flow circular dichroism spectroscopy. *Biochemistry* **34**, 12812-12819.

CHAPTER FIVE
DISCUSSION AND FUTURE DIRECTIONS

Kinetic intermediates

The goal of studying protein folding is to elucidate the protein folding code. The term, protein folding code, refers to the information required for a protein to achieve its native structure, stability and the mechanism for its conversion from an unfolded state to the native state. It is known that all the information required to achieve a protein's native structure and stability is contained within its amino acid sequence.

The histone oligomer H2A/H2B is an attractive model for studying the determinants of protein stability and folding. H2A and H2B are small, and form a predominately α-helical, highly basic dimer, in which each monomer contains a similar structure called the histone fold. Interestingly, even though these two proteins contain very divergent sequences (~ 4% sequence identity), they still fold to a very similar structure. This histone fold is seen in a number of other proteins with divergent amino acid sequences, including, the other histone proteins, H3 and H4, which forms a heterodimer, the homodimeric archael histones, and many other oligomeric DNA binding proteins including some of the TAF's (*1, 2*).

H2A and H2B heterodimerize in a head-to-tail manner called the "handshake" motif. This dimerization involves some intertwining of the six helices and buries a significant amount of surface area. The "handshake" motif has been described as a segment swapped. This is an extension of the domain swapping hypothesis for the creation of oligomeric protein interfaces (*3, 4*); these are a class of proteins in which corresponding domains or segments are exchanged between monomers to create the dimerization domain (*5*). We have studied several dimerization motifs, that are intertwined, segment swapped, α-helical DNA binding oligomeric proteins with diverse topologies. These include the H3/H4 dimer/tetramer, archael histone proteins, FIS (Factor for Inversion Stimulation) and Trp repressor. Comparison of the stabilities and kinetic folding mechanism of this class of oligomers will help to elucidate redundancies within the protein folding code.

Chapter Four determines the kinetic folding mechanism of the H2A/H2B dimer. The mechanism is proposed to involve two sequential steps with the formation of an obligatory intermediate. In the first step, the two monomers dimerize to form an on-pathway, obligatory intermediate. A first-order reaction then converts this intermediate to the native dimer in the second, rate-determining step. The role of kinetic intermediates is a point of contention with in the protein folding community. One view of kinetic intermediates is as follows:

> "For a given set of products, transition states, and reactants, a reaction proceeds most rapidly if no intermediates are populated. Any populated intermediate between the products and the transition state will increase the height of the barrier, assuming that the transition state remains unchanged."(*6*)

An opposing view states:

> "As a protein progresses from the unfolded state to the folded state, the number of interactions formed increases, as does the strength of these individual interactions. If enough of these weak interactions are formed before the transition state, they will stabilize an intermediate conformation. However, if these same interactions stabilize the transition state more than the intermediate, they will result in a net acceleration of the folding process."(*6*)

The results presented in Chapter Four clearly support the model of the potential for kinetic intermediates to accelerate the folding of a protein. For H2A/H2B, the data clearly indicate that >98% of the protein folds through the on-pathway, dimeric intermediate. This dimeric intermediate is not only seen in the folding of H2A/H2B, but also in other structurally similar proteins such as FIS (*7*), H3/H4 (*8*) and Trp repressor (*9, 10*). However, when the mechanism is compared to the structurally similar archael histones some interesting observations can be made. The folding of the archael histones, hPyA1 and hMfB, has been reported (*11*). hMfB requires the formation of a monomeric intermediate, hPyA1, however folds to the native dimer in a single step. What is most intriguing is that the folding rates of the hPyA1 and hMfB dimers are much slower than the other dimers discussed here, which fold via a dimeric intermediate.

Furthermore, hMfB, which folds via a monomeric intermediate, folds faster than hPyA1, which folds without the formation of any observable intermediates. This data strongly suggests that kinetic intermediates are not only productive but may enhance the rate of folding.

Nucleosome dynamics

The Nucleosome Core Particle (NCP) is a highly dynamic structure, and alteration of this structure is important for nuclear processes such as replication, repair, transcription and recombination. The association of the H2A/H2B dimers with the NCP has been shown to be a dynamic process. Several studies have demonstrated that the H2A/H2B dimer can readily exchange between nuclesosomes both i*n vivo* and *in vitro* (*12-14*). Furthermore, transcriptionally active chromatin is often depleted in H2A/H2B dimers (*12, 15*), and it has been shown that RNA pol II can displace H2A/H2B dimers during transcription (*16*). Therefore, there is an important equilibrium between the mature, fully assembled NCP and partially unfolded NCPs in which the H2A/H2B dimers are less tightly bound or completely dissociated. Histone variants or histone post-translational modifications can impact this equilibrium by altering the free energy of the mature NCP OR by altering the free energy of the dissociated dimer (*17*). Therefore, the stability of the free dimer will impact this equilibrium, and the state of nucleosome assembly is intimately linked to histone stability. A more stable H2A/H2B dimer should favor a more unfolded, dissociated state of the NCP. We have previously shown that the highly basic N-terminal tails destabilize the H2A/H2B dimer by electrostatic repulsion (*17, 18*). The charge state of the tails are modulated by post-translational modifications such as Ser phosphorylation and Lys acetylation, which should stabilize the free H2A/H2B dimer, and certainly hyperacetylation correlates with transcriptional activity and depletion of the H2A/H2B dimer. In this report, we have shown that the free H2A.Z/H2B dimer is unstable, and this

instability correlates with a shift of the equilibrium toward a more stable, assembled NCP, making the dimers less likely to dissociate under conditions that lead to dissociation of the H2A/H2B dimer (*19*).

Chapter Two determines the effect of the highly basic N-terminal tail regions on the stability of the H2A/H2B dimer. It was found that, while the individual tails have a small effect on the stability, the effect appears to be primarily caused by electrostatic repulsion between the residues in the tails as well as between the tails and the helical regions (*18*). This is of interest because the most well studied modifications of the histone tails (methylation, acetylation, and phosphorylation) all affect the charge state and electrostatic properties of the histone N-terminal tails. These results support our working hypothesis that altering the charge within the tails may have an effect on the stability of the H2A/H2B dimer and therefore the dynamics of the entire NCP. This hypothesis may help explain the apparent opposing roles of chromatin. On one hand, chromatin is responsible for binding to and compacting DNA within the nucleus. This role is generally thought to be repressive to processes such replication, repair and transcription. On the other hand, the chromatin must be altered to allow access to the DNA for these same processes to occur. However, during such events as transcription or DNA repair, it is important for the cell to restrict this access to localized regions of the chromatin without expanding and unpackaging the entire genome. Our stabilty results suggest the possibility that destabilizing NCP's within a defined region of the genome may increase the accessibility of the DNA by promoting release of H2A/H2B through its stabilization without opening up the entire genome to modification.

Further evidence for the importance of protein stability as a means to affect the NCP dynamics is provided in Chapter Three. This chapter examines the effect of the incorporation of a particular histone variant, H2A.Z, on the stability of the dimer. The dimer containing the variant H2A.Z is significantly destabilized, exhibiting ~ 50% of the stability the H2A/H2B dimer. Therefore, our hypothesis is that a NCP containing H2A.Z will favor the fully

assembled state as compared to an H2A-containing NCP. A recent report showed that a NCP containing H2A.Z is more stable to salt-induced dissociation of the dimer than a NCP containing the major H2A (*19*). These observations support the proposed role of H2A.Z as having a function in the formation and maintenance of heterochromatic, transcriptionally repressed regions of the genome.

Future Directions

Now that the stabilities and folding mechanisms of the histone oligomers, H2A/H2B dimer (*17, 18*) and H3/H4 tetramer (*8, 20*), have been determined; it is important to extend this work to the entire NCP. The elucidation of the dynamics of the NCP will help resolve the apparently conflicting roles of chromatin as mentioned previously. How does chromatin fulfill its role in compacting the DNA, while still allowing access to other nuclear proteins? To further the understanding of this, it will be important to determine in detail the folding and unfolding mechanism of the entire nucleosome, including characterizing any intermediates along the pathways of assembly and disassembly and to determine the biological function of these intermediates. Once the detailed biophysical equilibrium and kinetic mechanisms of NCP folding/unfolding have been determined for the NCP containing the major, unmodified histone oligomers, it will be important to test our working hypotheses with variant or modified histones: 1) How does electrostatic repulsion in the N-terminal tails of H2A and H2B affect the dynamics and stability of the NCP? How does altering the charge state of the N-terminal tails by post-translational modifications affect NCP dynamics? 2) How does incorporation of histone variants affect the dynamics and stability of the NCP? Specifically, does the variant H2A.Z stabilize the NCP compared to the H2A containing NCP? There are also a number of other H2A variants which may also affect the NCP stability, such as, MacroH2A or H2A-BBD.

Monitoring the kinetics of nucleosome assembly and disassembly with typical stopped-flow techniques utilizing intrinsic tyrosine or tryptophan fluorescence would not be feasible. A technique such as FRET (fluorescence resonance energy transfer) would be far more useful in

determining the on and off rates of the H2A/H2B dimer, for example. Specific donor-accepter pairs could be engineered into either the histone proteins or the DNA itself. NCP containing these altered histones and/or DNA can then be reconstituted. By making several different donor-accepter pairs the mechanism of assembly and disassembly for the entire NCP can be determined.

The work presented in this thesis advances the understanding of the biology of the NCP by: 1) Determining the effect of the N-terminal tail regions on the stability and kinetics of the H2A/H2B dimer. 2) Determining the effect of H2A.Z on the stability of the H2A/H2B dimer. This work also contributes to the understanding of how electrostatic interactions within the NCP might affect cellular processes such as replication, transcription and repair. Furthermore, this work also contributes to the understanding of protein folding with the observation that a dimeric intermediate is required for the folding of H2A/H2B, as well as a number of other intertwined, α-helical, segment-swapped dimers, and this intermediate is not only required but appears to accelerate the folding.

REFERENCES

1. Xie, X., Kokubo, T., Cohen, S. L., Mirza, U., Hoffmann, A., Chait, B. T., Roeder, R. G., Nakatani, Y., and Burley, S. K. (1996) Structural similarity between TAFs and the heterotetrameric core of the histone octamer *Nature 380*, 316-322.
2. Birck, C., Poch, O., Romier, C., Ruff, M., Mengus, G., Lavigne, A. C., Davidson, I., and Moras, D. (1998) Human $TAF_{II}28$ and $TAF_{II}18$ interact through a histone fold encoded by atypical evolutionary conserved motifs also found in the SPT3 family. *Cell 94*, 239-49.
3. Liu, Y., and Eisenberg, D. (2002) 3D domain swapping: As domains continue to swap *Protein Sci 11*, 1285-99.
4. Bennett, M. J., Schlunegger, M. P., and Eisenberg, D. (1995) 3D domain swapping: a mechanism for oligomer assembly *Protein Sci 4*, 2455-68.
5. Xu, D., Tsai, C. J., and Nussinov, R. (1998) Mechanism and evolution of protein dimerization *Protein Sci 7*, 533-44.
6. Spudich, G., and Marqusee, S. (2000) A change in the apparent m value reveals a populated intermediate under equilibrium conditions in Escherichia coli ribonuclease HI *Biochemistry 39*, 11677-83.
7. Topping, T. B., Hoch, D. A., and Gloss, L. M. (2004) Folding mechanism of FIS, the intertwined, dimeric factor for inversion stimulation *J Mol Biol 335*, 1065-81.
8. Banks, D. D., and Gloss, L. M. (2004) Folding mechanism of the $(H3\text{-}H4)_2$ histone tetramer of the core nucleosome. *Protein Sci 13*, in press.
9. Gloss, L. M., and Matthews, C. R. (1998) Mechanism of folding of the dimeric core domain of *Escherichia coli Trp* repressor: A nearly diffusion-limited reaction leads to the formation of an on-pathway dimeric intermediate. *Biochemistry 37*, 15990-15999.

10. Gloss, L. M., Simler, B. R., and Matthews, C. R. (2001) Rough energy landscapes in protein folding: Dimeric E. coli Trp repressor folds through three parallel channels. *J. Mol. Biol. 312*, 1121-1134.

11. Topping, T. B., and Gloss, L. M. (2004) Stability and folding mechanism of mesophilic, thermophilic and hyperthermophilic archael histones: The importance of folding intermediates *J. Mol. Biol.*, in press.

12. Louters, L., and Chalkley, R. (1985) Exchange of histones H1, H2A, and H2B in vivo *Biochemistry 24*, 3080-5.

13. Louters, L., and Chalkley, R. (1984) In vitro exchange of nucleosomal histones H2a and H2b *Biochemistry 23*, 547-52.

14. Kimura, H., and Cook, P. R. (2001) Kinetics of core histones in living human cells: little exchange of H3 and H4 and some rapid exchange of H2B *J Cell Biol 153*, 1341-53.

15. Jackson, V. (1990) In vivo studies on the dynamics of histone-DNA interaction: evidence for nucleosome dissolution during replication and transcription and a low level of dissolution independent of both *Biochemistry 29*, 719-31.

16. Kireeva, M. L., Walter, W., Tchernajenko, V., Bondarenko, V., Kashlev, M., and Studitsky, V. M. (2002) Nucleosome Remodeling Induced by RNA Polymerase II. Loss of the H2A/H2B Dimer during Transcription *Mol Cell 9*, 541-52.

17. Gloss, L. M., and Placek, B. J. (2002) The Effect of Salts on the Stability of the H2A-H2B Histone Dimer *Biochemistry 41*, 14951-14959.

18. Placek, B. J., and Gloss, L. M. (2002) The N-terminal Tails of the H2A-H2B Histones Affect Dimer Structure and Stability. *Biochemistry 41*, 14960-14968.

19. Park, Y. J., Dyer, P. N., Tremethick, D. J., and Luger, K. (2004) A new fluorescence resonance energy transfer approach demonstrates that the histone variant H2AZ stabilizes the histone octamer within the nucleosome *J Biol Chem 279*, 24274-82. Epub 2004 Mar 13.

20. Banks, D. D., and Gloss, L. M. (2003) Equilibrium folding of the core histones: the H3-H4 tetramer is less stable than the H2A-H2B dimer *Biochemistry 42*, 6827-39.